Sustainable Production, Life Cycle Engineering and Management
Series Editors: Christoph Herrmann, Sami Kara

Wen Li

Efficiency of Manufacturing Processes

Energy and Ecological Perspectives

Springer

Sustainable Production, Life Cycle Engineering and Management

Modern production enables a high standard of living worldwide through products and services. Global responsibility requires a comprehensive integration of sustainable development fostered by new paradigms, innovative technologies, methods and tools as well as business models. Minimizing material and energy usage, adapting material and energy flows to better fit natural process capacities, and changing consumption behaviour are important aspects of future production. A life cycle perspective and an integrated economic, ecological and social evaluation are essential requirements in management and engineering. This series will focus on the issues and latest developments towards sustainability in production based on life cycle thinking.

More information about this series at http://www.springer.com/series/10615

Wen Li

Efficiency of Manufacturing Processes

Energy and Ecological Perspectives

Springer

Wen Li
Sustainable Manufacturing and Life Cycle
Engineering
University of New South Wales
Sydney
Australia

Additional material to this book can be downloaded from http://extras.springer.com.

ISSN 2194-0541 ISSN 2194-055X (electronic)
Sustainable Production, Life Cycle Engineering and Management
ISBN 978-3-319-17364-1 ISBN 978-3-319-17365-8 (eBook)
DOI 10.1007/978-3-319-17365-8

Library of Congress Control Number: 2015940982

Springer Cham Heidelberg New York Dordrecht London

Printed on acid-free paper

Springer International Publishing AG Switzerland is part of Springer Science+Business Media (www.springer.com)

Dedicated to my daughter Lynn Li, my wife Jie Zhu, and my parents

—Wen Li

Foreword

Energy and eco-efficiency of manufacturing processes are of great interest to manufacturers, consumers, government and others. This is due to the soaring energy costs and the environmental impacts caused by high-energy consumption levels. However, the energy consumption of manufacturing processes and the associated environmental impact has been historically overlooked. The unit process is the fundamental and dynamic element of any manufacturing system. Thus, it requires careful evaluation of its energy and eco-efficiency in order to derive further improvement measures.

In this book, Dr. Li has developed a reliable methodology for characterizing energy and eco-efficiency of unit manufacturing processes. The Specific Energy Consumption, SEC, has been identified as the key indicator for the energy efficiency of unit processes. An empirical approach has been used to develop unit process energy consumption models based on SEC. Then these models have been validated on different machine tools and manufacturing processes to characterise the relationship between process parameters and energy consumptions. The tested cases cover a wide range of manufacturing processes including turning, milling, grinding, injection moulding and electrical discharge machining. All the derived SEC models agree with a universal form, where the Material Removal Rate (MRR) or throughput rate plays a decisive role in the model. The statistical results and additional validation runs have further proved the high accuracy of the derived models which is capable of predicting energy consumption with an accuracy of over 90 %.

In order to characterise the eco-efficiency of manufacturing processes, Dr. Li also discussed the value and the associated environmental impacts of the processes. Besides the electricity energy consumption, other resource consumptions such as tool and coolant have been taken into account. The interrelationship among process parameters, process value and the associated environmental impact has been integrated in the characterization of eco-efficiency. The results have been further investigated to develop strategies for improving the energy and eco-efficiency of manufacturing processes.

In addition, Dr. Li has further decomposed the derived SEC models of manufacturing processes in order to explore the mechanism of the model coefficients. A clustered model has been also generated for a rough estimation. In order to overcome the high efforts of empirical modelling, the methodology has been modified for the implementation in an industrial environment. Moreover, the derived SEC models can be used for improving the quality of life cycle inventory (LCI) databases. As a result, it encourages progress in industry and research towards sustainability in manufacturing.

Prof. Christoph Herrmann
Technische Universität Braunschweig

Prof. Sami Kara
The University of New South Wales

Acknowledgments

The present book has been developed mainly in the context of my work as a researcher within the Sustainable Manufacturing and Life Cycle Engineering Research Group at The University of New South Wales (SMLCE@UNSW). First and foremost, I owe my sincerest gratitude to my supervisor and mentor, Prof. Sami Kara, who has supported me throughout my research with his patience and knowledge. It was always joyful and fruitful to discuss research questions as well as philosophical topics with him during all kinds of occasions. I greatly appreciate the excellent example he has provided as a successful academic. One simply could not wish for a better or friendlier supervisor.

I would also offer my sincere gratitude to Prof. Dr.-Ing. Christoph Herrmann in Sustainable Manufacturing and Life Cycle Engineering Research Group at Technische Universität Braunschweig (TUBS). During my research visit to TUBS, I have been well supported and warmly welcomed by Prof. Herrmann and his research team. He has not only provided constructive suggestions for my research, but also integrated me as a member in his research team.

I am indebted to many of my colleagues in the SMLCE@UNSW research group. Their encouragement and companionship has been very important to me. I would like to particularly acknowledge Dr. Seung Jin Kim and Dr. Supachai Vongbunyong for the friendship that I am keen to maintain. It was also a great pleasure to work with colleagues from the TUBS team, particularly Dr.-Ing. Sebastian Thiede, Dr.-Ing. André Zein, Dr.-Ing. Gerrit Posselt and Mr. Marius Winter, Dr.-to-be. Their enthusiasm, professionalism and knowledge for the research of sustainable manufacturing have deeply encouraged me for my research. Special thanks go to Ms Anne-Marie Schlake who heartened me to finish this book.

I greatly appreciate Advanced Manufacturing CRC (AMCRC) for funding this research. Also, I have received great supports from the School of Mechanical and Manufacturing Engineering, UNSW, especially from Mr. Martyn Sherriff for assisting me with all the experiments. I would like to extend my gratitude to all the technicians from Sydney City TAFE who has also provided voluntary assistance for this research.

Last but not least, I would like to attribute this book to my family for their love and encouragement. Most of all is for my loving, supportive and encouraging wife, Jie Zhu, whose faithful support is so appreciated. Equally important and appreciated is my daughter, Lynn Li, who is the true driving force for me to accomplish this book. Also, I thank my parents Rong Han and Fangze Li who have unconditionally supported me in all my pursuits. I would like to further thank Jie's parents who have provided me with unending encouragement and support.

Sydney Dr. Wen Li
May 2014

Contents

Chapter 1
Introduction

1.1 Problem Statement and Scope

The global population has already exceeded 7 billion in 2011, and the growth rate is not evidently slowing down in the coming years (UNFPA 2011). Pressure from the population and increasing demand has urged an important question that needs to be answered by politicians, economists, scientists, and engineers: 'how can our planet be sustainable?' Although reducing population or curbing demand is infeasible in any near future, all types of resources can be used more efficiently, i.e. energy and eco-efficiency.

Manufacturing is one of the major energy and resource end-users compared to other sectors such as transport, households, services and others. Globally, this sector consumed the largest share of total energy generated in 2005 (33 %), with the corresponding highest proportion of CO_2 emissions (38 %), (IEA 2008). In addition, the energy price has increased sharply as well as the resource price for producing energy such as fossil fuels, coal, natural gas, and crude oil. Consequently, energy costs have become a topic high on the agenda for manufacturing enterprises. Therefore, improving energy and eco-efficiency can reduce not only these costs but also the associated environmental impacts. This is particularly important for those countries having high carbon intensity during energy generation, for instance, Australia and China. Moreover, regulations form another driving force to push manufacturers to practice energy efficiency measures more actively. The carbon tax passed in Australia is a good example, which has already raised the awareness among its industries. In addition to government action, customers are also starting to demand more environmental-friendly products. Thus, improved energy and eco-efficiency would not only enhance the competitiveness of the manufacturers, but also become a key survival skill in future markets.

W. Li, *Efficiency of Manufacturing Processes*, Sustainable Production,
Life Cycle Engineering and Management, DOI 10.1007/978-3-319-17365-8_1

Therefore, the research about characterizing manufacturing processes from energy and ecological aspects is of great interest to all parties including manufacturers, consumers, government and others.

Unit process is the fundamental element of any manufacturing system. It refers to process one unit volume of material, such as turning 1 cm^3 of mild steel. The unit process is generally a dynamic system, resulting in dynamic energy consumption and associated environmental impact. In fact, unit process is the operational level for executing improvement measures. On the one hand, energy and eco-efficiency improvements need to have a holistic view of the entire manufacturing system to avoid any shifting problems. On the other hand, dynamic behavior of unit processes should also be considered with an adequate evaluation of their energy and eco-efficiency.

However, energy consumption of manufacturing processes or machine tools has been historically overlooked. Machine tools are poorly documented in terms of their energy consumption and associated environmental impacts. In order to enable any improvements in energy and eco-efficiency, the first step is to develop a systematic methodology to characterize individual manufacturing processes. Although the energy consumption and the associated environmental impacts can be physically measured and monitored, the improvement measures can be only performed retrospectively. Therefore, there is a desire for models or tools to describe and even predict energy consumption of manufacturing processes, as well as the associated environmental impacts.

1.2 Research Objective and Approach

According to above problem statement, the overall research objective is to develop a reliable methodology for evaluating energy and eco-efficiency of unit manufacturing processes. This objective involves developing accurate models to describe and predict energy consumption and the associated environmental impacts of manufacturing processes. First, the development of energy consumption models should fulfil the following requirements:

- Reliable: it refers to the capability of describing and predicting energy consumption with an accuracy over 90 %;
- Generic: the model should be transferable and comparable among different machine tools and processes;
- Specific: the model should also be specific for one machine or process in order to evaluate the energy efficiency of each specific process.

Then, the energy efficiency models should be extended with the other aspects including process value and the associated environmental impacts, namely evaluating the eco-efficiency of unit processes.

To achieve the objective, the development of the research approach is structured in 7 chapters, as shown in Fig. 1.1.

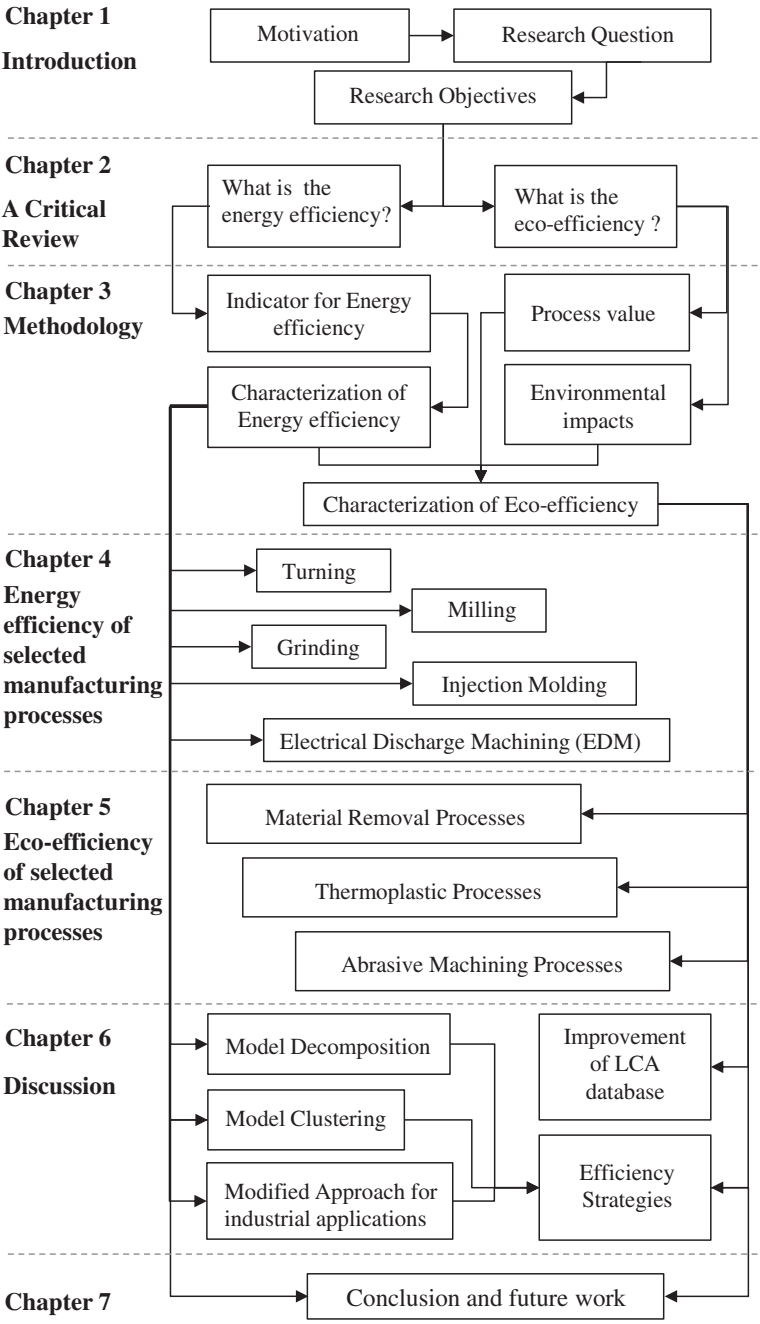

Fig. 1.1 Structure of the research approach

Chapter 2 starts with a critical review regarding the aforementioned research objectives. Two main questions have been asked: what is the energy efficiency and what is the eco-efficiency for unit manufacturing processes? Based on existing literatures, the appropriate indicator is selected to characterize the energy and eco-efficiency of unit processes.

Chapter 3 proposes the methodology of characterizing the efficiency of manufacturing processes from both energy and ecological aspects. An empirical approach is used to first characterize the energy efficiency of unit processes. Based on derived energy efficiency models, the eco-efficiency can be evaluated accordingly.

Following on, Chap. 4 presents the implementation of the proposed methodology to characterize the energy efficiency of different machine tools and manufacturing processes. The covered processes include conventional manufacturing processes (e.g. turning, milling, grinding, injection molding), as well as unconventional manufacturing processes (e.g. electrical discharge machining).

Chapter 5 presents the eco-efficiency characterization of manufacturing processes including material removal processes, thermoplastic processes, and abrasive machining processes.

Furthermore, Chap. 6 discusses the derived models and the results of evaluation for the tested manufacturing processes. The energy consumption models are first decomposed. Then, a clustered model is presented for rough estimation. The challenges of implementing the proposed method in an industrial environment are also discussed, and a modified modeling methodology is then proposed and validated with an industrial extrusion case. The current LCI database is also compared with results of energy and eco-efficiency characterization. Based on the discussion, a number of strategies are proposed in order to improve the energy efficiency of manufacturing processes from different perspectives.

The findings and the potential future work are concluded in Chap. 7.

References

International Energy Agency (IEA) (2008) Worldwide trends in energy use and efficiency-key insights from IEA indicator analysis, Online publication: http://www.iea.org/Papers/2008/Indicators_2008.pdf, Last visited 01/02/2012

UNFPA (2011) State of world population 2011, online publication: http://www.unfpa.org/swp/, Last visit 01/03/2012

Chapter 2
Review on the State of the Research in Energy and Eco-efficiency of Manufacturing Processes

Researches in the field of manufacturing processes traditionally focused on the mechanical performances, such as cutting forces, machinability, surface roughness, dimensional accuracy, etc. The energy consumption and the associated environmental impact of manufacturing processes had been overlooked in the past. Due to the soaring energy price and increasing awareness on environmental impacts, energy and eco-efficiency has become one of the most extensively researched topics in the field of manufacturing. New researches and papers have been published in order to improve the energy and eco-efficiency of manufacturing processes. However, there are few fundamental questions remaining unanswered. For example, "what does energy and eco-efficiency mean to manufacturing processes?", and "how to evaluate them" still remains to be answered. The following sections present the currently available methodologies in the literature that attempt to answer those fundamental questions and define the research gap which still requires to be addressed.

2.1 What Is Energy Efficiency

Energy efficiency now has a frequent appearance in the public domain, which has been discussed intensively in relation to economics, industrial competitiveness, energy security, as well as global warming and climate change (Eichhammer and Mannsbart 1997). In general, energy efficiency refers to the ratio of the useful output of a process to the energy input into a process. Better energy efficiency means using less energy to produce the same amount of useful output. Although it is primarily an engineering term, the definition has already extended to encompass

W. Li, *Efficiency of Manufacturing Processes*, Sustainable Production, Life Cycle Engineering and Management, DOI 10.1007/978-3-319-17365-8_2

economic measures. Patterson (1996) provided a thorough and a critical review of different energy efficiency indicators which can be classified into four main groups:

- Thermodynamic: both of the process output and energy input are derived from the science of thermodynamics.
- Physical-thermodynamic: these are hybrid indicators where the energy input is measured in thermodynamic units, but the output is measured in physical units.
- Economic-thermodynamic: Instead of using physical units, the output is measured by the market price, while the input energy is still in thermodynamic units.
- Economic: Both the energy input and process output are enumerated in monetary terms.

The first two groups are true to the engineering definition of energy efficiency, whereas the economic indicators are generally used in a macro scale for policy making, for instance, the "energy cost: GDP" ratio for a specific industry sector. Since this research focuses on the unit process level, the economic indicators are thus excluded in the further discussions.

2.1.1 Thermodynamic Approach

The thermodynamic indicators are often defined as the science of energy and energy processes, where the heat content or work potentials are measured in terms of thermodynamic terms, such as enthalpy, entropy, exergy and so forth (Patterson 1996). These indicators offer unique and objective measures for a given process in the context of physical conditions, i.e. temperature, pressure, etc. From an enthalpy point of view, the energy efficiency (η) can be defined as Eq. 2.1.

$$\eta_{\Delta H} = \frac{\Delta H_{out}}{\Delta H_{in}} \tag{2.1}$$

where ΔH_{out} refers to the sum of useful energy outputs of a process; ΔH_{in} refers to the sum of all the of the energy inputs into a process.

In the context of industries and manufacturing, the useful energy is generally associated with the minimum energy requirements to perform a task. For instance, Giacone and Mancò (2012) took a glass melting case to demonstrate the calculation procedure of thermodynamic energy efficiency. The useful energy output was computed as the sum of theoretical heat required regarding the temperature changes and chemical reactions of glass melting. However, this thermodynamic approach was only validated on the thermal processes or a furnace. Other machining processes, such as turning, milling and grinding, were initially excluded. For those processes, it is difficult to determine the minimum energy requirement from a thermodynamics perspective, since the temperature changes in the chip-formation areas are extremely sensitive to the combination of workpiece material, tool geometry, cutting parameters and other process conditions (O'Sullivan and

Cotterell 2001). One alternative is to use cutting forces to estimate the minimal energy requirement of a machining process, as shown in Eqs. 2.2 and 2.3.

$$P_t = F_c \times V \tag{2.2}$$

$$\mathrm{E} = \int_{t_1}^{t_2} P_t \cdot d_t \tag{2.3}$$

where P_t refers to the instantaneous power; F_c refers to the cutting force; V refers to the cutting speed; E refers to the energy consumption from time t_1 to t_2.

There were different theories and approaches for cutting force prediction, such as orthogonal machining theory, empirical modelling, finite element method, etc. As cutting force prediction is not the main research objective, a few leading researches about this topic have been reviewed.

Oxley's model is one of the widely accepted theories of cutting force prediction. He has investigated the mechanics of machining based on a geometrical model of chip formation (Oxley 1998). This model is very useful for predicting cutting forces, tool life as well as optimizing cutting conditions. However, this model still had several major limitations. One of them is that the model was limited to plain carbon steel work materials. To extend this approach, as Oxley suggested, the high strain-rate/high temperature flow stress of other materials in appropriate machining conditions should be developed. Another limitation of this model is that it assumed a plane cutting face tool, whereas many industrial tools have chip breaking devices such as obstructions located on the tool's face. Also, the model assumed that the cutting edge keeps perfectly sharp during the machining process. Lee has extended Oxley's machining theory in 2007 (Lee 2007). The author conducted a series of experiments to verify the methodology under various cutting conditions such as cutting speed, feed, tool nose radius, material hardness etc. Lee introduced the magnitude of tool radius into this model, which improved the model by not assuming that the cutting edge is perfectly sharp. Johnson-Cook's flow stress model also has been included in the model in order to extend the range of Oxley's model. However, Lee only experimentally validated this approach on hardened alloy steel. In 2009, Liu et al. presented a similar work, who also introduced Johnson-Cook's flow stress model into Oxley's model (Liu et al. 2009). They validated the methodology only on aluminum alloy work pieces.

Armarego is another leading researcher in the field of cutting force modelling for turning and milling processes. Different cutting force models have been published through the use of both theoretical and empirical approach. The theoretical investigation was initially conducted to analyze two oblique cutting processes (Armarego and Wiriyacosol 1978). The model has suggested the existence of a common oblique cutting theory, which has formed the fundamental tool for further researches on cutting force modelling. Different models have been published for turning and milling processes (Whitfield and Armarego 1986; Budak et al. 1996; Armarego and Samaranayake 1999). Although the cutting force models showed

a high accuracy of predicting cutting forces, the models were only validated for a specific case. Critically, the consistency among those cutting force models was lacking. The empirical modelling approach was also used in some of the researches (Armarego et al. 2000). In that paper, a large amount of available database and empirical models has been reviewed since Taylor's work in 1907. Some attempts to optimize the cutting force, surface roughness and tool life have been documented in Armarego and Brown's (1969) seminal book. Although the existing equations have covered a wide range of process conditions, the values of exponents and constants in the empirical equations were found unreliable.

Other researchers have also provided different types of cutting force models (Kline et al. 1982; Stephensen 1989; Axinte 2001). The models have all claimed achieving a great accuracy, but the uncertainty of the cutting forces has been also stated.

For a more complex machining process, like grinding, the cutting force prediction is more problematic. For instance, grinding force consists of three stages, ploughing, cutting and rubbing. Each one of them has resulted in a complicated model (Li and Fu 1980; Liu et al. 2008; Doman et al. 2009; Durgumahanti et al. 2010). Thus the estimations of minimum energy requirement based on cutting forces are not as applicable as they may first appear.

Another alternative for estimating the minimal energy consumption is to use the specific cutting energy or specific grinding energy for material removal processes. Kalpakjian and Schmid have included a table of specific cutting energy for different materials in their book (Kalpakjian and Schmid 2005). The recommended value for steel ranged from 2.7 to 9.3 w $\cdot$ s/mm^3. However, how to determine the specific energy was not presented. Malkin and Joseph (1975) presented a more detailed work for grinding process, plotting specific grinding energy against the specific material removal rate. However, the exponent and constant were still missing for an applicable estimation. He also suggested an average enthalpy increase between ambient temperature and liquid state as 10.5 kJ/cm^3 for iron and steels (Malkin and Guo 2008). Despite the approximation, the value tested was over-estimated since the material does not all melt completely. Besides the academic researches, the tool suppliers also provide some useful information for specific cutting force estimation. SECO® tools, a major turning and milling insert supplier, has included a specific cutting force (k_c) calculation in its catalogue, as Eq. 2.4 (SECO® 2009).

$$k_c = \frac{1 - 0.01\gamma_0}{(f \sin\alpha)^{mc}} k_{c1.1} \tag{2.4}$$

where f refers to the feed rete; α refers to the approach angle; γ_0 refers to the rake angle; mc refers to material exponent; $k_{c1.1}$ refers to the shear stress of the workpiece material. A complete dataset of exponents and constants for different cutting tools and workpiece material can be found in the catalogue, which makes the specific cutting energy estimation most applicable. However, it can be only applied to turning and milling processes.

Despite the sophisticated calculation of minimal energy consumption, the definition of useful energy output has been criticized by different authors due to the

implicit value judgment (Boulding 1981; Patterson 1996). For instance, the turning process also requires energy for spindle rotation; if only the cutting energy is considered as useful output, all the other energy requirements are considered as waste heat, resulting in a biased estimation of energy efficiency.

In addition, another problem with the enthalpy energy efficiency is that it does not consider the energy quality of the inputs and the useful outputs (Patterson 1996). However, this problem becomes significant when applying to a complex system where a mix of energy resources is used. For instance, the majority of manufacturing processes require electricity as energy input, but the electricity generation and the material processing consume various natural resources. To overcome the problem, the thermodynamic quality measures are introduced, such as exergy. The definition of exergy is, "*the amount of work obtainable when some matter is brought to a state of thermodynamic equilibrium with the common components of the natural surroundings by means of reversible processes involving interaction only with the above mentioned components of nature*" (Szargut et al. 1988). Gutowski et al. has used this concept to provide a platform to evaluate the environmental impacts among material preparation phases to manufacturing process, as shown in Fig. 2.1. The methodology was adapted from several thermodynamics books (Szargut et al. 1988; Smith et al. 2001; Gyftopoulos and Beretta 2005). As the Fig. 2.1 shows, there are three important aspects of manufacturing processes: (1) the energy requirements for the materials; (2) the energy requirements for manufacturing processes themselves; and (3) the efficiency of the material and exergy transformations in manufacturing processes. The definition of energy, enthalpy, entropy, heat, work, temperature and exergy can be

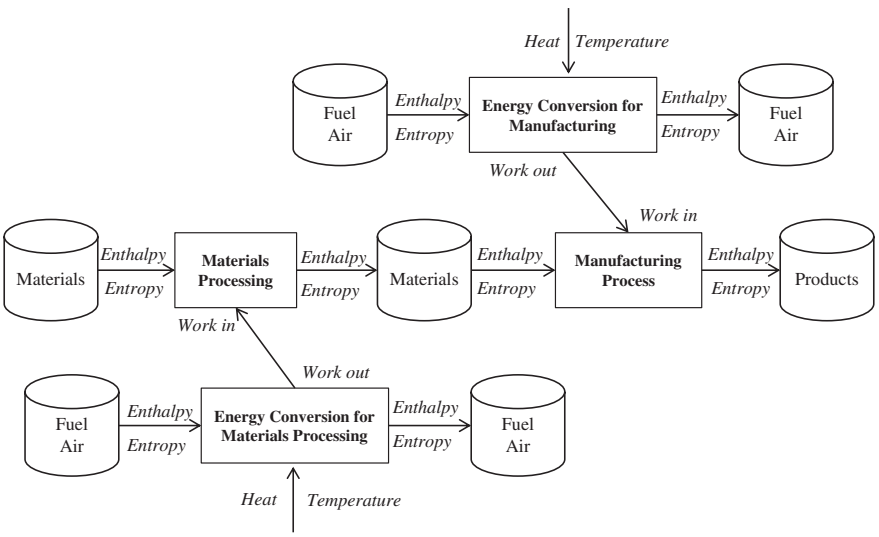

Fig. 2.1 Overview of the thermodynamics of manufacturing processes (Gutowski et al. 2007)

found in aforementioned books. Although the framework provides little information about energy efficiency of manufacturing processes themselves, it is still valuable to have the overall picture of the entire production stage. As Gutowski et al. suggested, once providing a reliable prediction of the energy consumption of manufacturing processes, the environmental impact of the entire manufacturing industry will then be obtained in conjunction with the energy efficiency of material processing.

2.1.2 Physical-Thermodynamic Approach

Besides the challenges of determining the useful output in terms of either heat content or work potential, the thermodynamic measurement does not reflect the end use service required by consumers. Hence, the efficiency ratios measure the output in physical units rather than in thermodynamic terms, whereas the input energy is still measured in traditional thermal terms, such as joule. For instance, the function of a general turning process is to remove material to achieve a round profile. This output can therefore be measured by cm^3.

As suggested by Patterson, one advantage of using physical measures is that they can be objectively measured as thermodynamic measures can, meanwhile they have the added advantage that they directly reflect what consumers are actually requiring in terms of an end use service. Furthermore, the market value of the output can be further converted from the physical measures, which enables longitudinal analyses (Patterson 1996). Therefore, these hybrid physical-thermodynamic measures of energy are widely used in industrial, residential, commercial and other sectors.

Obviously, the energy intensity indicator, which is the input energy consumption per part or a unit service, is the inverse of the physical-thermodynamic measures of energy efficiency. It is also called as specific energy consumption, SEC, as shown in Eq. 2.5. The use of energy intensity or SEC can be found in numerous industrial cases. For instance, Phylipsen et al. defined the energy efficiency indicators for the iron and steel, aluminum, cement, and other energy intensive industries. The specific energy consumption was selected to compare among different countries and industries (Phylipsen et al. 1997). Tanaka compared different energy efficiency measurements, such as absolute energy consumption, energy intensity and thermal efficiency. The specific energy consumption was finally selected for the case of iron and steel industry in Japan (Tanaka 2008).

$$SEC = \frac{Energy\ input\ into\ a\ process}{Physical\ output\ of\ a\ process} \tag{2.5}$$

For a unit manufacturing process, the specific energy consumption is more favorable than other energy efficiency indicators. The aforementioned specific cutting energy or specific grinding energy is actually the form of energy intensity measures. Notably, these indicators only refer to the minimum energy requirement,

which is completely different from the specific energy consumption of a unit process. In other words, the energy consumptions of auxiliary components need to be taken into account. In that sense, the total energy consumption of a machine tool needs to be measured in addition to the cutting energy or the spindle energy demand.

More importantly, the specific energy consumption is not constant for a unit manufacturing process. Owing to its dynamic nature, the specific energy consumption varies according to different process parameters, workpiece materials. For example, Eq. 2.4 has already shown the dynamics of specific cutting force, which directly affects the loads on the machine spindle as well as the total energy input into the process. Therefore, a model is required to characterize the relationship between the specific energy consumptions and process parameters. Ideally, the model should offer a reliable prediction of specific energy consumption for a given process, which will enable further environmental analysis and development of energy efficiency strategies.

2.1.3 The Predictions of SEC

Prior to this research, the prediction of SEC for unit manufacturing process remains unreliable or inapplicable. The existing models or methodologies fail to cope with the total energy consumption of a machine tool, or the dynamic behaviors of the energy consumption, as reviewed below.

One attempt is to link the minimal cutting energy requirement with the total energy consumption of a machine tool, which primarily assumes that the minimal cutting energy is predictable. In other words, the machine or motor efficiency (η) is targeted for modelling. However, no existing work has been conducted at machine tool level. Draganescu et al. (2003) attempted to model the spindle motor efficiency on a vertical milling machine. The motor efficiency has been defined as Eq. 2.6, where P_c refers to the minimal cutting power; P_{mc} refers to the consumed power by the spindle drive motor.

$$\eta = \frac{P_c}{P_{mc}} \tag{2.6}$$

The authors used the response surface methodology to establish the relationship between the machine tool efficiency and working parameters such as spindle speed (n) and torque (M_t). The derived model for the tested milling machine is shown in Eq. 2.7; and the efficiency surface response is shown in Fig. 2.2.

$$\begin{aligned}\eta = \exp\big[&-9.136 + 2.362\ln n + 1.135\ln M_t - 0.166(\ln n)^2 \\ &- 0.141(\ln M_t)^2 \\ &- 0.083(\ln n)(\ln M_t)\big]\end{aligned} \tag{2.7}$$

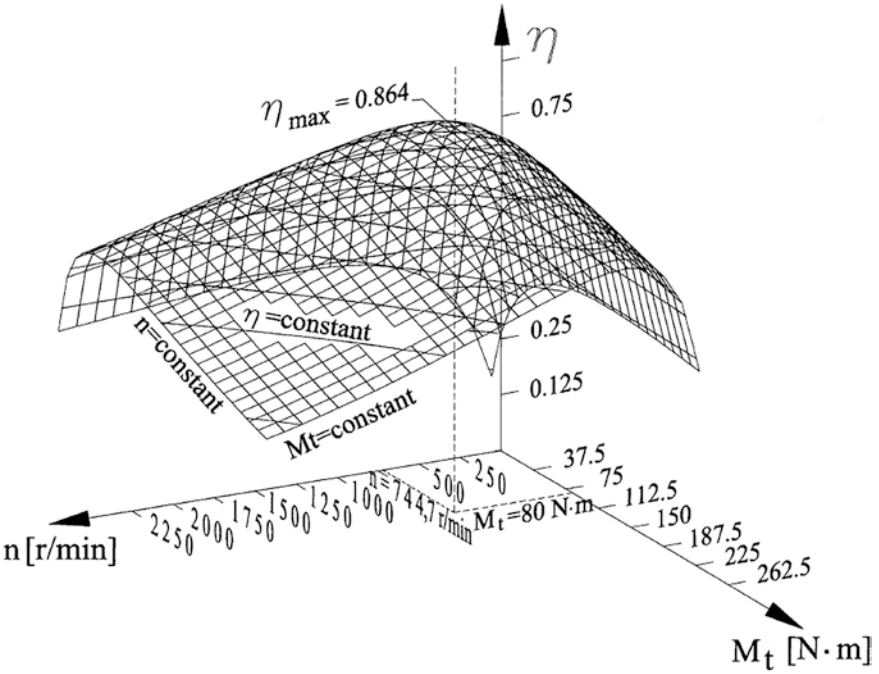

Fig. 2.2 The efficiency surface response for a tested spindle motor of a machine tool (Draganescu et al. 2003)

As the model suggests, the efficiency of the spindle motor has shown a complex trend against the load on the machine tool. However, the derived empirical model for motor efficiency is unlikely to be applied for specific energy consumption of the machine tool. Moreover, this statistical analysis was limited to one specific machine when operating on aluminum alloy. The reliability of the efficiency model cannot be guaranteed with other machines or processes.

On the contrary, disregarding the machine efficiency would result in failure of the prediction of energy consumption. Klocke et al. (2010) has presented a theoretical calculation of the cutting power. The total energy consumption of the machine tool was assumed as the sum of idle power and cutting power. However, the prediction has failed to match the measured energy consumption. The reason was mainly due to the exclusion of waste energy (e.g. heat) during the metal removing period. In other words, the energy consumption of a machine tool is not just fixed power plus working power. The internal energy conversions and transmissions remains as a complex manner, yet unknown.

Other researchers consider the dynamics of machine tools as the different states from power on to off, such as start-up, stand-by, ramp-up, processing, ramp-down, and power-off. Dietmair and Verl (2008) accomplished a case study of energy consumption forecasting based on the measurement of a machine tool at different states. Figure 2.3 shows the machine states over a measuring cycle.

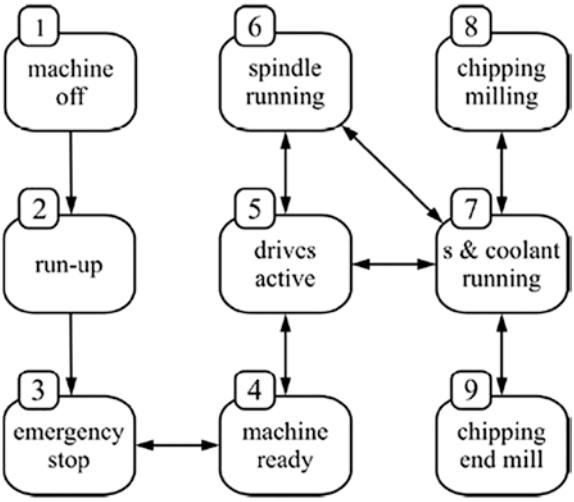

Fig. 2.3 Operational states and the measuring steps (Dietmair and Verl 2008)

This approach is very helpful to allocate the energy consumption of each component, which does not require direct measurement at the component level. Alternatively, the power change between operational states was associated with activated or deactivated components. The authors also claimed the ability to forecast the energy consumption of milling a sample piece. However, the process parameters during the milling process were kept constant throughout the research. In other words, the method was incapable of handling the dynamics of the removal loads.

The initiative—Cooperative Effort on Process Emissions in Manufacturing (CO_2PE!) has been launched by a worldwide collaboration of universities, aiming to document and analyze the environmental impact for available manufacturing processes (Duflou et al. 2010). Since the electricity consumption of unit process is the main contributor of induced environmental impacts, the electricity consumption has been the focus in this initiative. A screening approach was proposed which was similar to the Dietmair's state-based description of machine tools. The power consumption of the machine tool was recorded under different states such as ramp up, standby, processing, ramp-down, etc. However, the energy consumption regarding the change of process load has not been modelled. Therefore, the results cannot respond to the dynamic process load.

Since most of manufacturing processes mainly consume electricity, the exergy concept has been adapted to assess the electricity requirements of manufacturing processes (Gutowski et al. 2009). The energy consumption of the machine tools were simply separated into two parts, one for actual machining, one for other activities such as work handling, lubrication, tool changing, etc. This relationship was expressed as Eq. 2.8.

$$P = P_0 + k\dot{m} \tag{2.8}$$

where, P refers to the total power demand of the machine tool; P_0 refers to the idle power; $\dot{m}$ refers to the process rate (mass/s); and, k is a constant (J/mass). The

equation can be converted into a form of specific electricity consumptions (B_{ele}) as Eq. 2.9.

$$B_{ele} = \frac{P}{\dot{m}} = \frac{P_0}{\dot{m}} + k \tag{2.9}$$

However, the definition of the involved factors remains uncertain, for instance, how to determine the constant k, which consists of the idle power. Moreover, there was no experimental evidence to prove this exergy relationship. The estimation of specific energy consumption also requires accurate value of each factor, such as idle power and the constant for specific machines and processes. Without being given the values and clear definitions, the prediction of specific energy consumption for manufacturing processes remains infeasible.

Instead of using experimental data, the specific energy consumptions from subtractive processes, to net shape processes have been calculated based on rough estimation and averaged data. Gutowski et al. (2005) then collapsed all the specific energy requirements into one single chart (see Fig. 2.4). This figure has mainly used to address the increasing trend of energy intensity for advanced manufacturing processes. For instance, oxidation, EDM and sputtering sit in the upper left end of the trend, where as conventional machining and injection molding process were located at the lower right end. In addition, the authors used the exergy equation (Eq. 2.9) to describe trend. However, there is little information about the specific k or P_0 values found in the paper. Therefore, the prediction of unit process energy consumption was still not applicable.

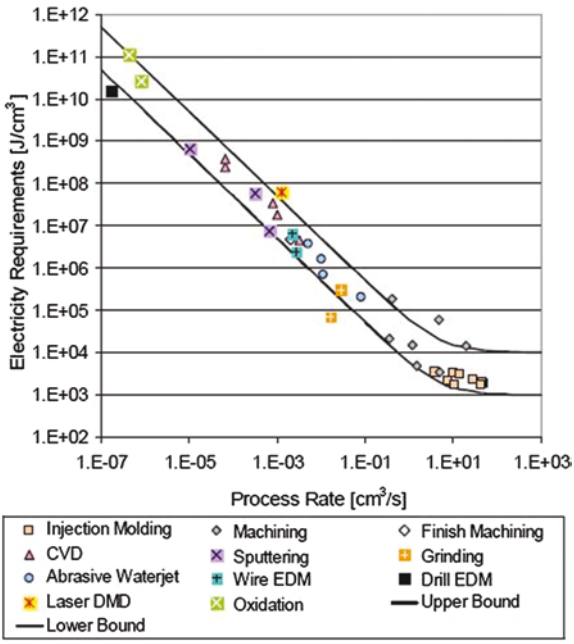

Fig. 2.4 Specific energy requirements for various manufacturing processes (Gutowski et al. 2005)

Renaldi et al. have continued to define the exergy efficiency of manufacturing processes (2011). The authors have compared different definitions for a variety of manufacturing processes. However, the definition for a specific case was still found unclear. Therefore, the exergy concept and framework still remain at a theoretical level, which is not suitable for evaluating and predicting specific energy consumption of manufacturing processes.

In summary, the aforementioned studies do not provide a reliable methodology to estimate and predict specific energy consumption of a unit process, thus calling for the need for such ability that will be developed in this research.

2.1.4 Energy Efficiency Practices in Manufacturing

The energy efficiency is not just an indicator. The definition given by World Energy Council (WEC) suggests that "*Energy efficiency improvements refer to a reduction in the energy used for a given service (heating, lighting, etc.) or level of activity*" (WEC 2008). The understanding of energy efficiency has evolved from a simple input/output ratio towards the global efforts for energy reduction. The researches and practices in the field of manufacturing have been conducted in the different levels from component, to unit process, and factory level.

At the component level, the researches of machine tools have also showed great efforts to improve the energy efficiency. Abele et al. (2010) has reviewed the state-of-the-art technologies and researches for machine tool main spindle units. Normally, the spindle unit is the biggest energy consumer in the machine tool. Different models and simulation tools have been developed for improving the design of spindle motor. However, the focus still remained on the quality performance of the spindle unit, such as accuracy and reliability. There also exist plenty of mechanical design solutions and drive methods to achieve a high-speed production but not compromising any other quality indicators. Mori et al. (2011) has given a perspective from machine tool builder side. A new acceleration control method was developed to reduce the time for non-value adding activities, such as tool change, positioning, acceleration, returning, etc.

At the unit process level, Munoz and Sheng (1995) has proposed an analytical approach to evaluate the environmental impact of machining processes by considering process mechanics, wear characteristics and lubricant flows. Although the tool wear and the efficiency of applying cutting fluid can be improved, the gap towards environmentally-conscious manufacturing remains large due to the exclusion of energy consumptions. In addition, isolating the process from the machine tool cannot provide the true efficiency of any manufacturing processes. Anderberg et al. (2009) has developed a cost model to evaluate both cost and energy efficiency of a CNC lathe machine. The proposed model covered multiple types of cost, such as energy cost, machine cost, tool cost, operational cost, carbon dioxide emission cost, etc. Although the direct energy cost was not comparable with direct machining cost (tool cost and labor cost), the high energy consumption did reflect

the least cost-efficient alternative. The author also suggested a better knowledge about the relationship between important machining parameters and energy consumption will increase the energy efficiency for the CNC machining processes.

At the factory level, simulation has been used to characterize the energy and material flow within the factory. Thiede and Herrmann (2010) presented a holistic view of simulating a manufacturing system considering the interrelationship among processes and the technical building services. But the dynamic behavior of individual process was not modelled. The energy efficiency improvements would be more useful if the unit energy consumption model can be integrated within the simulation system.

Besides the above mentioned energy efficiency practices, Herrmann et al. (2009) provided an extended perspective. They have strategically pointed out the limitation of solely improving energy efficiency. According to their suggestions, all the relevant input and output flows should be considered, including heat, compressed air, coolant, periphery system, etc. In other words, all the consumed energy and resources need to be considered to avoid shifting the problem shifting as well as to enable the overall efficiency of a machine tool. This suggestion leads to the discussion of the second keyword of this research, eco-efficiency.

2.2 What Is Eco-efficiency?

2.2.1 The General Definition of Eco-efficiency

The original meaning of eco-efficiency is defined by World Business Council for Sustainable Development (WBCSD):

> Eco-efficiency is achieved by the delivery of competitively-priced goods and services that satisfy human needs and bring quality of life, while progressively reducing ecological impacts and resource intensity throughout the life-cycle to a level at least in line with the earth's estimated carrying capacity. (WBCSD 2000)

The eco-efficiency is generally measured by Eq. 2.10 (WBCSD 2000):

$$\text{Eco-efficiency} = \frac{\text{Product or Service Value}}{\text{Environmental Impact}} \tag{2.10}$$

The numerator in the ratio is normally indicated by either quantity of product produced/sold or net sales of a business, while the denominator considers energy consumption, water consumption, material consumption, greenhouse gas (GHG) emissions as well as ozone depleting substance (ODS) emissions (WBCSD 2000).

This concept was primarily applied to evaluate the profitability and environmental responsibility of a corporation or a product throughout its life cycle (Sinkin et al. 2008; Aoe 2007). Strategies for improving eco-efficiency have then been proposed accordingly. However, the main interests of manufacturers are the activities within the factory or during manufacturing stage. In fact, the operations as well as the improvement measures are mostly executed at unit process level.

Thus, the concept of eco-efficiency should be applicable for unit processes and transferable among different processes to magnify the benefits at corporate level or throughout product life cycle.

Gutowski (2010) has initially discussed eco-efficiency for unit manufacturing process, where he recommended that eco-efficiency is often the reciprocal of some intensity metric, e.g. energy intensity. It is true for those processes whose energy consumption dominates their environmental impacts. However, this perspective should be extended by considering processes and materials which are needed to support the actual value creation process, because these supporting materials (e.g. coolant) and supporting processes (e.g. coolant filter) have significant environmental impacts. Therefore, a more holistic view of evaluating eco-efficiency for unit process is necessary, but still remains absent.

2.2.2 Environmental Studies of Manufacturing Processes

One of the differences between energy efficiency and eco-efficiency is the consideration of environmental impacts of the unit process. A series of environmental analysis has been conducted among different manufacturing processes. Since the environmental impact of the most tested process is mainly due to the electricity usage, those environmental analyses all started with energy consumption studies. Essentially, there is no difference between energy efficiency and eco-efficiency at this point.

Kordonowy (2002) experimentally measured the energy consumption of selected machines for his B.Sc. thesis. In his thesis, the energy consumed by a machine could be broken down to three stages, such as constant start up stage, constant operation stage, machining stage. A similar state-based measurement was conducted to assign energy consumptions for each machine component. Kordonowy further measured the machining power when applying different material removal rates to the machines. According to the results, the machining power consumption varies dramatically due to different material removal rates. But Kordonowy did not explain how the process parameters impact on the energy consumption. Instead of establishing the relationship between energy consumption and process parameters, the research focused on the constant parts, and tried to theoretically calculate the idle power consumption by using the machine specifications. However, this estimation was unsuccessful especially when applied to the lathe machine (calculated 21810 W vs. measured 1770 W).

Nevertheless, Kordonowy's thesis had provided some useful information for further rough analysis. By referring Kordonowy's findings, Dahmus and Gutowski (2004) then presented a system level environmental analysis of machining processes where grinding process was excluded. In this paper, the authors stated that the energy necessary to actually cut the material is only an insignificant fraction of the total energy consumption, and the differences between different cutting conditions were ignored when attempting to assess the total system energy requirement.

Those statements were based on the previous research of Toyota production processes by Gutowski et al. (2005). By creating an annual production scenario, the actually machining energy consumption was assumed to be only 14.8 % of the total energy consumption. However, this analysis was embodied in the entire production line for a long period of time. The fraction of machining energy consumption was dependent on how many vehicles were produced during that time. Thus, it is unacceptable to ignore the impact of machining parameters on total energy consumption in a smaller scale of production or in unit process analysis. Later, the roughly estimated energy consumption for material removal has then been compared with other energy requirement such as material production, cutting fluid preparation, tool preparation, tool construction and others. The results showed that the embodied energy in the material dominate the energy involved in the material removal processes. However, the energy requirement during the material production does not belong to the unit process, as the material is not created or consumed by the process itself. Therefore, the involvement of embodied energy of raw material can result in a biased conclusion of environmental impacts of unit process.

In 2006, Thiriez and Gutowski conducted series of power measurements on three types of injection molding machines: hydraulic, hybrid and all-electric machines. A similar procedure was conducted to allocate energy consumption to each component. In addition, Thiriez (2006) attempted to model the relationship between energy consumption and throughput rate in his thesis. However, the results were quite poor. The derived regression models showed low *R*-square values for the tested machine tools (less than 0.5); and, the models did not agree with the proposed exergy framework (Eqs. 2.8 and 2.9).

In that research, besides the basic energy consumption analysis, the life cycle inventory analysis of injection molding process was also included. It has identified that the major contributor for the environmental impacts is due to raw material production. Similar to the results of material removal processes, the embodied energy in the raw material has overweighed the energy consumption during other stages. But this does not mean that the energy consumption during manufacturing stage can be neglected. On the contrary, the manufacturing stage is more dynamic than material production; and the total energy consumption due to manufacturing is still considerable. Hence, the improvement of energy consumption and environmental impacts of unit manufacturing processes is still demanded.

Overall, the above mentioned environmental analysis only considered an average specific energy consumption of a unit process, which resulted in constant results of environmental impact of tested process. Consequently, the process dynamics have been excluded in the current studies. More importantly, the energy for material production was incorrectly included in the analysis of unit process. From the unit process point of view, the material is only changed in its geometric, surface and other features from raw material to end product. The material amount is not created from zero to certain gram for an injection molding process; or, the chips do not disappear for a turning or milling processes. Therefore, the embodied energy for a material should be considered from a product point of view, not unit process; and the environmental impacts during material production stage need to be studied separately.

2.2.3 LCC/LCA Approach

Calculating eco-efficiency based on a ratio between life cycle costs and life cycle assessment (LCC/LCA) is proposed by different authors (Kicherer et al. 2007; Huppes and Ishikawa 2005; Lyrstedt 2005).

According to Westkämper et al., LCA is a technique to assess environmental impacts associated with a function. Generally, it is applied to a product, but the product is defined as an object to fulfil a certain function. A holistic view is essential for LCA, which should cover the entire life cycle of the product or the function, as well as different types of environmental impacts. The LCC refers to the valuation of the costs of production, installation, usage and disposal (Westkämper et al. 2000). By assuming that life cycle cost reflects the value of the product or a function, the LCC/LCA can theoretically provide the information for its eco-efficiency (Lyrstedt 2005; Kicherer et al. 2007). However, the proposed cases were originally for the assessment of a product or company in order to support decision making. Huppes and Ishikawa (2005) provided a theoretical approach for assessing eco-efficiency of society. To adapt this LCC/LCA method for unit process, the information about every involved life cycle activities need to be provided. Taking grinding process as an example, besides the electricity consumption, the resources consumptions such as coolant, the grinding wheel also should be included in the eco-efficiency analysis. In that sense, the cost and the environmental impacts of producing and consuming those resources need to be estimated. However, none of the information can be found in either previous literature or Life Cycle Inventory (LCI) databases. In order to gather above information, it needs a joint effort from machine tool builders, cutting tool suppliers, coolant makers and the users.

In short, due to the high demand of input information, the LCC/LCA is inapplicable for the case of unit process at the moment. Therefore, the methodology of evaluating the eco-efficiency of unit process is required in this research.

2.3 Ensuing Need for Research

This chapter has mainly reviewed the existing methods for characterizing energy and eco-efficiency of unit manufacturing processes. The indicator for evaluating energy efficiency has been selected, and the specific energy consumption is favored due to the objective measurements, as well as the meaningful reflection of customer requirements. However, the current methodology faces shortages to either describe or predict the dynamic behavior of unit manufacturing processes. Therefore, there is an essential need to develop unit energy consumption models to characterize the relationship between specific energy consumption and process parameters, in order to evaluate the energy efficiency of a unit process.

The eco-efficiency for unit process is also under development. Although the eco-efficiency can be simplified as the reciprocal of energy intensity for processes that only consume electricity, other resource consumptions need to be taken into

account for a relatively complex process, such as grinding. In addition, the process value remains undefined for the case of unit process. Therefore, the methodology of characterizing eco-efficiency for unit process also needs a systematic development.

References

Abele E, Altintas Y, Brecher C (2010) Machine tool spindle units. CIRP Annals Manufact Technol 59(2):781–802

Anderberg S, Kara S, Beno T (2009) Impact of energy efficiency on computer numerically controlled machining. Proc Inst Mech Eng Part B J Eng Manufact 224(4/2010):531–541

Aoe T (2007) Eco-efficiency and ecodesign in electrical and electronic products. J Clean Prod 15:1406–1414

Armarego EJA, Brown RH (1969) The machining of metals. PrenticeHall Inc., New Jersey

Armarego EJA, Samaranayake P, (1999) Performance prediction models for turning with rounded corner plane faced lathe tools. II. Verification of models. J Mach Technol 3(2):173–200

Armarego EJA, Wiriyacosol S (1978) Oblique machining with triangular form tools—I. Theoretical investigation. Int J Mach Tool Design Res 18(2):67–80

Armarego EJA, Ostafiev D, Wong SWY, Verezub S (2000) Appraisal of empirical modeling and proprietary software databases for performance prediction of machining operations. J Mach Sci Technol 4(3):479–510

Axinte DA, Belluco W, De Chiffre L (2001) Evaluation of cutting force uncertainty components in turning. Int J Mach Tools Manufact 41(5):719–730

Boulding KE (1981) Evolutionary economics. Sage Publications, CA

Budak E, Altintas Y, Armarego EJA (1996) Prediction of milling force coefficients from orthogonal cutting data. J Manufact Sci Eng Trans ASME 118(2):216–224

Dahmus JB, Gutowski T (2004) An environmental analysis of machining. in American Society of Mechanical Engineers. Manufacturing Engineering Division, MED. Anaheim

Dietmair A, Verl A (2008) Energy consumption modeling and optimization for production machines. In: IEEE international conference on sustainable energy technologies, ICSET, Singapore

Doman DA, Warkentin A, Bauer R, (2009) Finite element modeling approaches in grinding. Int J Mach Tools Manufact 49(2):109–116

Draganescu F, Gheorghe M, Doicin CV (2003) Models of machine tool efficiency and specific consumed energy. J Mater Process Technol 141(1):9–15

Duflou JR, Kellens K, Dewulf W (2010) Unit process impact assessment for discrete part manufacturing: a state of the art. CIRP J Manufact Sci Technol (in press)

Durgumahanti USP, Singh V, Rao PV (2010) A new model for grinding force prediction and analysis. Int J Mach Tools Manuf 50(3):231–240

Eichhammer W, Mannsbart W (1997) Industrial energy efficiency-indicators for a European cross-country comparison of energy efficiency in the manufacturing industry. Energy Policy 25(7–9):759–772

Giacone E, Mancò S (2012) Energy efficiency measurment in industrial processes. Energy 38(1):331–345

Gutowski T (2010) The efficiency and eco-efficiency of manufacturing. Int J Nanomanuf 6(1–4):38–45

Gutowski T, Murphy C, Allen D, Bauer D et al (2005) Environmentally benign manufacturing: observations from Japan, Europe and the United States. J Clean Prod 13(1):1–17

Gutowski T, Dahmus J, Thiriez A, Branham M, Jones A (2007) A thermodynamic characterization of manufacturing processes. In: IEEE International symposium on electronics and the environment, Orlando

Gutowski T, Branham MS, Dahmus JB, Jones AJ, Thiriez A, Sekulic DP (2009) Thermodynamic analysis of resources used in manufacturing processes. Environ Sci Technol 43(5):1584–1590
Gyftopoulos EP, Beretta GP (2005) Thermodynamics: foundations and applications. Dover Publications Inc, New York
Herrmann C, Thied S, Zein A, Ihlenfeldt S, Blau P (2009) Energy efficiency of machine tools: extending the perspective. In: 42nd CIRP international conference on manufacturing systems. Grenoble
Huppes G, Ishikawa M (2005) A framework for quantified eco-efficiency analysis. J Ind Ecol 9(4):25–41
Kalpakjian S, Schmid SR (2005) Manufacturing engineering and technology, 5th edn. Prentice Hall
Kicherer A, Schaltegger S, Tschochohei H, Pozo BF (2007) Eco-efficiency combining life cycle assessment and life cycle costs via normalization. Int J Life Cycle Assess 12(7):537–543
Kline WA, DeVor RE, Lindberg JR (1982) The prediction of cutting forces in end milling with application to cornering cuts. Int J Mach Tool Design Res 22(1):7–22
Klocke F, Schlosser R, Lung D (2010) Energy and resource consumption of cutting processes—how process parameter variation can optimise the total process efficiency. In: 17th CIRP international conference on life cycle engineering. Hefei
Kordonowy DN (2002) A power assessment of machining tools, in mechanical engineering. Massachusetts Institute of Technology, Cambridge
Lee TH (2007) An experimental and theoretical investigation for the machining of hardened alloy steels. PhD thesis in School of mechanical and manufacturing engineering, UNSW, Sydney
Li L, Fu J (1980) A study of grinding force mathematical model. CIRP Annals Manufact Technol 29:245–249
Liu Q, Chen X, Wang Y, Gindy N (2008) Empirical modelling of grinding force based on multivariate analysis. J Mater Process Technol 203(1–3):420–430
Liu HT, Sun YZ, Lu ZS, Han LL (2009) The prediction model of cutting forces based on Johnson-Cook's flow stress model. Key Eng Mater 392–394:1–6
Lyrstedt F (2005) Measuring eco-efficiency by a lcc/lca ratio an evaluation of its applicability—a case study at ABB. Master Thesis, Chalmers University of Technology, Göteborg
Malkin S, Guo C (2008) Grinding technology—theory and applications of machining with abrasives, 2nd edn. Industrial Press, New York
Malkin S, Joseph N (1975) Minimum energy in abrasive processes. Wear 32(1):15–23
Mori M, Fujishima M, Inamasu Y, Oda Y, (2011) A study on energy efficiency improvement for machine tools. CIRP Annals Manufact Technol 60(1):145–148
Munoz AA, Sheng P (1995) An analytical approach for determining the environmental impact of machining processes. J Mater Process Technol 53(3–4):736–758
O'Sullivan DO, Cotterell M (2001) Temperature measurement in single point turning. J Mater Process Technol 118:301–308
Oxley PLB (1998) Development and application of a predictive machining theory. J Mach Sci Technol 2(2):165–189
Patterson MG (1996) What is energy efficiency? Concepts indicators and methodological issues. Energy Policy 24(5):377–390
Phylipsen GJM, Blok K, Worrell E (1997) International comparisons of energy efficiency-methodologies for the maufacturing industry. Energy Policy 25(7–9):715–725
Renaldi Kellens K, Dewulf W, Duflou JR, (2011) Exergy efficiency defnitions for manufacturing processes. In: 18th CIRP international conference on life cycle engineering. Braunschweig
SECO® Tools (2009) MN2009-turning. The Machining Navigator Catalogue
Sinkin C, Wright CJ, Burnett RD (2008) Eco-efficiency and firm value. J Acc Public Policy 27:167–176
Smith JM, Van Ness HC, Abbott MM (2001) Chemical engineering thermodynamics, 6th edn. McGraw-Hill
Stephensen DA (1989) Material characterization for metal-cutting force modelling. J Eng Mater Technol Trans ASME 111(2):210–219

Szargut J, Morris DR, Steward FR (1988) Energy analysis of thermal, chemical, and metallurgical processes. Hemisphere Publishing Corporation and Springer-Verlag, New York

Tanaka K (2008) Assessment of energy efficiency performance measures in industry and their application for policy. Energy Policy 36(8):2887–2902

Thiede S, Herrmann C (2010) Simulation-based energy flow evaluation for sustainable manufacturing systems. In: 17th CIRP international conference on life cycle engineering. Hefei

Thiriez A (2006) An environmental analysis of injection molding. Master thesis in MIT, Cambridge

Thiriez A, Gutowski T (2006) An environmental analysis of injection molding. In: IEEE international symposium on electronics and the environment, Scottsdale

Westkämper E, Alting Arndt (2000) Life cycle management and assessment: approaches and visions towards sustainable manufacturing (keynote paper). CIRP Annals Manufact Technol 49(2):501–526

Whitfield RC, Armarego EJA (1986) Predictive milling force models for cad/cam systems. Aust, Inst of Engineers, Newcastle

World Bussiness Council for Sustainable Development (WBCSD) (2000) Eco-efficiency: creating more value with less impact, Geneve

World Energy Council (2008) Energy efficiency polices around the world: review and evaluation, online publication: http://www.worldenergy.org/publications/energy_efficiency_policies_around_the_world_review_and_evaluation/default.asp, Last visited 1 March 2012

Chapter 3
Methodology for Characterizing Energy and Eco-efficiency of Manufacturing Processes

As concluded in Chap. 2, specific energy consumption is a representative indicator for the energy efficiency of unit manufacturing processes. A physical measurement should be selected as an indicator of process outputs, the selection of which is made according to the mechanism of the process. For example, grinding is a metal machining process, therefore volume of removed material can be chosen as the physical output. However, a reliable methodology for describing and predicting SEC remains absent. There are several obstacles for deriving mechanistic models based on either kinematics or thermodynamics. This is primarily due to the complexity of energy conversion and losses within a machine tool system. Even if the mechanism of energy flow can be described for a specific machine tool, it may not be transferable to other machine tools or processes owing to inherent differences among machine tools. Alternatively, empirical modelling offers an equivalent ability to characterize the relationship between process variables and responses. Therefore, empirical modelling has been applied to establish the methodology for characterizing the energy efficiency of unit processes, as presented in Sect. 3.1.

In addition to energy efficiency, the unit process also requires other resources and periphery processes. Thus, the concept of eco-efficiency can be introduced to the level of unit process. There are two elements required to evaluate the eco-efficiency of a unit process: one is its value (or process value); and, the other one is the direct or indirect environmental impacts. However, neither of these two elements has been defined for a unit process, particularly the former one, since process value is determined by not only the quantity of the product but also the quality. Taking the case of grinding, surface roughness, dimensional accuracy and other quality measures are closely related to the process value. Therefore, owing to the variety of manufacturing processes, the definition of eco-efficiency should be given according to the nature and purpose of a unit process, as discussed in Sect. 3.2.

W. Li, *Efficiency of Manufacturing Processes*, Sustainable Production,
Life Cycle Engineering and Management, DOI 10.1007/978-3-319-17365-8_3

3.1 Methodology of Energy Efficiency Evaluation for Unit Process

3.1.1 Empirical Modelling

Models are frequently used by engineers in problem formulation and solution. In some cases, these models are based on underlying physical, chemical, engineering or other scientific knowledge of the phenomenon, and can be called mechanistic models (e.g. the Oxley's model as reviewed in Sect. 2.1.1). However, there are many situations in which two or more variables of interest are related, and a mechanistic model relating these variables is unknown. In this case, another modelling method, empirical modelling is required, which is built on the observed data relating the variables. As suggested by Montgomery, an empirical model can be manipulated and analyzed in the same way as a mechanistic model (Montgomery et al. 2007).

As discussed in Chap. 2, the relationship between process parameters and energy consumption is not known. Even if the minimum energy requirement could be calculated based on a mechanistic model, efficiency of the machine and the impact of process parameters on this efficiency remain unidentified. Therefore, empirical modelling is selected as an effective approach to derive prediction models. This approach considers a machine tool as an integrated system configured by process parameters. Hypothetically, different configurations of process parameters would result in different energy consumptions, disregarding energy transmission and its conversions within the system. As a result, it is expected that the models are able to characterize the total energy consumption of a machine tool (using process parameters) regardless of its size and type.

Montgomery provided guidelines for designing an experiment in his book about experimental design (Montgomery 2009). The book provides seven basic tasks as listed below:

1. Recognition of and statement of the problem
2. Selection of the response variable
3. Choice of factors, levels, and ranges
4. Choice of experimental design
5. Performing the experiment
6. Statistical analysis of the data
7. Conclusions and recommendations

It is also important to retain a few valuable points suggested by Montgomery: to use non-statistical knowledge of the problem; to keep the design and analysis as simple as possible; to recognize the difference between practical and statistical significance; and, that most experiments are iterative (Montgomery 2009). It is also important to adapt above mentioned guidelines for a specific case or in relation to the problem statement.

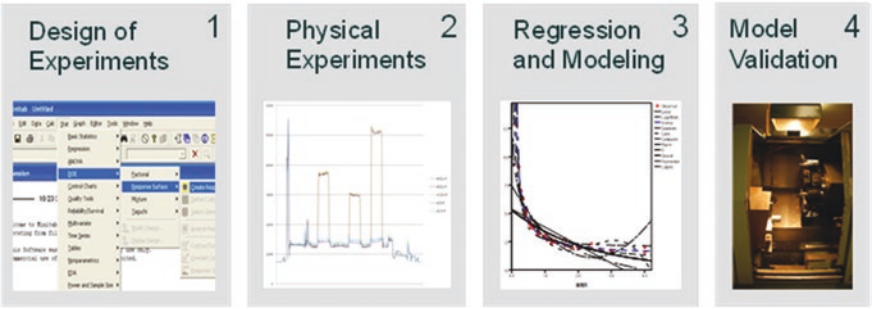

Fig. 3.1 The procedure of empirical modeling approach

In this research, the empirical approach follows four stages: Design of Experiments (DoE); physical experiments; regression and modelling; and, model validation as shown in Fig. 3.1.

- **Stage I**: The Design of Experiments (DoE) uses two methods to separate the experiments into two steps. As there are multiple variables involved in one unit process, it is inefficient to develop the energy consumption models with the complete combination of all the process variables. Therefore, a factor screening procedure is firstly applied in order to eliminate the insignificant variables. Then Response Surface Methodology (RSM) is used for model development which includes at least 3-level of variance. The detailed methodology is discussed in Sect. 3.1.2.
- **Stage II**: During the physical experiments step, data acquisition is essential for empirical modelling, as the accuracy of the model depends on the reliability of collected data. Hence, an accurate energy metering and monitoring system is required and discussed in Sect. 3.1.3.
- **Stage III**: The collected data is then processed with statistical analysis for regression and modelling using various methods. Curve-estimation is firstly performed to test the best-fit model; followed by, multiple-linear regression to test the impact of different variables. The detailed analysis methods are discussed in Sect. 3.1.4.
- **Stage IV**: Once the model is derived, a validation test is conducted in order to compare the difference between predicted energy consumption and actual measured energy consumption. A different combination of process parameters, which is not used for modelling development, is used for model validation.

The selection of model response is critical for empirical modelling, since it should meet the original aim of the project or study (Montgomery et al. 2007). Specific Energy Consumption, SEC, is primarily selected as model response according to the review of all the energy efficiency indicators (Sect. 2.1). In this research, SEC refers to the total energy consumed by a machine tool to process a unit material, as illustrated in Fig. 3.2. This value includes the energy consumptions of

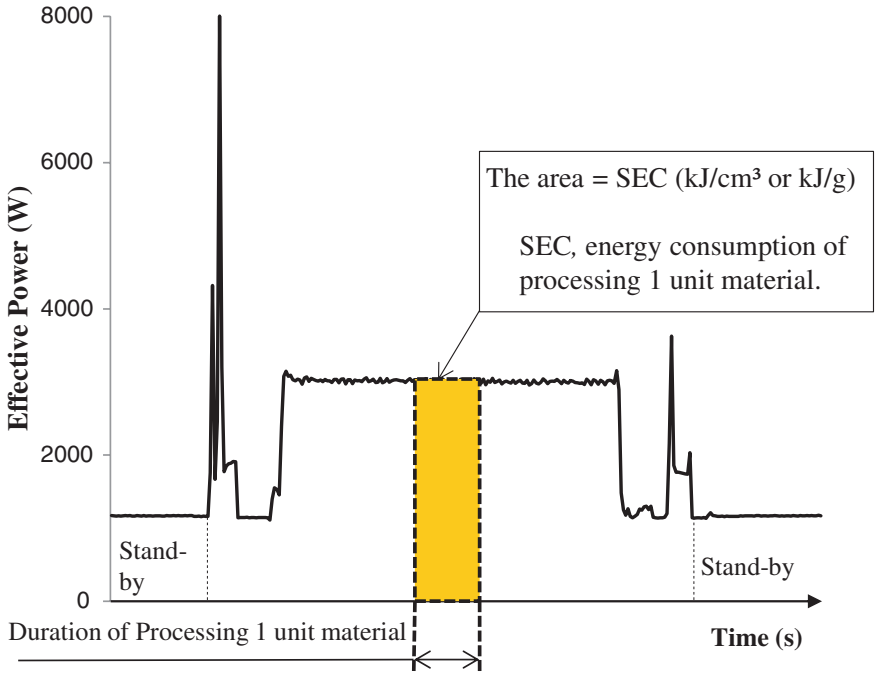

Fig. 3.2 Illustration of specific energy consumption (SEC)

both processing load and base load. It can also be transferable and comparable among different machine tools and manufacturing processes (Kara and Li 2011). Nevertheless, the unit of SEC varies depending on the feature of the processes. For example, turning is a material removal processes which is configured by volumetric parameters. Thus, SEC for turning process would be the total energy consumption of a lathe to remove a unit volume of material. For the case of injection molding, plastics are firstly melted in a heated chamber and then solidified in a mold, where the processed material is normally measured by mass. Hence, SEC for an injection molding process would be the total energy consumption of the machine tool to inject a unit mass of material. It should also be noted that the unit of SEC can be easily converted from per volume to mass by multiplying the material density, or vice versa. Therefore, the modelling objective can be interpreted as characterizing the relationship between process parameters and specific energy consumptions.

3.1.2 Stage I: Methodology of Design of Experiments (DoE)

Stage I can be considered as a sequential learning procedure to investigate the effects of process parameters on energy consumption, which leads to full scale

experimentation for regression models. Two objectives need to be fulfilled in this stage: one is to eliminate insignificant factors impacting energy consumptions, i.e. factor-screening; and, second is to generate a complete schedule of experiments for stage II.

The purpose of the first objective is to screen out unimportant factors whilst identifying important ones for further investigation. For a unit process, there are numerous factors involved such as tool geometries, workpiece material, cutting parameters, cooling fluid, working environment, etc. Some of these variables have an obvious impact on unit process energy consumption, while some factors are uncontrollable, insignificant or negligible. Thus, all the factors need to be listed and classified into different categories.

According to (Montgomery 2009), factors involved in a process or system can be classified as either potential design factors or nuisance factors. Further classification is suggested, such as: design factors; held-constant factors; allowed-to-vary factors; controllable and uncontrollable nuisance factors; and, noise factors. The key criterion used for classification depends on whether the factor is of interest in relation to current experiments. It is also unnecessary to utilize all the aforementioned sub-groups. Hence, a modified classification is proposed specifically for this research:

- *Design factors*: the factors identified by existing knowledge or tested by factor screening who have significant impacts on specific energy consumption of a unit process;
- *Screening factors*: the factors that may have effects on unit process energy consumption and cannot be identified directly without statistical analysis prior to the model development.
- *Held-constant factors:* the factors that have insignificant effects on unit process energy consumption according to the results of factor-screening, which will be held at one particular level for the model development.
- *Nuisance factors:* the factors that are identified as insignificant by existing knowledge or uncontrollable during experiments; such as, the unit-to-unit variability of workpiece, humidity of the working environment, etc.

The definition of SEC offers hints as to determine whether a process parameter is a design factor prior to factor-screening. Since energy consumption is an integration of instantaneous power over a period of time (see Eq. 2.3), the duration for processing a unit material should have a direct impact on the SEC. Multiple literature has shown evidence that machine tools consume more power for base load than variable loads, as discussed in Chap. 2. It is reasonable to believe that the factors in relation to the duration of process are significant factors; because, they determine the amount of base load accumulated during processing of unit material. In other words, a factor which has direct or indirect impact on process speed is considered as a design factor in this research; for instance, cutting speed, feed rate, cycle time, etc.

The other potential design factors also need to be considered with factor-screening procedures. There are different statistical methods available for

factor-screening, such as one-factor-at-a-time, factorial experiment designs, fractional factorial experiment designs, Taguchi methods, and Plackett-Burman designs (Montgomery 2009). One-Factor-at-a-Time (OFAT), as its name suggests, is to vary one factor at a time until all factors have been varied (Daniel 1973). Factorial experiment is that in which each complete replicate of the experiment involves all possible combinations of factor levels. The other methods use different orthogonal matrices and arrays to select a subset of complete factorial experiments. Although current researches favor the factorial experiment design due to its strengths of accessing interactions, OFAT can still remain effective in certain scenarios. (Qu and Wu 2005) stated the attractive features of OFAT, as "*run size economy, fewer level changes and providing protection against the risk of premature termination of experiments*". More importantly, OFAT offers a sequential learning process, which provides information for experimenters after each run. In that sense, the main effect of a factor can be accessed efficiently, and can promptly be identified as a design factor. Therefore, OFAT is selected for factor-screening procedure in this research.

Since the time-related factors have been pre-determined as design factors, the screening factors may have effects only on instantaneous power. The screening procedure starts with a baseline where all the factors are at their default setting, whereby each screening factor is varied over its range with all other factors held at baseline. The instantaneous power for both baseline run and varied run needs to be recorded for an adequate period. The two groups of data are then performed with a *t*-test to assess the difference in means. As the variances are unknown and not necessarily equal, the test statistic and the degrees of freedom should be calculated using Eqs. 3.1 and 3.2 (Montgomery 2009).

$$T_0^* = \frac{\overline{X_1} - \overline{X_2} - \Delta_0}{\sqrt{\frac{S_1^2}{n_1} + \frac{S_2^2}{n_2}}} \tag{3.1}$$

$$DF = \frac{\left(\frac{S_1^2}{n_1} + \frac{S_2^2}{n_2}\right)^2}{\frac{\left(S_1^2/n_1\right)^2}{n_1 - 1} + \frac{\left(S_2^2/n_2\right)^2}{n_2 - 1}} \tag{3.2}$$

where

T_0^* is the test statistic;
DF is the degrees of freedom, which should be rounded down to the nearest integer;
$\bar{X}_1, \bar{X}_2$ are the means of two group data;
n_1, n_2 are the number of data;
S_1, S_2 are the standard deviations of two group data; and,
Δ_0 is the test of interest, in this case, it should equal to 0.

The statistical chart of t distribution can be used to determine the P-value. If the P-value is greater than 0.05, the statistical analysis would suggest that the main effects of the tested factor are insignificant, thus the factor will be grouped as a held-constant factor for further steps. Otherwise, the factor will be considered as a design factor, and included for model development.

After factor-screening, all the design factors are determined for model development. However, the interaction among design factors may affect the reliability of derived models. Hence, OFAT will no longer be suitable for modelling purpose. As mentioned before, factorial experiments are favored by many researchers for assessing the interactions between factors, but the typical 2-level factorial experiment design (2^k design) has its own drawbacks. It initially assumes that the regression between the factors and model response is almost linear. Therefore, a more complicated approach, Response Surface Methodology (RSM), is then introduced.

Response Surface Methodology, or RSM, is a collection of mathematical and statistical techniques useful for modelling and analysis in applications where a response of interest is influenced by several variables; and, the original objective is to optimize this response (Montgomery 2009). RSM is also a sequential procedure. If the response is well modelled by a linear function of the independent variables, the approximating function is the first-order model (Eq. 3.3).

$$Y = \beta_0 + \beta_1 x_1 + \beta_2 x_2 + \cdots + \beta_k x_k + \epsilon \tag{3.3}$$

If there is curvature in the system, a polynomial of higher degree must be used, such as the second-order model (Eq. 3.4).

$$Y = \beta_0 + \sum_{i=1}^{k} \beta_i x_i + \sum_{i=1}^{k} \beta_{ii} x_i^2 + \sum_{i<j} \sum \beta_{ij} x_i x_j + \epsilon \tag{3.4}$$

In theory, the RSM can provide the most reliable empirical models in this research. But the necessity of second-order model remains uncertain at this stage. Similar to factor-screening, there are multiple methods for experimental designs of RSM, such as full 3^k factorial design, Box-Behnken design, and central composite design (NIST 2010). The first two methods are excluded in this research due to the disadvantage of run size. Central Composite Design (CCD), however, is a favorable option of many engineering projects as well as this research. It contains an embedded factorial or fractional factorial design with center points which allow estimation of curvature (NIST 2010). There are three types of CCD: Circumscribed Central Composite (CCC), Inscribed Central Composite (CCI), and Face Centered Composite (CCF). The difference among those three specific methods is illustrated in Fig. 3.3.

The pre-defined lower and upper levels of each factor are noted as start points. The additional levels generated by CCD are the center points shown as red dots in Fig. 3.3. It clearly visualizes the center points derived by CCC exceed the range of the start points, which may result in infeasible runs for a constraint system. On the contrary, CCI can be seen as a scaled down CCC. It causes difficulties in selecting starting points whilst using center points to test the system limits. Alternatively,

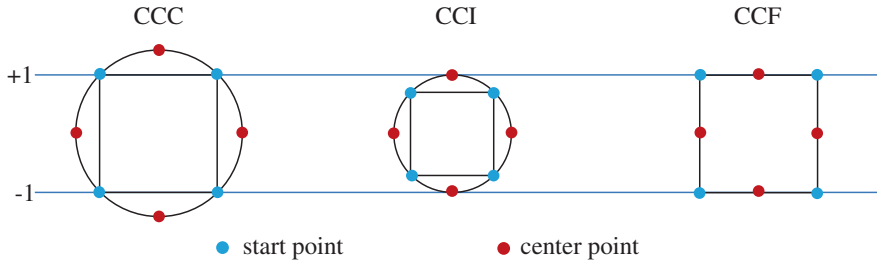

Fig. 3.3 Comparison of circumscribed, inscribed and face centered composite design for response surface methodology

CCF only requires the maximum range of a factor as starting points, and generates the center points as the midpoints between the maximum and minimum value, the method of which is considered as the best choice for this research.

The statistics package, MiniTab® Version 15, is used to generate the schedule of experiments. It offers a design of experiment module with the function of RSM and CCF. In this research, trial runs are required to determine the range of each design factor. Experts' opinion can be also helpful for this case. Once the ranges of all design factors are determined, the upper and lower levels of each factor can be input into MiniTab®. In order to avoid any human induced trend, the randomization function needs to be enabled when generating the experiment schedule.

In short, there are three key steps in stage I: firstly, all the involved factors are classified into different groups; secondly, a factor-screening procedure is conducted for uncertain factors by using one-factor-at-a-time method; then, response surface methodology and face centered composite design is used to generate a full schedule of experiments with the assists of MiniTab®.

3.1.3 Stage II: Energy Metering and Monitoring System

Collecting accurate and adequate data from the experiments is essential for this research. Kara et al. (2011) pointed out the importance of energy metering and monitoring in manufacturing systems in their keynote paper. They have provided not only the guidelines for establishing an energy metering and monitoring system, but also discussed the technical aspects from factory level to unit process level. As the keynote suggested, a clear metering task needs to be defined in the first place. Then the measurands, resolution and communication interface can be selected accordingly.

The energy consumption behavior of a machine tool is highly dynamic in most cases. For example, current motor technologies offer rapid acceleration and deceleration in order to achieve operational readiness as quick as possible. Consequently, instantaneous power peak occurs during these processes. This behavior desires a high resolution of energy metering and monitoring system to

capture these peaks. Similarly, the communication interface needs to be compatible with the sampling resolution and be capable of handling large amount of data on a real time basis. Effective power which is the actual energy consumed for work done is the main measurand of interest for this research. However, other measurands such as apparent power, reactive power, and power factor also provide useful information about how effectively a machine tool draws energy from the grid. In addition, the time should be recorded simultaneously. It can be achieved by having constant sampling interval, so the duration of the process can be calculated by counting the number of recorded samples. As the experiments are conducted temporarily, a portable solution is preferred. Therefore, the strategies of energy metering and monitoring for this research is proposed as following:

- Output resolution should be no larger than 0.1 s;
- Constant sampling interval is an essential feature;
- Effective power, apparent power, reactive power and power factor needs to be recorded;
- Communication 1interface must be compatible with data sampling resolution;
- The monitoring system can process large amount of data on a real time basis; and,
- The system needs to be portable and easy-to-install.

Based on above strategies, an energy metering and monitoring system has been developed. It consists of a hardware subsystem and a monitoring platform. Since the proposed model should consider the total energy consumption of a machine tool, the metering point should be located at the main bus of the machine tool. The structure of the energy metering and monitoring system is illustrated in Fig. 3.4.

The tasks of the hardware subsystem are to acquire power information from a machine tool and to transfer the information to the monitoring platform. With the National Instruments® (NI) system, two modules are applied to measure voltage and current separately. The NI 9225 module (see in Fig. 3.4b) is selected to measure the voltage, which provides a full measurement range of 300 Vrms for 3 channel high voltage measurement applications with high-speed simultaneous sampling at 50 kS/s per channel. The voltage cables are directly mounted at the main bus of a machine tool. The NI 9229 module (see in Fig. 3.4c) is chosen for measuring current. It is a 4-channel, 24-bit C Series analogue input module whose range is ±60V. It requires additional equipment to transform the current measurands into voltage signals, where FLUKE® i200s current clamps (see in Fig. 3.4a) are used. The i200s current clamps have a dual range of 20 and 200 A with voltage output as 10 or 100 mV/Amp respectively. The two NI modules, 9225 and 9229, are plugged into a NI data acquisition chassis, cDAQ-9172 (see in Fig. 3.4d). It can hold up to eight C series I/O modules, which have a high speed connection to a laptop PC via a USB cable.

The monitoring platform is developed under NI LabVIEW environment. It is a sophisticated programming environment with hundreds of built-in libraries. It also offers high integration with NI data acquisition hardware (National Instruments 2010). The “electrical power calculation” program was developed with NI engineers. The block diagram is a graphic programming environment as shown

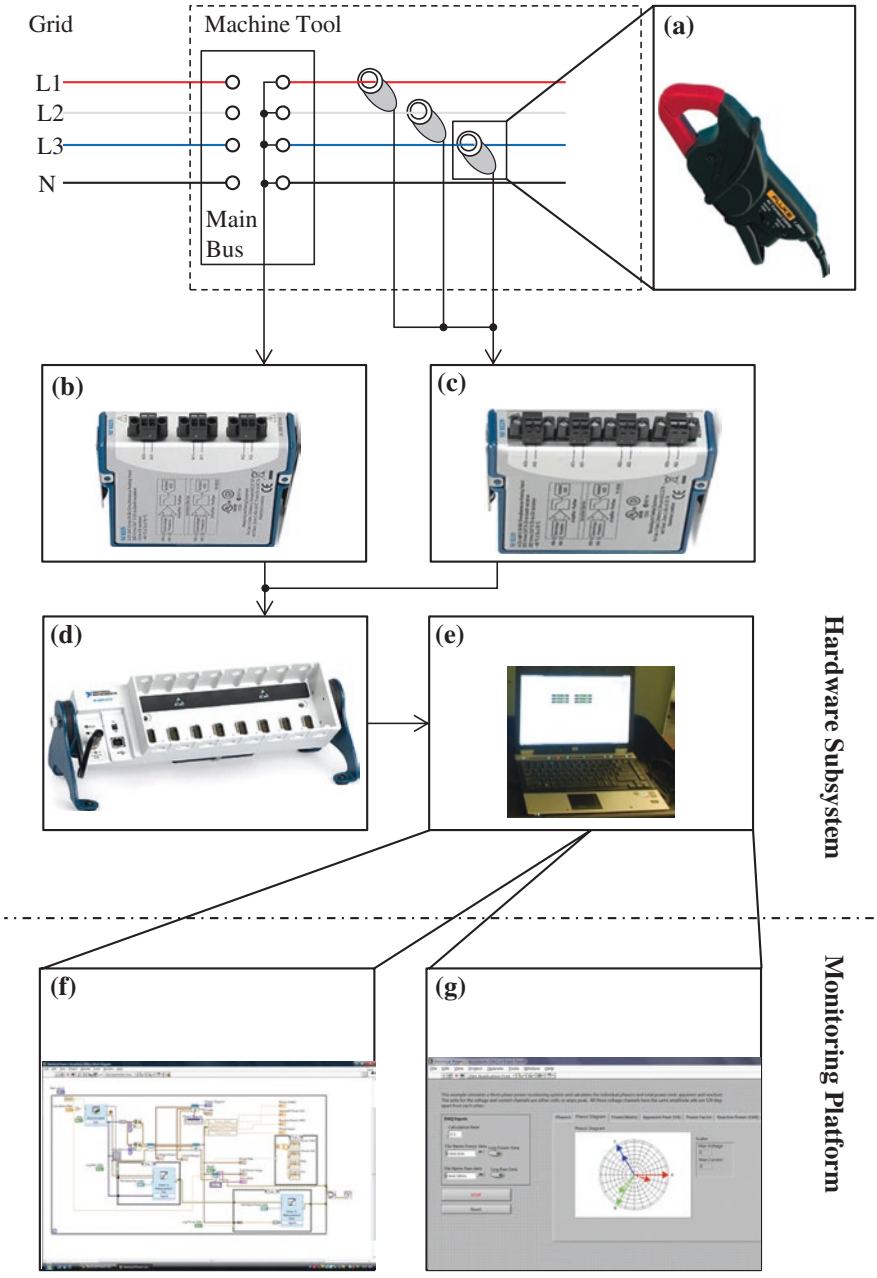

Fig. 3.4 Structure of energy metering and monitoring system for unit processes. **a** Current clamp FLUKE® i200s. **b** Voltage Module NI 9225. **c** Current Module NI 9229. **d** NI cDAQ-9172. **e** Laptop PC. **f** Block diagram of LabVIEW Program. **g** Front panel of LabVIEW Program

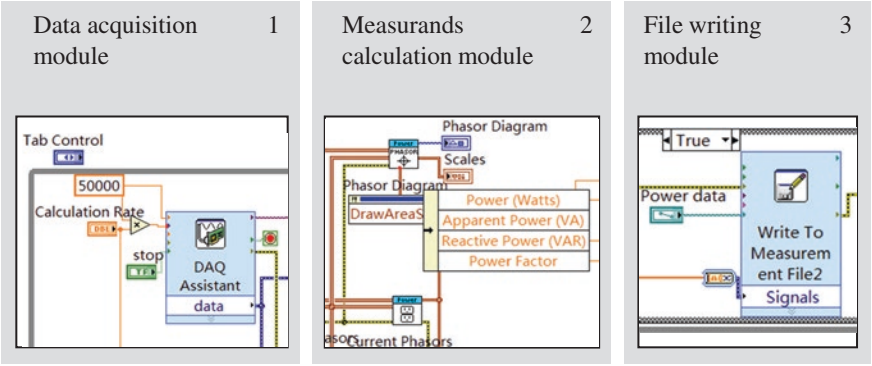

Fig. 3.5 Structure of LabVIEW program "electrical power calculation"

in Fig. 3.4f. This program consists of three modules: the data-acquisition module reads and processes the data via NI cDaq-9172 chassis; the calculation module uses built-in subroutines called visual instruments (VIs) to calculate desired measurands, such as effective power, apparent power, reactive power and power factor; and, the file writing module saves the calculated results in a LabVIEW data file (.lvm), as shown in Fig. 3.5.

The user interface, or front panel, allows experimenters to start or stop the measurements, name and locate saved data files, as well as monitor measurements in real time, as shown in Fig. 3.4g. This system can record energy information with a constant sampling interval down to 0.1 s. Therefore, all the proposed energy metering and monitoring strategies have been achieved.

3.1.4 Stage III: Statistical Analysis and Regression Methods

The objective of this stage is to statistically express the relationship between the process variables and observed responses. In order to achieve the reliability of the empirical models, the statistical techniques should be coupled with "*good engineering or process knowledge and common sense*" (Montgomery 2009).

As specific energy consumption (SEC) is not directly measurable, the proposed responses need to be computed from other measurable values. Firstly, the total energy consumption during the processing period is integrated from the recorded data. Then, the total volume or mass of processed material is theoretically calculated or directly measured. Since the current computer numerical control (CNC) machine tools have achieved a high level of precision, the volume of processed material can be assumed equal to what each process program commands. For the case of injection molding, the mass of injected material varies depending on the material type, melting temperature, viscosity of melted material, etc. Thus, all

Fig. 3.6 Photograph of Wedderburn Precisa® precision weighing scales

the injected parts need to be weighted by a Wedderburn Precisa® precision weighing scale, which offers accuracy ±0.005 g (see in Fig. 3.6). Finally, the SEC can be calculated by dividing total energy consumption by the volume or mass of processed material. The detailed calculation procedures are presented with the specific cases in Chap. 4.

Although the experiments are designed with RSM, the higher-degree polynomial model may not be favored as it normally cannot be transferred or compared with other machine tools or processes. In order to keep the model generic and transferable, the main effect, which is the effect of a single factor, is focused in this work (Montgomery et al. 2007). In addition, the correlation of factors can also be considered as a single factor separately. For example, Material Removal Rate (MRR) is an important parameter for machining processes suggested by Kalpakjian and Schmid (2005). It is the product of cutting speed, feed rate and depth of cut for turning processes, which can be considered as a single factor for regression. Since the relationship between process variables and response (SEC) can be either linear or non-linear, the curve-estimation is the most suitable analysis to estimate the main effects of each factor. A statistical package, SPSS®, is used here, which provides 11 different models for curve-estimation, such as quadratic, logarithmic, exponential, inverse, logistic, etc. SPSS® also provides R-square values (R^2) for each combination of model type and tested factor. It is referred to the proportion of variability in the observed response that is explained by the regression model. The large R^2 (close to 1) indicates the regression model is well fitted with observed trends. The manual calculation of R^2 is shown as Eq. 3.5.

$$R^2 = 1 - \frac{SS_E}{SS_T} \tag{3.5}$$

where, SS_E refers to the error sum of squares (or unexplained variability); and, SS_T refers to the total sum of squares (or total variability). Each of these can also be calculated according to Eqs. 3.6 and 3.7.

$$SS_E = \sum_{i=1}^{n} \left(y_i - \widehat{y}_i\right)^2 = \sum_{i=1}^{n} e_i^2 \tag{3.6}$$

$$SS_T = \sum_{i=1}^{n} (y_i - \overline{y})^2 \tag{3.7}$$

where, y_i is the observed response; $\widehat{y}_i$ is the predictor value; e_i is the error in the fit of the model to the ith observation, or called residual; and, $\overline{y}$ is the observed mean of response. If the R^2 is larger than 0.9, the model can be concluded as sufficient, as more than 90 % of observed data can be explained with the model.

In addition, the residuals of a good model should be randomly distributed or normal. Thus, the residuals need to be plotted against the predictor values. If the distribution is not random or normal, it suggests that other factors have certain impacts on the system which need to be statistically included in the model.

A more accurate model can be derived from multiple-linear regression. As any regression model can be rewritten in a linear form regardless of the shape of the observed surface, the derived models from curve estimation can be converted into a linear format (Montgomery 2009). For instance, if the factor x_1 fits the inverse model for predicting response Y as in Eq. 3.8; the reciprocal of x_1 can be noted as a new factor x_1'; whereby, the inverse model can be also written as the linear one shown in Eq. 3.9.

$$Y = c_0 + \frac{c_1}{x_1} \tag{3.8}$$

Let $x_1' = \frac{1}{x_1}$, then:

$$Y = c_0 + c_1 \cdot x_1' \tag{3.9}$$

By using the stepwise function of linear regression in SPSS®, all the significant factors are introduced to the model sequentially according to the significance of their impacts. However, this method will certainly increase the complexity of the model, and affect the consistency among different machines and processes. Thus, the model derived from curve-estimation can be accepted as a generic model, whereas the results of multiple-linear regression explore the detailed interrelationship within the system.

3.1.5 Stage IV: Validation Methods

Besides the statistical evidence obtained during model developments, additional runs should be conducted to further validate the models. The selection of process parameters for validation run should differ from the ones used for model development. The difference between predicted SEC and measured SEC are calculated in percentage as shown in Eq. 3.10.

$$\text{Difference} = \frac{\left|y_i - \widehat{y_i}\right|}{y_i} \times 100\,\% \tag{3.10}$$

This research aims to achieve the discrepancy between prediction and measurement less than 10 %. This index can be also used to compare the accuracy between a simple model and relatively complex model derived from curve-estimation and multiple-linear regression respectively. It would suggest whether there is a significant benefit to introduce multiple factors in a model for predicting energy consumption.

3.1.6 Summary of Model Development

As discussed above, different techniques and devices are involved in developing energy consumption models for unit processes. The experimenters need to follow a logic procedure as displayed in a flow chart, Fig. 3.7.

3.2 Methodology of Eco-efficiency Evaluation for Unit Process

3.2.1 Definition of Eco-efficiency Evaluation for Unit Process

Eco-efficiency is originally defined by the World Business Council for Sustainable Development (WBCSD). In short, the eco-efficiency is to "*create more value with less impact*" (WBCSD 2000).

A unit process can be considered as a service which generates value for the products as well as consuming energy and other resources. As shown in Fig. 3.8, it can be constructed as three layers; on the upper layer, unit process transforms raw materials into output products by changing material attributes, such as geometric features, surface roughness, hardness and etc.; on the bottom layer, it consumes energy and other auxiliary resources inducing environmental impacts; and in the center, process parameters define the actual performance of the process.

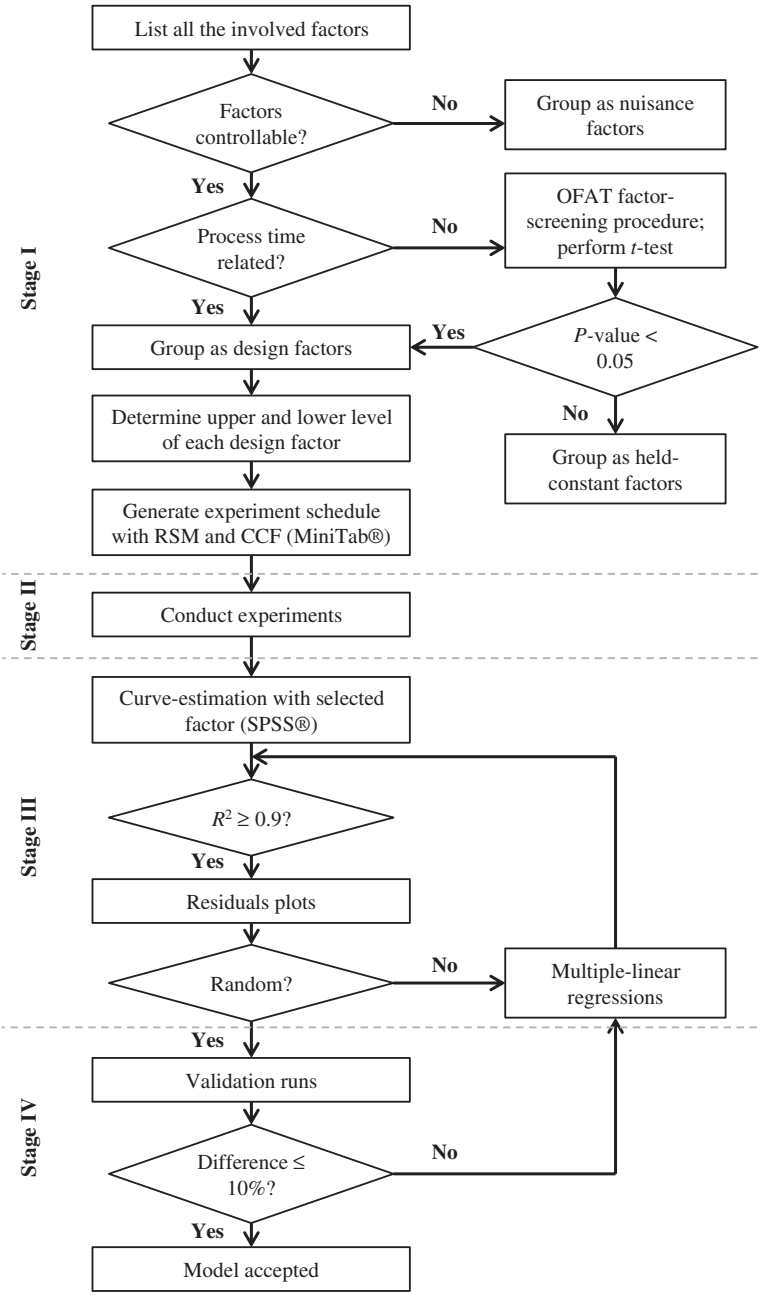

Fig. 3.7 Flowchart of developing unit process energy consumption models

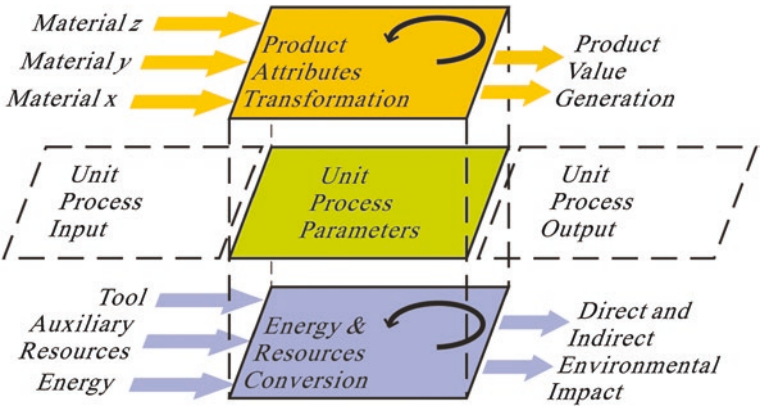

Fig. 3.8 Layers of the unit process eco-efficiency (Li et al. 2012)

According to the original definition, the eco-efficiency of a unit process can be adapted as to generate more product value but induce less environmental impact. It refers to the right side in Fig. 3.8. However, most unit processes are dynamic systems. Varying process parameters will result in different outputs and different environmental impacts. Thus, improving eco-efficiency requires linking the process parameters with the value of the process and its environmental impacts. The eco-efficiency of unit process can therefore be written in the form of Eq. 3.11, which is a function of process parameters. The method for assessing process value and the environmental impacts are discussed in the following sections.

$$\begin{aligned} Eco{-}efficiency &= \frac{Process\ Value}{Process\ Environemental\ Impacts} \\ &= f(Process\ Parameters) \end{aligned} \tag{3.11}$$

3.2.2 The Value of a Unit Process

Economic indicators are a common reference when discussing value or cost issues. However, those indicators are found inapplicable for the case of unit process due to two main reasons. One is that the economic value is always product not process dependent. From a unit process point of view, there is no difference between turning aluminum or steel, besides the achieved shape and dimensional accuracy. The other reason is that the changing market value of materials, products and other resources would directly influence the economic value of a unit process. This would lead to a biased impression of the unit process efficiency; for instance, the unit process may remain unchanged but the efficiency may seem increased due to an increased market value. Therefore, those economic indicators cannot provide a true objective measure for the value of unit process.

Alternatively, the physical indicators can be objective, whilst being meaningful for the value of the process. For example, the steel industry produces tons of steel every day; the value of the processes is depending on the amount of steel produced, which is measured by weight. The same concept should apply to unit manufacturing process. For the case of material removal processes, the amount of material removed from the raw workpiece is actually the main value of the process.

However, the value of unit process is not just the mass or volume; the other physical dimensions need to be considered such as dimensional accuracy, surface roughness, etc. These physical measures regarding the part quality describe how well the customer requirement has been achieved by the unit process. Taking an injection molding process as an example, the completeness of mold shape, flash or shrinkage rate determines whether the part is acceptable or not; thus, these physical measurements directly affect the value of the process. However, it is also insufficient to consider every quality measurements for the evaluation of eco-efficiency, since they are not comparative to each other. Alternatively, the primary objective of the unit process can be considered and the associated physical measurements can be selected according to the process value. A number of selected manufacturing processes are discussed below:

- Turning and milling (roughing and general purpose): they are conventional material removal processes, whose primary objective is to remove material from raw workpiece; thus, the volumetric unit is representative for the process value.
- Grinding: it is an abrasive machining process, which is normally considered as a surface finishing process; thus, the achieved surface roughness is representative for the process value. This can also be applied to the finishing turning and milling processes.
- Injection molding: it is a material addition process, whose primary objective is to form and shape plastics; thus, the weight of injected part is representative for the process value.

The selected manufacturing processes cover a range of processes from material removal to material addition. Other manufacturing processes can refer to the relevant selected type of process. For instance, casting also belongs to the category of material addition which can be related to injection molding. Other characteristics of these processes are initially neglected such as typical surface finish, porosity, shape complexity, dimensional accuracy, due to the lack of precise measurement. Ideally, those characteristics should be included and a matrix of process characteristics can be developed to evaluate the value of process in the future.

3.2.3 The Associated Environmental Impacts

Environmental impacts can be generally summarized into the following three categories according to the United Nations Environmental Program—Society for Environmental Toxicology and Chemistry (UNFP-SETAC 2005):

- Environmental interventions such as emissions, extractions, and land use;
- Midpoint impacts through main environmental mechanisms such as global warming, acidification, and toxicity; and,
- Endpoints of relevant items as related ultimately to human health (e.g. morbidity and mortality), environmental quality as an independent value of the life support system (e.g. biodiversity) and to human affluence (as reflected in production functions, land scape and cultural heritage).

For the case of manufacturing processes, the environmental impacts are mainly induced by energy consumption as well as the usage of tool and cutting fluid. As discussed in Sect. 2.2.2, the embodied energy during material production should excluded for the eco-efficiency analysis of unit process.

Energy consumption has been believed to be a major driver for environmental impact and most current machine tools use electricity as their primary energy source. In this sense, the study of a unit process' energy efficiency benefits the evaluation of its eco-efficiency. It is important to note that energy consumption not only accounts for processing workpiece materials but should also consider the energy consumption for auxiliary components and periphery processes. For example, grinding requires dressing processes to maintain the sharpness of grinding wheels, therefore the energy consumption of dressing process needs to be included. From the environmental impact point of view, the energy induced impacts for manufacturing processes are sensitive to the location, since electricity is generated from both renewable and non-renewable resources and the ingoing mix is location specific. For example, the environmental impact of turning 1 cm^3 metal in Australia is different from turning the same amount in European countries as the carbon intensity of electricity generation varies from region to region. Thus, typical locations were selected for the comparison, such as Australia, USA, European Union and Brazil. The environmental impact of consuming 1 kJ of electricity can be easily calculated by using Life Cycle Inventory (LCI) database, such as Ecoinvent Version 2.2.

The direct environmental impact of tool usage is believed to be limited due to their relatively long life. Dahmus and Gutowski have suggested that the production of carbide tools requires energy intensive materials and processes, such as physical vapor deposition or chemical vapor deposition etc. However, environmental cost of these tools and their maintenance is often amortized over numerous products and it can thus be ignored (Dahmus and Gutowski 2004). This statement was based on the assumption of low tool wear rate. In fact, tool selection has a significant impact on the process behavior in terms of tool wear rate, surface integrity, cutting speed and thus material removal rate. Although little environmental analysis can be found for tools (such as carbide tools, grinding wheel etc.) it is important to consider the tool selection regarding its impact on material removal rate, surface roughness as well as tool wear rate.

Furthermore, to address the environmental impact of tool usage, a screening Life Cycle Assessment (LCA) has been conducted to analyze the environmental impacts of grinding wheels (see in Sect. 5.3.2). LCA is a well-established

methodology to study the environmental performance of products throughout the entire life cycle from cradle to grave (i.e., from raw material extraction through material processing, manufacture, distribution, usage and end-of-life). According ISO 14040:2006, there are four main phases for LCA: goal and scope definition, inventory analysis, impact assessment and interpretation (ISO 2006). Firstly, LCA requires a clear definition of an overall purpose, a system boundary for study and any assumptions or limitations to be addressed. Secondly, a Life Cycle Inventory (LCI) can be calculated by mapping the flow of all inputs (e.g. energy, water, raw materials, etc.) and outputs (e.g. waste, emissions, etc.) of the defined product system. This inventory can be quantified by different means, such as literature, national statistics, commercialized database, etc. Inventory analysis is followed by impact assessment including characterization and classification. There are different impact categories used for Life Cycle Impact Assessment (LCIA) (Finnveden 2009). For example, Global Warming Potentials (GWP) is an index to measure the emission of greenhouse gases, measured in CO_2 equivalents; Abiotic Depletion Potential (ADP) is an indicator of abiotic resource consumption, measured in antimony equivalents; whereas, Eco indicator 99 encompasses most of the environmental impact categories represented by a single score. Several software packages are available for LCIA, such as GaBi®, SimaPro®, Umberto®, etc. In this research, SimaPro® with Ecoinvent® Version 2.2 was used at this phase; and, CO_2 Fossil Fuel Emissions (CO_2 Fossil) was selected as an exemplary indicator to demonstrate the environmental impact of unit manufacturing processes. Finally, significant issues need to be identified based on the results of LCIA. Further evaluation is necessary for considering the completeness, sensitivity and consistency of the study whereby conclusions and recommendations are generated.

Cutting fluids normally consist of oil, chemicals and a large amount of water. Applying coolant does not only require electricity for generating the coolant flow but the composition of coolant itself has an important environmental impact. The environmental analysis of coolant forms a research topic itself and a systematic summary regarding this topic remains absent. Byrne et al. (2003) have briefly summarized the related environmental impacts and health issues of cooling fluid. In general, the chemical substances are hazardous such as those containing hydrocarbons, sulphur, phosphorus, chlorine, surfactants/emulsifiers and biocides. The pre-treatment and treatment of cutting fluids cannot eliminate the potential environmental damage; for instance, fluid splashing, spillage and improper disposal can contaminate lakes, rivers and groundwater sources. In addition, human health is related to the contact and exposure to cutting fluids through dermal and inhalation pathways. However, little quantitative analysis of those environmental impacts is available at the moment. Nevertheless, a fair amount of coolant is lost throughout every day activities. Dahmus and Gutowski (2004) estimated the annual consumption of concentrated metalworking fluid use per machine tool is 53 gallons, excluding the use of water. Therefore, an assumption of coolant consumption is made for the evaluation of process eco-efficiency. The quality of the evaluation can be certainly improved by enhancing the study of environmental impacts of coolant and the behaviors of coolant loss.

In order to reduce the environmental impacts of cutting fluids and lubrication, improvement efforts have been concentrated on: elimination of hazardous chemicals; development of alternative bio coolant; prolonging tool and lubricant life; recovery and reuse of lubricants; dry machining; and, Minimal Quantity Lubrication (MQL) (Bay et al. 2010). The benefits of applying these environmentally benign coolant technologies can be evaluated via the proposed eco-efficiency evaluation of unit process in the future.

Overall, the total energy and resource consumption of a unit process can be classified and characterized into different environmental impact categories. Based on current available data, CO_2 Fossil was selected to indicate the environmental impacts of manufacturing processes. Other impact categories (GWP, ADP, Eco indicator-99, etc.) can be further calculated once the data quality of cutting tools and coolants is improved.

3.2.4 The Interrelationship Within a Unit Process

Owing to a dynamic nature, process parameters play a central role linking both process value and environmental impacts, as shown in Fig. 3.8. The amount of process output has a direct link with the process parameters, which determines how much volume or weight of material can be processed during a unit time. The process parameters have a more significant influence on other quality measurements. The studies about surface integrity and process precision have generated a number of models to characterize the relationship between process parameters and quality measurements (Jawahir et al. 2011).

Section 3.1 has proposed a methodology to derive SEC models for unit process. The results of these SEC models can be directly used for evaluating the associated environmental impacts. Thus, there exists a platform to encompass all the three layers including process value, environmental impact and process parameters; and, it is possible to quantitatively describe their interrelationships.

Based on above analysis, a methodology for evaluating eco-efficiency of unit process is proposed as Fig. 3.9. Due to the lack of information about the environmental analysis of every energy and resource involved, the application requires assumptions and simplifications.

3.3 Summary

This chapter has provided methodologies for the evaluation of energy and eco-efficiency of unit processes. According to the review in Chap. 2, the specific energy consumption (SEC) is the appropriate indicator for evaluating energy efficiency of unit process. The proposed methodology uses empirical modelling to derive

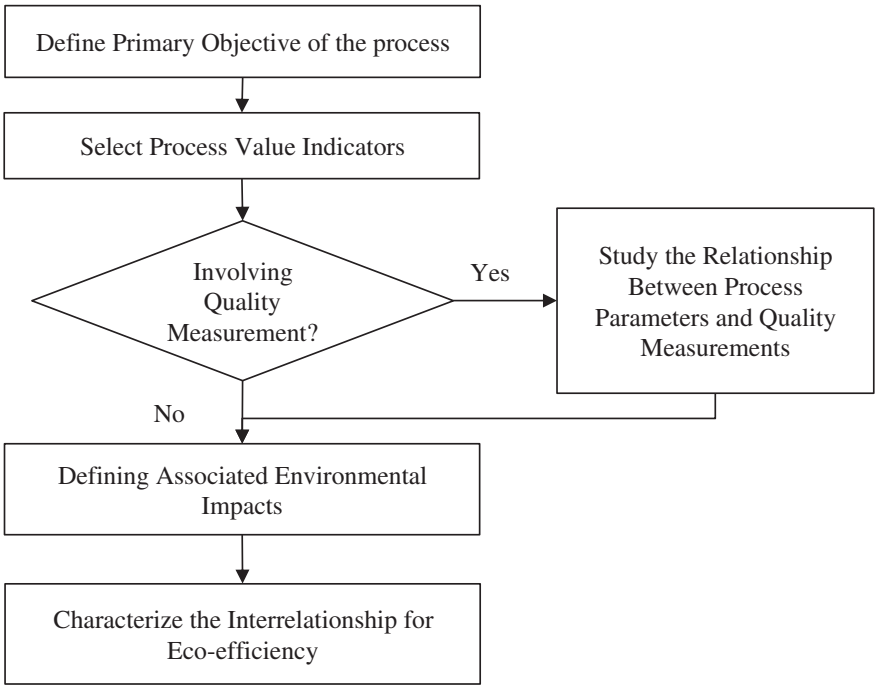

Fig. 3.9 Flow chart of evaluating eco-efficiency of unit process

relationships between specific energy consumption and process parameters. It involves a sequential procedure and a series of statistical analyses.

In addition to energy efficiency evaluation, eco-efficiency attempts to provide a holistic view of the unit process, which considers the process value and the associated environmental impacts of the process. Instead of using economic indicators, the process value can be measured by the physical indicators according to the nature of the process. Quality measurements are also recommended to be added into the valuation of unit process. Besides environmental impact due to electricity consumption, other resource and energy usage needs to be taken into account for environmental impact analysis. On top of these analyses, an integrated result should be delivered in which process parameters play a center role to link the process value with environmental impact. Therefore, the dynamic nature of unit process eco-efficiency can be described with this integrated model.

References

Bay N, Azushima A, Groche P, Ishibashi I, Merklein M, Morishita, M, Nakamura T, Schimid S, Yoshida M (2010) Environmentally benign tribo-systems for metal forming. CIRP Annals—Manuf Technol 59(2):760–780

Byrne G, Dornfeld D, Denkena B (2003) Advanced cutting technology. CIRP Ann—Manuf Technol 52(2):483–507

Dahmus JB, Gutowski T (2004) An environmental analysis of machining. American Society of Mechanical Engineers, Manufacturing Engineering Division, MED, Anaheim, CA

Daniel C (1973) One-at-a-time plans. J Am Statist Assoc 68(342):353–360

Finnveden Gl, Hauschild MZ, Ekvall T, Guinée J, Heijuns R, Hellweg S, Kohler A, Pennington D, Suh S (2009) Recent developments in life cycle assessment. J Environ Manage 91(1):1–21

ISO 14040:2006 (2006) Environmental management—life cycle assessment—principles and framework

Jawahir IS, Brinksmeier E, M'Saoubi R, Aspinwall DK, Outeiro JC, Meyer D, Umbrello D, Jayal AD (2011) Surface integrity in material removal processes: recent advances. CIRP Ann—Manuf Techonol 60(2):603–626

Kalpakjian S, Schmid SR (2005) Manufacturing engineering and technology, 5th edn. Prentice Hall, Upper Saddle River

Kara S, Li W (2011) Unit process energy consumption models for material removal processes. CIRP Ann—Manuf Technol 60(1):37–40

Kara S, Bogdanski G, Li W (2011) Electricity metering and monitoring in manufacturing systems. In: 18th CIRP international conference on life cycle engineering, Braunschweig, Germany

Li W, Winter M, Kara S, Herrmann C (2012) Eco-efficiency of manufacturing processes: a grinding case. CIRP Ann—Manuf Technol 61(1):59–62

Montgomery DC (2009) Design and analysis of experiments, 7th edn. Wiley, New York

Montgomery DC, Runger GC, Hubele NF (2007) Engineering statistics, 4th edn. Wiley, New York

National Instruments (2010) Getting started with LabVIEW, online publication. http://digital.ni.com/manuals.nsf/websearch/EC6EF8DE9CB98742862576F7006B0E1E. Last visited 3 Jan 2012

NIST/SEMATECH (2010) e-handbook of statistical methods, online publication. http://www.itl.nist.gov/div898/handbook/. Last visited 3 Jan 2012

Qu X, Wu CFJ (2005) One-factor-at-a-time designs of resolution V. J Statsit Plan Infer 131(2):407–416

UNEP/SETAC (2005) Life cycle approaches-the road from analysis to practice, online publication: http://www.unep.fr/shared/publications/. Last visit 3 Jan 2012

World Bussiness Council for Sustainable Development (WBCSD) (2000) Eco-efficiency: creating more value with less impact, Geneve

Chapter 4
Energy Efficiency Characterization of Manufacturing Processes

With the proposed methodology in Sect. 3.1, this chapter selects a wide range of manufacturing processes to characterize their energy efficiency. The presented cases range from single cutting-edge machining (e.g. turning) to multiple cutting-edges machining (e.g. milling), from geometrically defined cutting-edge machining to geometrically undefined cutting-edge machining (e.g. grinding), from metal machining to thermoplastic processes (e.g. injection molding), from conventional manufacturing processes to unconventional manufacturing processes (e.g. electrical discharge machining). For each process, a number of different machine tools are presented in order to validate the proposed methodology.

4.1 Energy Efficiency Characterization for Turning Processes

4.1.1 Background

Turning is a conventional material removal process in which the workpiece is machined whilst it is rotating. It is widely used for producing straight, conical, curved or grooved workpieces such as shafts, spindles and pins (Kalpakjian and Schmid 2005). Various materials can be machined by turning processes such as aluminum, copper, steel, titanium and so on. Currently, these processes are usually performed on Computer Numerical Control (CNC) lathes due to high process precision. A typical CNC lathe includes several different motors, control systems and other auxiliary components as illustrated in Fig. 4.1. The spindle drive motor provides various rotation speeds for the workpiece. It is normally the most powerful component whose rated power indicates the capacity of the machine tool. The axes servo motors feed the cutting tool at different speeds. As the cutting load depends on the workpiece

W. Li, *Efficiency of Manufacturing Processes*, Sustainable Production,
Life Cycle Engineering and Management, DOI 10.1007/978-3-319-17365-8_4

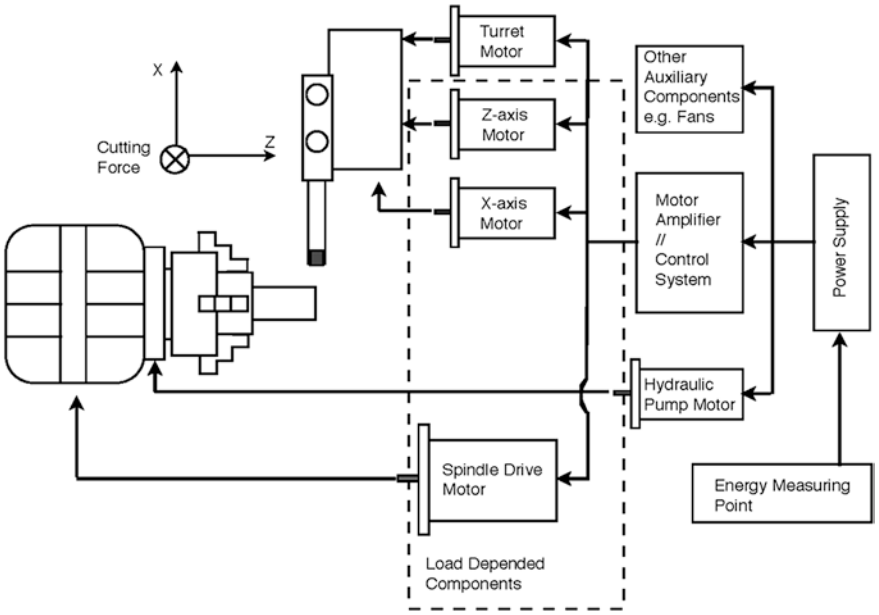

Fig. 4.1 Schematic diagram of a CNC lathe (Li and Kara 2011)

material, cutting parameters and other factors three motors are grouped as load dependent components. However, a turret servo motor is only activated while changing the cutting tool. A hydraulic pump motor provides constant clamping pressure for holding the workpiece, which requires relatively static power throughout the process. Energy consumption of other components such as amplifiers, fans and other auxiliary components remains constant and form the base load of the machine tool.

Five different CNC lathes have been selected for modelling (as displayed in Fig. 4.2) and they cover a variety of machine ages, spindle power and transmission systems. The first two lathes were located in the manufacturing laboratory of School of Mechanical and Manufacturing Engineering, the University of New South Wales whilst the other three were in Sydney City TAFE.

4.1.2 Design of Experiments

Since turning is a material removal process, in this case, specific energy consumption (SEC) refers to the total energy consumption of a CNC lathe for removing 1 cm^3 material. The objective of the experiments is to derive the relationship between SEC and process parameters. There are numerous factors that influence a cutting operation in a turning process. These can be generally classified into one of five categories:

- Tool condition: i.e. material, insert geometry, tool wear, etc.
- Workpiece material: generally referring to hardness and machinability.

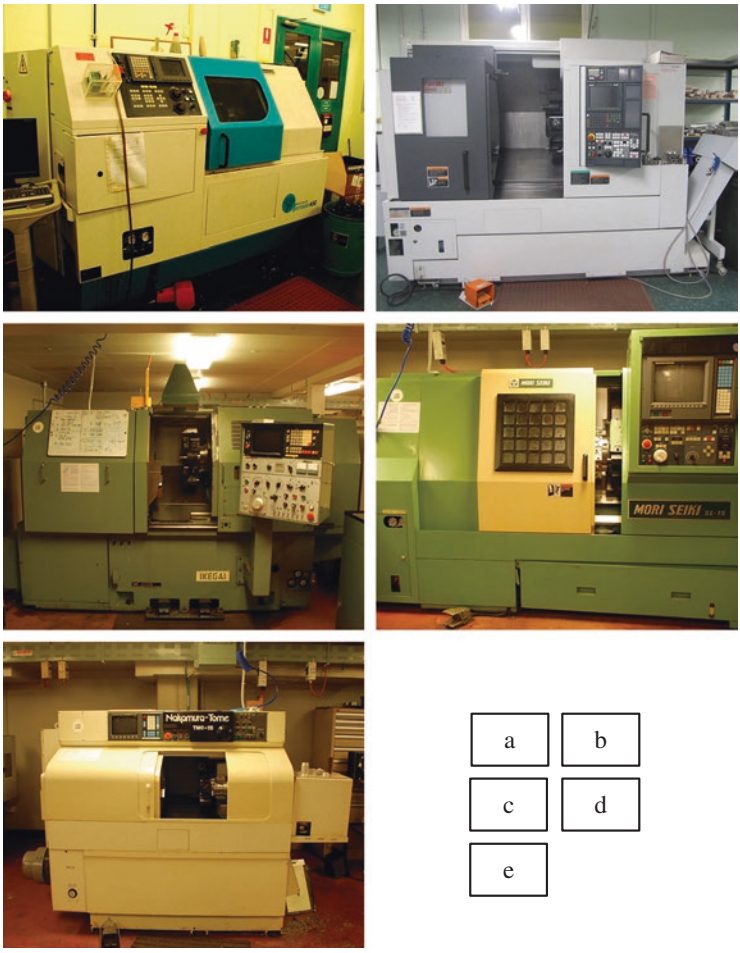

	Manufacturer & Model	Spindle No. (power)	Year
a	Colchester Tornado A50	1spindle (5.5 kW)	2000
b	Mori Seiki NL2000MC/500	2 spindles (11/3.7 kW)	2005
c	IKEGAI AX20	1 spindle	1970s
d	Mori Seiki SL-15	1spindle (11 kW)	1980s
e	Nakamura TMC-15	1 spindle (7.46 kW)	1990s

Fig. 4.2 Photograph of tested CNC lathes

- Cutting parameters: i.e. cutting speed (V), feed (f) and depth of cut (d).
- Cutting fluids: whether or not a coolant is used, type of coolant, etc.
- Operation environment: i.e. temperature, humidity, etc.

Cutting parameters determine the duration of removing 1 cm^3 material, thus they were grouped as design factors. As different workpiece materials feature different machinability, the available range of cutting parameters differs from material to material. For instance, cutting aluminum is relatively a fast process, the cutting speed of which has range from 200 to 400 m/min; while the cutting speed for machining low-carbon steel is normally under 150 m/min (Kalpakjian and Schmid 2005). Therefore, the type of workpiece material was also considered as a design factor.

Benefits of applying cutting fluid (wet machining) are to lubricate the cutting zone, to avoid workpiece damage, as well as to extend the tool life. However, the cost of coolant and the environmental concerns have driven the trend towards dry machining (Sreejith and Ngoi 2000). Several materials are recommended for dry machining, i.e. aluminum, copper, steels, etc. (Kalpakjian and Schmid 2005). From the energy consumption perspective, applying cutting fluid requires additional energy to power the coolant pump. Since power requirement of coolant pump remains constant, it can be added to the base load in the further stages. Therefore, the type of cutting fluids was considered as a held-constant factor.

As discussed in Sect. 2.1, cutting tools have significant impacts on cutting forces, which indirectly affect the loads on both servo and spindle motors. The type of cutting tool or insert is strongly dependent on workpiece material due to different machinability. Hence, the insert type was coupled with the workpiece material. According to Oxley's cutting force model, the geometric features of cutting tool first need screening. Cutting rake angle was selected for factor-screening, since different cutting force models universally suggest the significance of rake angle's impacts (Oxley 1998; Armarego and Wiriyacosol 1978; SECO® 2009).

Rake angle tests have been conducted on the Colchester Tornado A50. 50 mm diameter mild steel bars were used for testing with constant cutting speed, feed and depth of cut but various insert rake angles from $-6°$ to $6°$. 100 samples taken during the cutting process were randomly extracted from each run. Then, a t-test was performed according to the research methodology proposed in Sect. 3.1. The results of t-test are listed in Table 4.1. Since the P-value is larger than 0.05, the rake angle is an insignificant factor for the total energy consumption of the CNC lathe. The results can apply to other geometric factors of cutting tools, because their impacts are only limited at tool tip and the power requirements at tool tip only account for a small portion of the total power consumption of the machine

Table 4.1 t-test results of rake angle test on the Colchester Tornado A50

	Mean (W)	N	Standard deviation
Group 1: rake angle 6°	$\overline{X}_1 = 4349.82$	$n_1 = 100$	$S_1 = 5.01$
Group 2: rake angle −6°	$\overline{X}_2 = 4348.51$	$n_2 = 100$	$S_2 = 7.65$
$T_0^* = 1.484$	$DF = 170$		P-value = 0.141

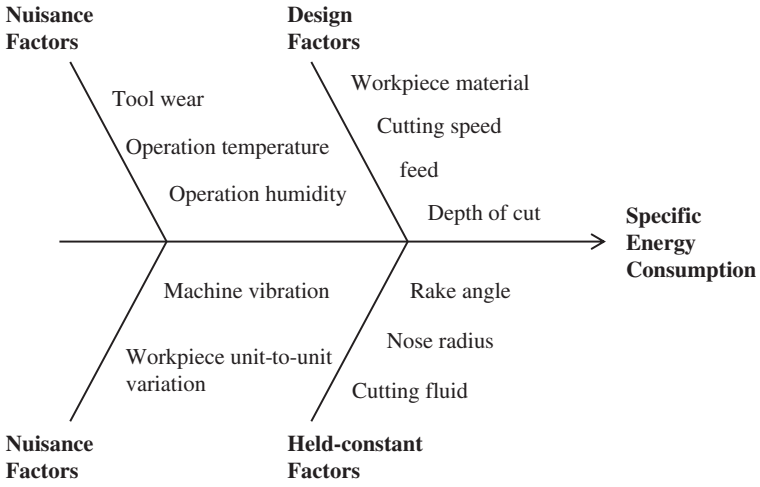

Fig. 4.3 Ishikawa diagram for tested turning processes

tool. Therefore, the geometric factors of cutting tools were assumed negligible and determined as held-constant factors for this research.

Other factors such as tool wear and operation environment were uncontrollable in this case and were grouped as nuisance factors. An Ishikawa diagram was developed to organize all the involved factors, as shown in Fig. 4.3.

Three workpiece materials were selected for investigation, i.e. aluminum alloy, mild steel and high tensile steel, as listed in Table 4.2. Aluminum alloy has an excellent machinability, whereas high tensile steel is relatively hard to machine. Consequently, the available range of cutting parameters differs from material to material. The levels of tested factors are listed in Table 4.3. It should be noted that the variable levels were modified according to machine capacity in order to investigate the widest possible range of cutting parameters. Then the schedule of experiments for each workpiece material was generated by MiniTab® as discussed in Sect. 3.1.3. A sample schedule for testing aluminum alloy on the Colchester Tornado A50 is presented in Appendix 1.

4.1.3 Experiment Details

Tool suppliers offer a wide range of cutting tools in terms of shape, size, chip-former, etc. The tools need to be carefully selected according to the workpiece material and the desired surface finish. According to the factor-screening results, geometric features of cutting tools were assumed negligible. Hence, it is both expensive and unnecessary to test different insert types. In this research, the

Table 4.2 Specifications of tested workpiece materials for turning processes

Material type	Composition typical analysis (Ave. values %)												Brinell hardness (HB)	Density (kg/dm^3)
Aluminum alloy 2011[a]	Cu		Fe	Pb		Bi		Si	Zn		Al		95	2.84
	5.5		0.7	0.4		0.4		0.4	0.3		92.0			
Bright mild steel 1020[b]	C	Si		Mn		P		S					120–140	7.87
	0.20	0.25		0.45		0.04		0.04						
High tensile steel 4140[b]	C		Si	Mn		Cr		Mo	S		P		269–331	7.85
	0.4		0.2	0.8		1.0		0.2	0.025		0.025			

[a]Supplied by Capral® Aluminum, Australia
[b]Supplied by Böhler Uddeholm®, Australia

Table 4.3 The levels of tested factors for turning processes

Material	Factors	Level 1	Level 2	Level 3
Aluminum alloy (2011)	V (m/min)	200	300	400
	f (mm/rev)	0.1	0.2	0.3
	d (mm)	1.0	1.5	2.0
Bright mild steel (1020)	V (m/min)	100	150	200
	f (mm/rev)	0.1	0.2	0.3
	d (mm)	0.5	1.0	1.5
High tensile steel (4140)	V (m/min)	90	120	150
	f (mm/rev)	0.1	0.15	0.2
	d (mm)	0.5	1.0	1.5

cutting tool was selected for general machining purposes. Both insert holders and inserts were supplied by ISCAR® tool. The selected insert holder was MWLNR/L 2020K-06W and the selected insert was WNMG 06T308-PP with grade IC9025. However, due to the difficulties of machining high tensile steel (4140), an alternative grade IC3028 was used. The PP chip-former offers very positive rake and sharp edges, which is recommended for aluminum alloys and low carbon steels. As the tool geometry was held constant, a number of tool damages occurred when cutting 4140 with a high level of depth of cut and feed. The situation can be improved by changing the chip-former type, which has a secure cutting edge. Nevertheless, the impacts of tool wear need to be considered when investigating the eco-efficiency of unit manufacturing processes, discussed later.

There were three stages of cutting within each experiment run, as illustrated in Fig. 4.4. An exemplary power measurement of one complete run was plotted against time at 0.1 s intervals as shown in Fig. 4.4a. As the figure shows, the power curve exactly mirrors each machining operation: first, the raw metal bar was corrected to a universal size of 49 mm in diameter, i.e. skin-off (see in Fig. 4.4b, c); second, two repetitive facing cuts were performed in order to examine spindle acceleration, in which a constant surface speed was applied (see in Fig. 4.4d); third, a 50 mm long horizontal cut was performed with the scheduled cutting parameters and this was replicated an additional two times (see in Fig. 4.4e).

The power curve showed a constant trend during horizontal cuts, where the analysis of data obtained for the facing cuts became problematic due to the inconsistency of MRR along single cuts. A spindle needs to accelerate exponentially when the workpiece diameter decreases in order to create a constant MRR. Thus, once the spindle reaches its capacity, 400 rev/min in the case of Colchester Tornado A50, and is no longer able to compensate the reduction in the diameter of the workpiece a decrease in MRR results. Moreover, facing operations only account for a small portion of total removal work in practice, which is normally less than 5 % of the total removal volume. Therefore, the analysis was mainly focused on the horizontal machining actions.

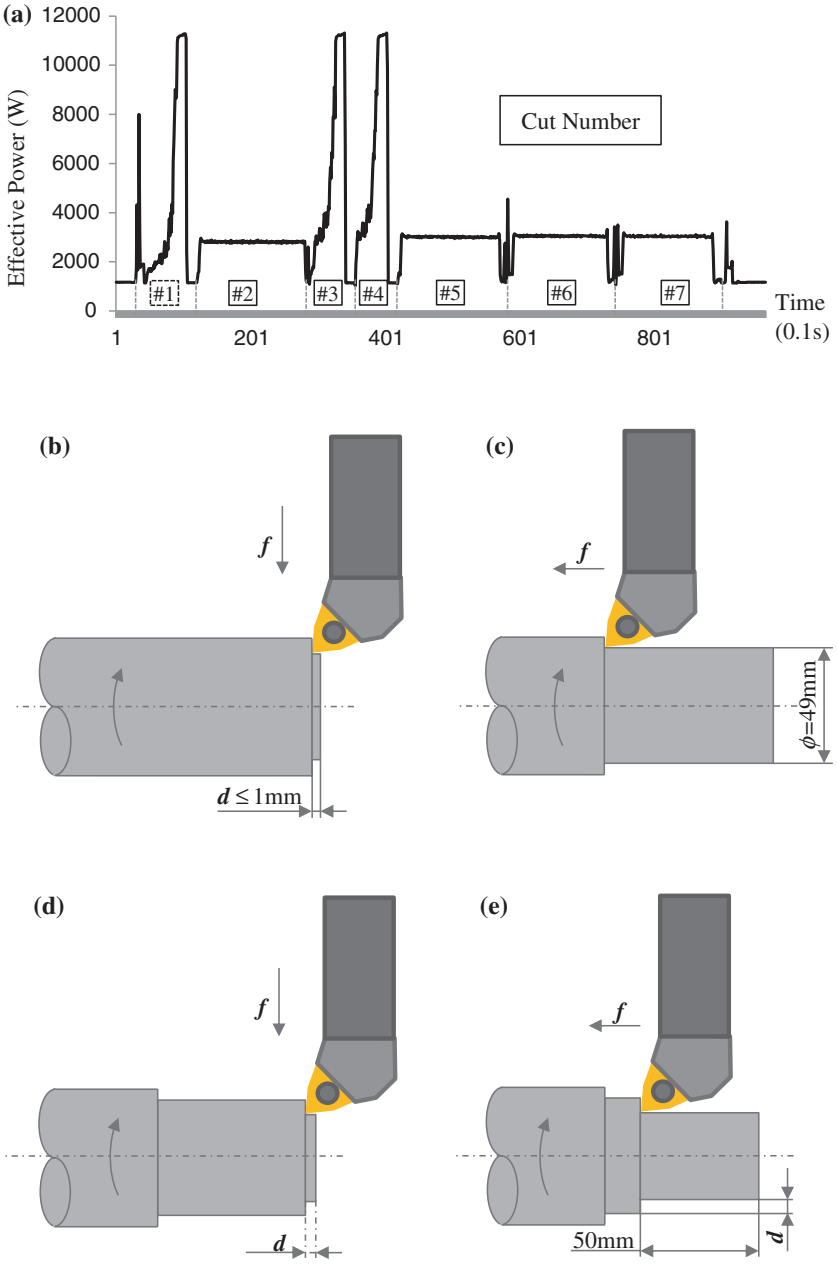

Fig. 4.4 Exemplary power curve of one turning experiment and illustrations of cutting steps. **a** An exemplary power measurement of one turning experiment. **b** Skin-off facing cut—cut #1. **c** Skin-off facing cut—cut #2. **d** Skin-off facing cut—cut #3 and 4. **e** Skin-off facing cut—cut #5, 6 and 7

4.1.4 Regression Results

First, each of three horizontal cuts was separated as shown in Fig. 4.4a. The energy consumption of each cut (E) is the integration of the power over the cutting period. The cutting volume (Q) was determined based on the scheduled cutting parameters (Eq. 4.1). Thus, SEC was also calculated (Eq. 4.2) as the response for modelling. Sample data including SEC values for the Colchester Tornado A50 are shown in Appendix 2.

$$Q = \left[\pi r_0^2 - \pi (r_0 - d)^2\right] \times l \tag{4.1}$$

$$SEC = \frac{E}{Q} = \frac{\int P_i d_t}{Q} \tag{4.2}$$

where r_0 refers to the original radius of the workpiece; and, l refers to the length of the horizontal cut, which was 50 mm here.

Each design factor was then processed using curve-estimation in relation to SEC. Although SPSS® offers 11 different types of model, the R-square was very low for using single cutting parameters to predict SEC. An example model plot between cutting speed and SEC on the Colchester Tornado A50 is displayed in Fig. 4.5.

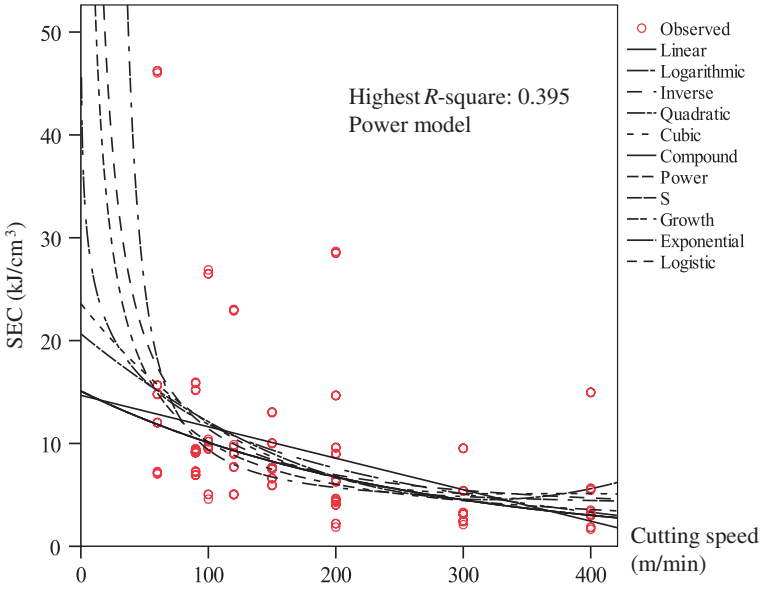

Fig. 4.5 Model plot between cutting speed and SEC for the Colchester Tornado A50

Table 4.4 Model summary of curve-estimation between MRR and SEC for the Colchester Tornado A50

Model type	Model summary					Equation
	R^2	F-value	DF_1	DF_2	P-value	
Linear	0.295	74.003	1	177	0.000	$y = 13.2 - 7.1x$
Logarithmic	0.728	472.591	1	177	0.000	$y = 2.3 - 7.52 \ln x$
Inverse	0.993	26,563.613	1	177	0.000	$y = 1.5 + \frac{2.2}{x}$
Quadratic	0.498	87.325	2	176	0.000	$y = 17.6 - 20.2x + 4.8x^2$
Cubic	0.681	124.615	3	175	0.000	$y = 24.9 - 55.6x + 38.2x^2 - 6.9x^3$
Compound	0.661	345.720	1	177	0.000	$y = 12.6 \times 0.38^x$
Power	0.978	7732.117	1	177	0.000	$y = 3.5x^{-0.79}$
S	0.761	563.737	1	177	0.000	$\ln y = 1.4 + \frac{0.17}{x}$
Growth	0.661	345.720	1	177	0.000	$\ln y = 2.5 - 0.97x$
Exponential	0.661	345.720	1	177	0.000	$\ln y = \ln 12.6 - 0.97x$
Logistic	0.661	345.720	1	177	0.000	–

As discussed in Chap. 2, several researchers have suggested that the process rate has significant impact on SEC from an exergy point of view. In the case of material removal processes, it should refer to the material removal rate (MRR). MRR is the volume of material removed per unit time (cm^3/s), which can be calculated according to Eq. 4.3. Thus, MRR was computed and added as another factor to the data spread sheet (Appendix 2).

$$MRR = V \cdot f \cdot d \tag{4.3}$$

Among all the tested machine tools, MRR has consistently resulted in the highest R-square value with an inverse model. The statistical results and model plot for the Colchester Tornado A50 are presented in Table 4.4 and Fig. 4.6 respectively. Other indicators such as F-value and P-value represent the results of hypothesis testing i.e. whether the relationship is random. A high F-value and close-to-zero P-value also suggests high significance of MRR. The analysis of variance (ANOVA) of inverse model and model plots for all the tested CNC lathes can be found in Appendix 3.

Although the current inverse model has achieved a high R-square value, the residual analysis needs to be conducted according to the methodology. Figure 4.7 plots the residuals against the predicted SEC in a case of the Colchester Tornado A50.

As shown by the dashed line in Fig. 4.7, the distribution of the residuals is not random. Thus, stepwise multiple-linear regression was performed after curve estimation. The reciprocal of MRR was used in this analysis as discussed in Sect. 3.1.4 (Eqs. 3.8 and 3.9). However, different machine tools showed different results as presented in Table 4.5. Without an exception, 1/MRR was the first accepted variable. Table 4.5a, b lists each step of the analysis for the Colchester Tornado A50 and Mori Seiki NL 2000MC/500 respectively.

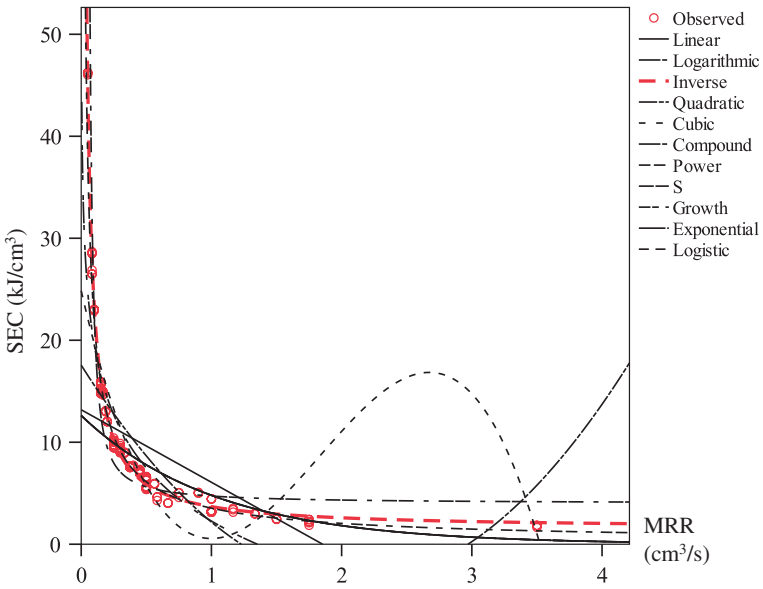

Fig. 4.6 Model plot between MRR and SEC for the Colchester Tornado A50

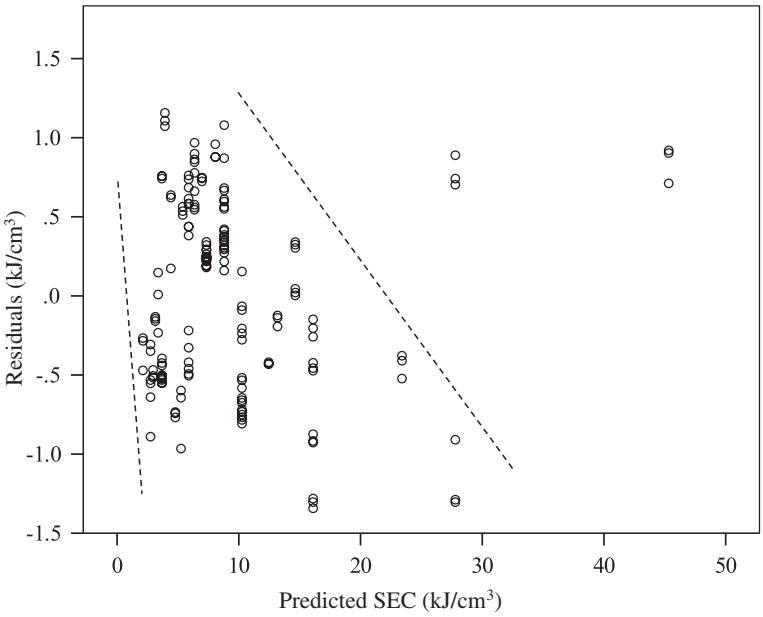

Fig. 4.7 Residuals plot of the inverse model for the Colchester Tornado A50

Table 4.5 Results of stepwise multiple-linear regression for tested turning processes

(a) Results for the Colchester Tornado A50

Step	Variable entered	R^2	Equation
1	1/MRR	0.993	$y = 1.5 + 2.2/MRR$
2	[1]HB	0.994	$y = 1.1 + 2.2/MRR + 0.003\text{HB}$

(b) Results for the Mori Seiki NL 2000MC/500

Step	Variable entered	R^2	Equation
1	1/MRR	0.927	$y = 3.6 + 2.4/MRR$
2	[2]f	0.942	$y = 6.4 + 2.3/MRR - 14.5f$
3	[3]d	0.963	$y = 10.7 + 1.9/MRR - 19.2f - 1.9d$
4	HB	0.966	$y = 9.9 + 1.8/MRR - 18.7f - 1.9d + 0.005\text{HB}$
5	[4]V	0.970	$y = 8.0 + 1.9/MRR - 19.5f - 1.7d + 0.008\text{HB} + 0.005V$

(c) Summary of all the tested machine tools

Machine	R^2	Equation
Colchester Tornado A50	0.994	$y = 1.1 + 2.2/MRR + 0.003\text{HB}$
Mori Seiki NL2000MC/500	0.970	$y = 8.0 + 1.9/MRR - 19.5f - 1.7d + 0.008\text{HB} + 0.005V$
IKEGAI AX20	0.988	$y = 0.9 + 4.2/MRR + 0.01\text{HB} - 0.005V + 0.5d$
Mori Seiki SL-15	0.971	$y = 4.1 + 1.8/MRR + 0.01\text{HB} - 8.2f - 0.7d$
Nakamura TMC-15	0.973	$y = 8.8 + 1.7/MRR - 18.4f + 0.009\text{HB} - 1.6d$

[1]HB refers to Brinell Hardness; [2]f refers to feed rate (mm/rev); [3]d refers to depth of cut (mm); [4]V refers to cutting speed (m/min)

The R-square value increases slightly by introducing other factors to the model. However, the contribution of the other factors in terms of R-square value is minimal (less than 5 %). In other words, the effects of other factors are negligible compared to MRR. Therefore, models derived from curve-estimation were favored, since their R-square values already exceeded 0.9. In addition, the simple models with a universal shape are easy to use for further studies and allow the comparison among different machine tools and processes. The energy consumption models of turning processes can be written as listed in Eq. 4.4. The values of coefficients c_0 and c_1 are also listed in Table 4.6 (Kara and Li 2011).

$$\text{SEC} = C_0 + \frac{C_1}{\text{MRR}} \tag{4.4}$$

Table 4.6 Summary of SEC models for tested turning processes

Machine	*R*-square	SEC MODEL[a]
Colchester Tornado A50	0.993	$SEC = 1.495 + \frac{2.191}{MRR}$
Mori Seiki NL2000MC/500	0.927	$SEC = 3.600 + \frac{2.445}{MRR}$
IKEGAI AX20	0.981	$SEC = 2.093 + \frac{4.415}{MRR}$
Mori Seiki SL-15	0.940	$SEC = 2.378 + \frac{2.273}{MRR}$
Nakamura TMC-15	0.929	$SEC = 3.730 + \frac{2.349}{MRR}$

[a]The unit of SEC is kJ/cm^3; the unit of MRR is cm^3/s

4.1.5 Model Validation

According to the proposed methodology (Sect. 3.1), additional experiments were performed in order to validate the above SEC models. Since the MRR is the only variable included in these models, different workpiece materials (brass and bright mild steel 1045) were used in the validation experiments. Four new sets of cutting parameters different to the ones used in stage II were used. The results for the Colchester Tornado A50 are listed in Table 4.7; and, the results for other machine tools can be found in Appendix 4. As results suggested, the SEC models were able to successfully predict the total energy consumption for a given combination of workpiece material and cutting parameters with a less than 10 % difference between predictions and measurements (Li and Kara 2011).

In summary, MRR has a decisive impact on the energy consumption of turning processes. The relationship between process parameters and SEC can be characterized in a simple equation as listed in Eq. 4.4. Due to the nature of empirical modelling, the meaning of coefficients c_0 and c_1 requires further investigation, presented in Chap. 6.

Table 4.7 Validation results of SEC model for the Colchester Tornado A50

	Brass		Mild steel 1045	
	Test 1	Test 2	Test 3	Test 4
V (m/min)	350	350	160	160
f (mm/rev)	0.2	0.1	0.2	0.1
d (mm)	2	0.5	1.25	0.8
MRR (cm^3/s)	2.333	0.292	0.667	0.213
Q (mm^3)	8792	2041	7497	4391
Predicted SEC (kJ/cm^3)	2.433	9.006	4.781	11.764
Predicted E (J)	21,390.9	18,381.2	35,838.2	51,656.8
Measured E_i (J)	23,491.4	19,990.5	39,385.4	54,052.8
Difference (%) (Eq. 3.10)	8.94	8.05	9.01	4.44

4.2 Energy Efficiency Characterization for Milling Processes

4.2.1 Background

Milling is another conventional material removal process in which a rotating, multi-tooth cutter removes material while traveling along various axes with respect to the workpiece. It is a versatile process, offering different types of operations, i.e. slab milling, face milling, end milling, straddle milling, form milling, etc. Milling can produce shapes more complex than external or internal round profiles (Kalpakjian and Schmid 2005). There is a wide selection of milling machines with numerous features, such as column-and-knee type machines, bed-type machines, profile milling machines, etc. Similar to turning processes, manual machine tools have been rapidly replaced by CNC ones which offer versatile operations and high production rates with repetitive accuracies. This research selected three different CNC milling and machining centers, as displayed in Fig. 4.8. They cover a variety of machine age, spindle motor size, transmission system, number of axes, etc. They are all suitable for face milling, in that the spindle has an

Fadal VMC4020
Year: 1998
Axes No.: 3
Spindle No.: 1
Motor Power: 11 kW

Mori Seiki Dura
Vertical 5100
Year: 2008
Axes No.: 3
Spindle No.: 1
Motor Power: 15 kW

DECKEL MAHO DMU 60P
Year: 2005
Axes No.: 5
Spindle No.: 1
Motor Power: 19 kW

Fig. 4.8 Photograph of tested CNC milling and machining centers

axis of rotation perpendicular to the workpiece surface. All of the three machine tools were located in the manufacturing laboratory of School of Mechanical and Manufacturing Engineering, the University of New South Wales.

4.2.2 Design of Experiments

Milling processes share a similar mechanism of chip formation with turning processes. Instead of rotating the workpiece, the rotation of cutter generates cutting forces for material removal. It is reasonable to assume that the SEC model for milling processes would agree with that of turning, where the material removal rate (MRR) plays a key role. Since the cutter contains multiple cutting edges, the equation of calculating MRR for face milling is slightly different than the one for turning, as shown in Eq. 4.5.

$$\text{MRR} = w \cdot d \cdot v \tag{4.5}$$

where w refers to the width of cut (mm); d refers to the depth of cut (mm); and, v refers to the linear speed of the workpiece (mm/min) which is determined by the selection of feed per tooth (f), number of teeth on cutter (n), rotation speed (N), cutting speed (V) and the cutter diameter (D), as shown in Eq. 4.6.

$$v = f \cdot n \cdot N = f \cdot n \cdot \left(\frac{V}{D}\right) \tag{4.6}$$

According to the above equations, more factors need to be considered as design factors in the milling case. The operators normally use rotation speed and workpiece speed to command a milling operation. The rotation speed has a direct impact on the power requirement of spindle motor, so the cutter diameter needs to be tested. In addition, the cutter diameter also affects the workpiece speed. Thus, the cutter diameter was believed to have a larger influence on the processes than the number of teeth. In addition, the cutting fluid was also applied to compare with dry machining, discussed in Sect. 4.2.6. Therefore, the Ishikawa diagram can be modified as Fig. 4.9.

The selection of workpiece materials was identical to turning experiments. They were aluminum alloy 2011, bright mild steel 1020 and high tensile steel 4140. Two different cutters were tested, diameter 32 mm (4 teeth) and diameter 63 mm (4 teeth). The width of cut was adjusted to fit the cutter diameter. The levels of tested factors are listed in Table 4.8. It should be noted that the variable levels were modified according to machine capacity in order to investigate the widest possible range of cutting parameters. Then the schedule of experiments for each workpiece material was generated by MiniTab® as discussed in Sect. 3.1.3.

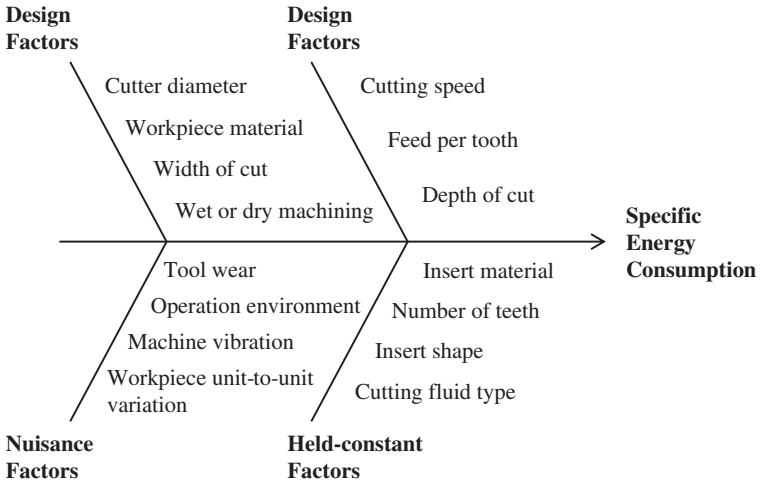

Fig. 4.9 Ishikawa diagram for tested milling processes

Table 4.8 The levels of tested factors for milling processes

Material	Factors	Variable levels		
Aluminum alloy (2011)	V (m/min)	200	300	400
	f (mm/rev·tooth)	0.1	0.2	0.3
	d (mm)	1.0	2.0	3.0
Bright mild steel (1020)	V (m/min)	120	160	200
	f (mm/rev·tooth)	0.1	0.15	0.2
	d (mm)	1.0	1.5	2.0
High tensile steel (4140)	V (m/min)	100	140	180
	f (mm/rev·tooth)	0.1	0.15	0.2
	d (mm)	0.5	1.0	1.5
Factors	Variable levels			
Cutting environment	Dry machining			Wet machining
Cutter diameter, D (mm)	32 (4 teeth)			63 (4 teeth)
Width of cut, w (mm)	10	15	25	10	30

4.2.3 Experiment Details

The workpiece was pre-machined to a 50 mm square bar with 200 mm length (l). Climb milling was performed, where the maximum chip thickness occurred at the start of the cut. Each combination of cutting parameters was repeated twice without coolant and a third time with coolant. A sample power curve and the schematic illustrations of each tool path are illustrated in Fig. 4.10 for the case of cutter diameter 32 mm.

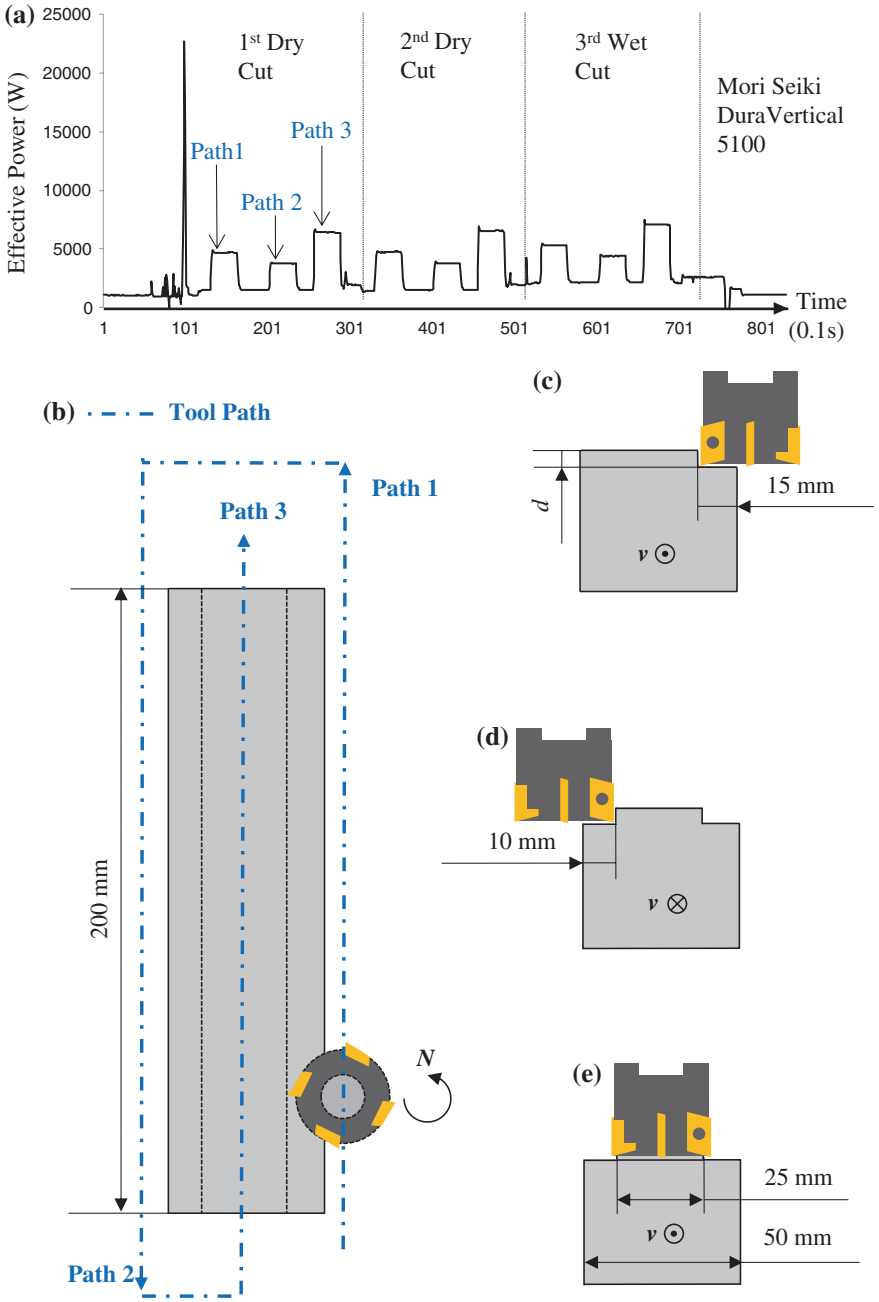

Fig. 4.10 Exemplary power curve of one milling experiment and illustrations of cutting steps (cutter diameter 32 mm). **a** Exemplary power curve of one complete experiment run (32 mm). **b** Schematic illustration tool path. **c** Tool path 1. **d** Tool path 2. **e** Tool path 3

Although the DECKEL MOHA DMU 60P (DMG DMU 60P) is a 5-axis machining center, only three axes were used in this research. There were two main reasons for this decision: one is to keep the consistency among all the three tested milling machine tools; the second is that the motor size for the two additional axes is much smaller than the others; correspondingly, the power demand of the spindle drive motor and other auxiliary components outweighs the consumptions of the other two servo motors significantly. Thus, the SEC model for DMG DMU 60P can still be assumed to be representative and reliable.

4.2.4 Regression Results for Dry Machining

First, each of three tool paths was separated as shown in Fig. 4.10. The energy consumption of each cut (E) is the integration of the power over the cutting period. The cutting volume (Q) was determined for the scheduled cutting parameters (Eq. 4.7).

$$Q = w \cdot d \cdot l \tag{4.7}$$

Thus, SEC was calculated similarly according to Eq. 4.2 as the response for modelling.

Then, each design factor was processed with curve-estimation in relation to SEC. The results are identical to those of the turning processes. Each single cutting parameter resulted in very low R-square values; while, the MRR with an inverse model can consistently achieve an R-square value of over 0.9 for all the tested machine tools. The model plot and statistical results for the Mori Seiki Dura Vertical 5100 are presented in Fig. 4.11 and Table 4.9 respectively.

The ANOVA analysis of inverse model and model plots for the other tested machine tools can be found in Appendix 3. Although the current inverse model has achieved a high R-square value, the residual analysis needs to be conducted from a statistical point of view. Figure 4.12 shows the residuals plotted against the predicted SEC for the case of the Mori Seiki Dura Vertical 5100. There is a visible trend between the residuals and the predicted value. Thus, stepwise multiple-linear regression was performed afterwards.

Similar to the turning process, different machine tools showed different model shapes as presented in Table 4.10. There is a lack of consistency of the accepted factors after final steps. More importantly, there was an insignificant growth of R-square value from inverse model to the multiple-linear regression model. For instance, the inverse model for the DMG DMU 60P has already achieved an R-square value at 0.997; after adding 6 other factors, the R-square value only increased by 0.001. Therefore, the contribution of the other factors for the SEC model can be concluded negligible.

In fact, the inverse model is more practical than the multiple-linear regression models, because it agrees with the model for turning processes as listed in Eq. 4.4, which enables cross comparison between turning and milling processes. The only difference among the tested machine tools is the value of the coefficients c_0 and

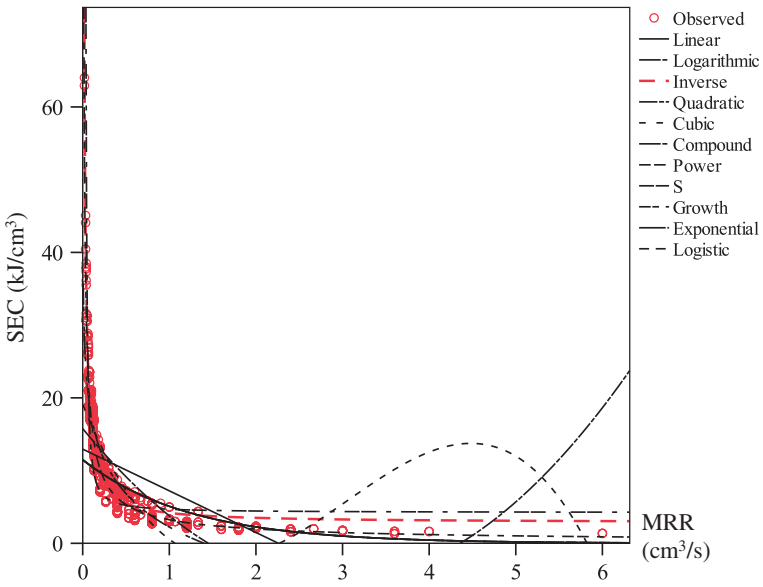

Fig. 4.11 Model plot between MRR and SEC for the Mori Seiki Dura Vertical 5100

Table 4.9 Model summary of curve-estimation between MRR and SEC for the Mori Seiki Dura Vertical 5100

Model type	Model summary					Equation
	R^2	F-value	DF_1	DF_2	P-value	
Linear	0.257	191.572	1	555	0.000	$y = 12.9 - 5.7x$
Logarithmic	0.730	1497.344	1	555	0.000	$y = 2.2 - 6.562 \ln x$
Inverse	0.947	9844.944	1	555	0.000	$y = 2.8 + \frac{1.3}{x}$
Quadratic	0.419	200.015	2	554	0.000	$y = 15.8 - 14.5x + 2.5x^2$
Cubic	0.556	230.901	3	553	0.000	$y = 19.1 - 29.6x + 12.4x^2 - 1.4x^3$
Compound	0.565	720.548	1	555	0.000	$y = 11.5 \times 0.44^x$
Power	0.929	7301.959	1	555	0.000	$y = 3.2x^{-0.72}$
S	0.653	1042.726	1	555	0.000	$\ln y = 1.4 + \frac{0.11}{x}$
Growth	0.565	720.548	1	555	0.000	$\ln y = 2.4 - 0.81x$
Exponential	0.565	720.548	1	555	0.000	$\ln y = \ln 11.5 - 0.81x$
Logistic	0.565	720.548	1	555	0.000	–

c_1, as discussed in Chap. 6. Moreover, the simple SEC model also requires less input for predicting energy consumption, which is a major advantage for deriving energy saving strategies. Therefore, this research prefers the model derived from curve-estimation; with the SEC models and the values of the coefficients for the tested CNC milling and machining centers listed in Table 4.11. The SEC models were then processed for validation.

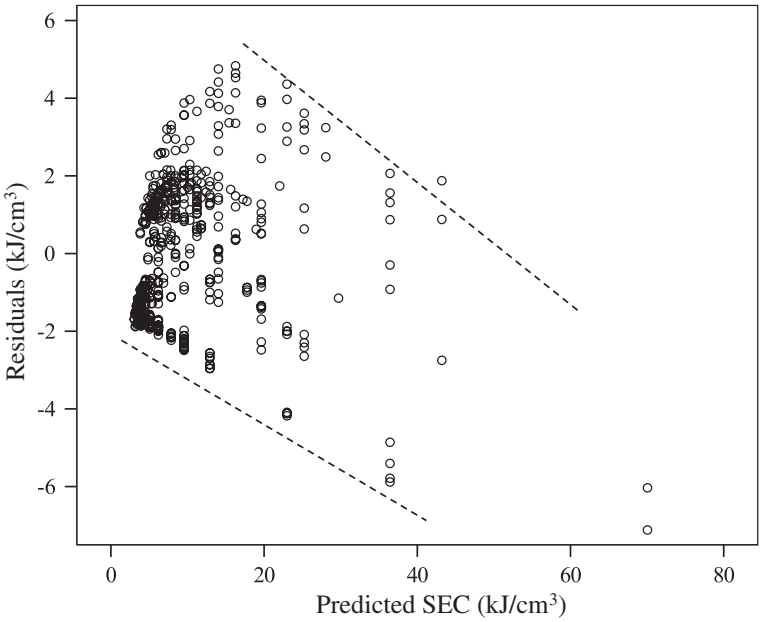

Fig. 4.12 Residuals plot of the inverse model for the Mori Seiki Dura Vertical 5100

Table 4.10 Results of stepwise multiple-linear regression for tested milling processes

(d) Mori Seiki Dura Vertical 5100		
Step	R^2	Equation
1	0.947	$y = 2.8 + 1.3/MRR$
⋮	⋮	⋮
10	0.986	$y = 2 + 1.1/MRR + 0.02\text{HB} - 0.01V - 6f - 0.04w - 0.4d + 0.04D + 0.001N$
(e) Fadal VMC4020		
Step	R^2	Equation
1	0.971	$y = 2.8 + 1.3/MRR$
⋮	⋮	⋮
8	0.991	$y = 7 + 1.1/MRR - 0.01HB + 0.4v - 0.8d - 0.06w - 11f - 0.001N - 0.001V$
(f) DMG DMU60P		
Step	R^2	Equation
1	0.997	$y = 2.4 + 5.9/MRR$
⋮	⋮	⋮
9	0.998	$y = 6 + 5.8/MRR + 0.01HB - 0.08D - 0.7d + 0.001V - 0.001N - 0.7v$

Table 4.11 Summary of SEC models for tested milling processes

Machine	*R*-square	SEC model
Mori Seiki Dura Vertical 5100	0.947	$SEC = 2.830 + \frac{1.344}{MRR}$
Fadal VMC 4020	0.971	$SEC = 2.845 + \frac{1.330}{MRR}$
DMG DMU 60P	0.997	$SEC = 2.411 + \frac{5.863}{MRR}$

4.2.5 Model Validation

The validation experiments were conducted without coolant, thus the above SEC models for dry machining can be tested. Since the MRR is the only variable included in the SEC models, a different workpiece material (bright mild steel 1045) was introduced for testing at this stage. Moreover, the number of teeth was initially tested as insignificant comparing with the impact of cutter diameter (Sect. 4.2.2). Hence, a new cutter with 3 teeth, and diameter 32 mm was used to further validate the model. Other cutting parameters, such as cutting speed, feed per rev per tooth and depth of cut, were changed to the ones which had not been used at stage II. The validation results for the DMG DMU 60P are listed in Table 4.12. The results for other milling processes are presented in Appendix 4.

As the results showed, the difference between the predicted and measured energy consumption remained under 5 % for the DMG DMU 60P. The validation results for other tested machine tools also showed less than 10 % discrepancy between prediction and physical measurements. In other words, the SEC models have achieved accuracy over 90 % for energy consumption prediction. Therefore, the SEC models for tested milling processes can be concluded as accurate and reliable.

Table 4.12 Validation results of SEC model for the DMG DMU 60P

Workpiece	High tensile steel 4140			Bright mild steel (1045)		
Cutter	32 mm; 3-tooth			63 mm; 4-tooth		
Cutting parameters	$V = 160$ m/min; N = 1600 rpm; $d = 1.8$ mm			$V = 160$ m/min; N = 900 rpm; $d = 1.8$ mm		
Tool path number	1	2	3	1	2	3
w (mm)	5	25	20	15	10	25
f (mm/rev·tooth)	0.2	0.18	0.14	0.18	0.2	0.16
MRR (cm^3/s)	0.144	0.648	0.403	0.292	0.216	0.432
Q (cm^3)	1.8	9.0	7.2	5.4	3.6	9.0
Predicted SEC (kJ/cm^3)	43.13	11.46	16.95	22.51	29.55	15.98
Predicted E (kJ)	77.63	103.13	122.06	121.59	106.40	143.84
Measured E_i (kJ)	79.91	105.85	126.05	123.67	109.29	151.13
Difference (%)	2.85	2.57	3.17	1.68	2.65	4.82

4.2.6 Comparison Between Dry and Wet Machining

Although there is a trend towards minimum coolant or lubricant use, wet cut is still widely used in industry for milling processes. From an energy point of view, applying coolant requires additional power to activate the coolant pump which is generally at a constant level. Different machines provide different pressure of output coolant. For some complex models, such as the DMG DMU 60P, an integrated coolant filter system consumes extra energy once the coolant pump is enabled. All the experiments have been repeated on 3 milling machine tools by using a low-mineral, water-miscible coolant (Eco Cool 68 CF2, FUCHS® Lubricants).

Table 4.13 compares the unit energy consumption models between dry and wet machining. The power profile presented in the table results from the measurement of air cuts (running the cutting program without contacting the workpiece); the blue and red curves are dry and wet air cut respectively. The gap between those two curves is the power demand for applying coolant, which is approximately equal to the difference between the coefficient c_1 of SEC models for dry and wet machining. For example, the coolant pump of the Mori Seiki Dura Vertical 5100 consumes 0.74 kW, whereas the c_1 value increases 0.675 from 1.344 to 2.019.

Table 4.13 Comparison of SEC models between dry and wet cutting environment (Kara and Li 2011)

Machine	Model		Power profile
Fadal VMC 4020	Dry	$SEC = 2.845 + \frac{1.330}{MRR}$	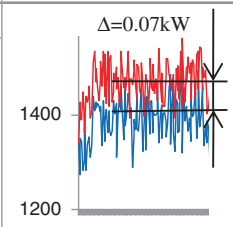
	Wet[a]	$SEC = 3.078 + \frac{1.397}{MRR}$	
Mori Seiki Dura Vertical 5100	Dry	$SEC = 2.830 + \frac{1.344}{MRR}$	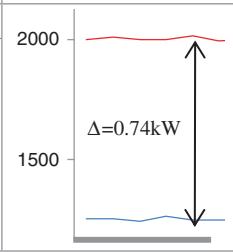
	Wet[a]	$SEC = 2.955 + \frac{2.018}{MRR}$	
DMG DMU 60P	Dry	$SEC = 2.411 + \frac{5.863}{MRR}$	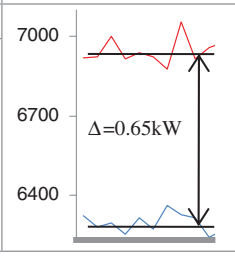
	Wet[a]	$SEC = 2.425 + \frac{6.422}{MRR}$	

[a]The ANOVA results and model plots for wet machining are presented in Appendix 3

It is also important to note that the environmental impact of applying coolant is not only due to electricity consumption of the coolant pump. The coolant itself has significant environment impacts, due to the use of chemical substances, emissions and losses during the operations, disposal and recycling phases. However, the process can also benefit from applying coolant, including longer tool life and better surface finish. For some processes like grinding, the coolant is essential for operation due to the substantial heat generated at the contacting zone. Therefore, the energy and ecological impacts of applying coolant need to be investigated in a systematic manner, discussed with a grinding case in Chap. 5.

4.3 Energy Efficiency Characterization for Grinding Processes

4.3.1 Background

Grinding is normally considered as a surface finishing process which uses bonded abrasives as the cutting medium. Unlike turning or milling, there are countless grains held by the softer bonding agent on a grinding wheel; and each grain acts as a microscopic cutting tool. Thus, grinding is classified as a geometrically undefined cutting-edge machining process. It features a very fine surface finish and high dimensional accuracy, and is capable of machining very hard and brittle materials. It is also a versatile process, offering different types of operations, i.e. surface, cylindrical, internal, and centerless grinding. Numerous products (e.g. bearings, pistons, cylinders, cutting tools, etc.) are machined by grinding in at least one stage of their production (Kalpakjian and Schmid 2005).

Due to the nature of grinding, only small amount of material is removed during this process, resulting in very high energy consumption per unit volume of material removal. However, modelling the grinding process is a very challenging task due to the irregular geometry of multiple cutting points, the high cutting speeds, and the small depths of cut which vary from grain to grain (Malkin and Guo 2008). During the last few decades, the grinding process has been studied extensively. As discussed in Sect. 2.1, cutting force and specific grinding energy has been modelled at a microscopic level, which has proved the possibility of characterizing this complex process; but, along with other manufacturing processes, the energy consumption of the entire machine tool has been neglected. Thus, the grinding process is an ideal case to validate the proposed empirical approach for deriving energy consumption models.

Internal cylindrical grinding processes were selected for this research where a small grinding wheel is rotating at a high speed to grind the inside diameter of a workpiece rotating in the opposite direction. As a result, a substantial amount of heat is generated at the contacting zone necessitating the use of cutting fluids or coolant. Throughout the experiments, the coolant was applied as a part of stream lubrication through a tangential nozzle into the contact zone. Due to the microscopic

Reinecker ISA 110
Year: 1980s
Numerical Control

Studer S120
Year: 2007
Internal Grinding Wheel Spindle
Motor Power: 10 kW
Max RPM: 60000

Studer S40
Year: 2007
Internal Grinding Wheel Spindle
Motor Power: 7.5 kW
Max RPM: 60000

Fig. 4.13 Photograph of tested grinding machines

cutting mechanism, the formed chip or swarf is washed away by the circulated coolant. Moreover, the coolant is emitted to the air which contains hazardous and flammable substances. Hence, a coolant filter and an exhaust air filter are normally connected to grinding machines. The three tested machine tools are displayed in Fig. 4.13. They cover a variety of machine age, spindle motor size, control system, etc. All of the three machine tools were located in the Institute of Machine Tools and Production Technology (IWF), Technische Universität Braunschweig.

4.3.2 Design of Experiments

As mentioned above, grinding is a complex process in which numerous factors affect the process performance. They can be generally classified into one of six categories:

- Grinding wheel: e.g. abrasive material, bond type, geometry, etc.;
- Dressing parameters: e.g. dresser type, dressing ratio, dressing infeed, etc.;

- Workpiece material: generally refers to hardness and grindability;
- Cutting parameters: e.g. specific material removal rate (Q'_w), cutting speed (V), specific material removal volume (V'_w), etc.;
- Cutting fluid: e.g. coolant type, nozzle position, flow rate;
- Operation environment: e.g. temperature, humidity, etc.

Unlike turning or milling processes, grinding is very delicate and sensitive to minor changes. The selection of process parameters faces many constraints; otherwise, tool damages are expected to occur frequently. It is also important to keep the experiments practical, which would offer better implementations of the derived models. Therefore, the proposed research methodology needs to be modified and adapted for the grinding case.

The grinding wheel consists of both abrasives and bonding agents. The abrasives can be generally grouped as conventional abrasives and superabrasives. The typical abrasives in each group are aluminum oxide (Al_3O_2) and cubic boron nitride (CBN) respectively. Comparing those two materials, the CBN features higher hardness than the former one, which can grind harder material and relatively faster. The shape and the size of the abrasives can also affect the performances of grinding wheel, for instance, friability which refers to how long the abrasives can remain sharp. In addition to the abrasives, the bond type increases the variety of grinding wheels, such as vitrified, resinoid, rubber, and metal. A vitrified bond, or called ceramic bond is the most common and widely used bond, which can bond both conventional and superabrasives (Malkin and Guo 2008). In this research, two different grinding wheels were used, CBN (B126M8VD49) and Al_2O_3 (A120K9V3). Both of the selected grinding wheels are vitrified. The original diameter of the grinding wheel is 40 mm, which decreases during the grinding process due to the wear of grinding wheel as well as the dressing process.

Dressing is the process of correcting the conditions of grinding wheel in order to achieve a desired sharpness and roundness. The dressing process itself has formed a research field, where the type of dresser and dressing process parameters were studied. A well-defined dressing process can result in a better surface finish of the ground parts. Nevertheless, the dressing configurations were assumed as irrelevant to the energy consumption during the grinding process. Therefore, the dressing parameters were held constant. During the experiments, the dressing was performed with a CNC dressing form roller. The dressing ratio was 0.4, the dressing infeed was 1.0 μm and the dressing overlap was 5.0. It should be noted that the dressing process also consumes electricity, which needs to be considered and integrated within the unit process during the evaluation of eco-efficiency of the grinding processes, as presented in Sect. 5.3.

The results of turning and milling indicate that the workpiece material has indirect influences on the SEC models. It affects the energy consumption by limiting the range of material removal rate. However, these impacts in grinding process would be even less significant, because the available range of material removal rate is already restricted. Thus, instead of having three levels for workpiece material, two different materials were used for model development: a hardened high

carbon alloy steel 100Cr6 (62 HRC, Rockwell Hardness C scale), and a non-hardened low carbon alloy steel 16MnCr5 (35 HRC).

In internal cylindrical grinding, the specific material removal rate (Q'_w) is the primary parameter which refers to the removal rate per unit width of grinding (mm^3/mm s). The use of specific material removal rate reduces the number of variables and allows direct comparison of removal efficiency. The calculation of MRR can be simplified as Eq. 4.8.

$$MRR = Q'_w \cdot w \tag{4.8}$$

During the experiments, the width of grinding (w) was equal to the thickness of the workpiece (10 mm), which is less than the thickness of the grinding wheel. It was kept constant due to the use of a special workpiece holder. The turning and milling experiments have proved that MRR has a decisive impact on the SEC. Correspondingly, the design of experiments should seek as many levels as possible for Q'_w in order to authentically characterize the trends between MRR and SEC.

Other cutting parameters are also believed to have a certain influence on the energy consumption. For instance, the cutting speed (V) determines the rotation speed of the grinding wheel (N_s), while it is also correlated with the type of grinding wheel. Thus, the cutting speed was coupled with the type of grinding wheel. But for a given grinding wheel, the cutting speed is held constant according to the recommendations of the wheel suppliers. The rotation speed of the workpiece has a ratio (q_s) to the speed of grinding wheel. The ratio q_s can vary from 30 to 90. As the workpiece rotation speed is very slow comparing to the rotation speed of grinding wheel, q_s was initially considered as a screening factor.

Specific material removal volume (V'_w) is a unique process parameter for the grinding case. It refers to the material removal volume per unit width of grinding between two dressing processes (mm^3/mm). The topography of grinding wheel is constantly changing during the process due to the loss and self-sharpening of grains, resulting in different cutting actions and frictions. Correspondingly, the energy consumption may vary significantly during the grinding process, so V'_w was preceded for factor-screening.

The functions of cutting fluids are to reduce the temperature at the contacting zone, to improve the surface finish, to increase the dimensional accuracy, and to avoid excessive tool wear. There exists a variety of coolant used in industry i.e. mineral oil, water-based emulsions, etc. Not only the material composition of coolant, but the delivering of coolant can result in different lubricating and cooling effects, i.e. the nozzle position, the flow rate of the coolant. However, from the energy consumption perspective, the performance of coolant is out of the interest in this stage, except its impacts on power requirement during the grinding process. Thus, both mineral oil coolant and water-based emulsion are tested in the factor-screening step.

In order to estimate the impacts of specific material removal volume, one grinding process was separated into a few runs. With the CBN grinding wheel, 400 mm^3/mm materials were removed in total before dressing. Therefore, the experimenter configured each run by removing 100 mm^3/mm materials; and, after repeating 4 times, a dressing process was conducted. Figure 4.14 plots the averaged effective power against V'_w.

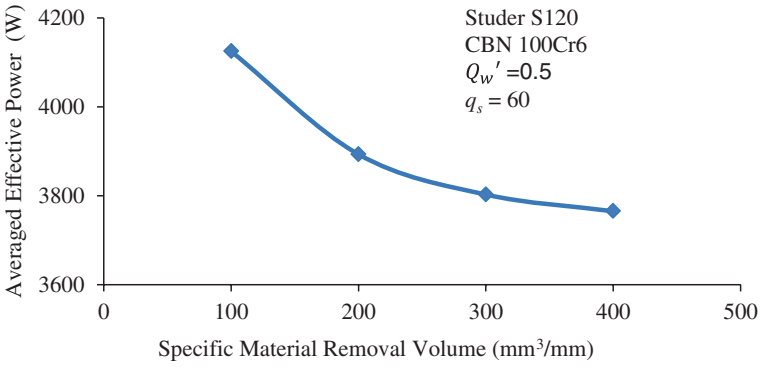

Fig. 4.14 Power plots against specific material removal volume

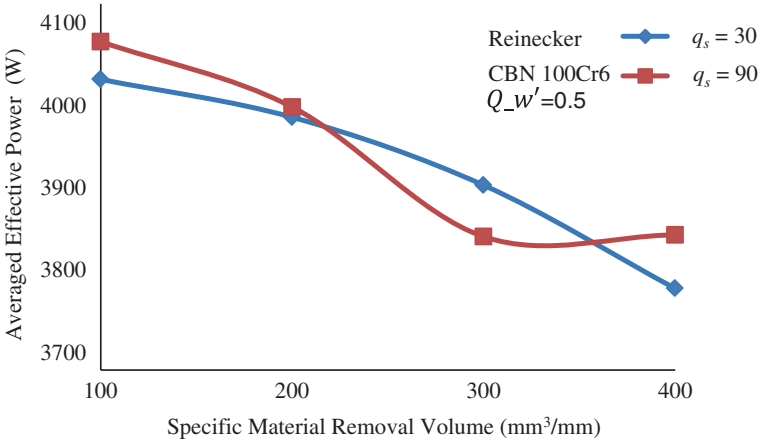

Fig. 4.15 Screening results: speed ratio of workpiece and grinding wheel

Figure 4.14 has shown a clear power decreasing trend when increasing the specific material removal volume. It is mainly because of the abrasive loss during the grinding process, which reduces the number of effective cutting points as well as the grinding forces. Therefore, V_w' was considered as a design factor.

Two different speed ratios of workpiece and grinding wheel were used to test its impact on the energy consumption, as shown in Fig. 4.15. The results suggested that the impacts of q_s are less significant than V_w'. Hence, it was held constant at further steps.

A similar procedure was conducted by using mineral oil and water-based lubrication. The results suggest that the type of coolant has a less significant impact on energy consumption comparing to the specific material removal volume, as shown in Fig. 4.16. Thus, the coolant type was considered as held-constant factor at the following stages.

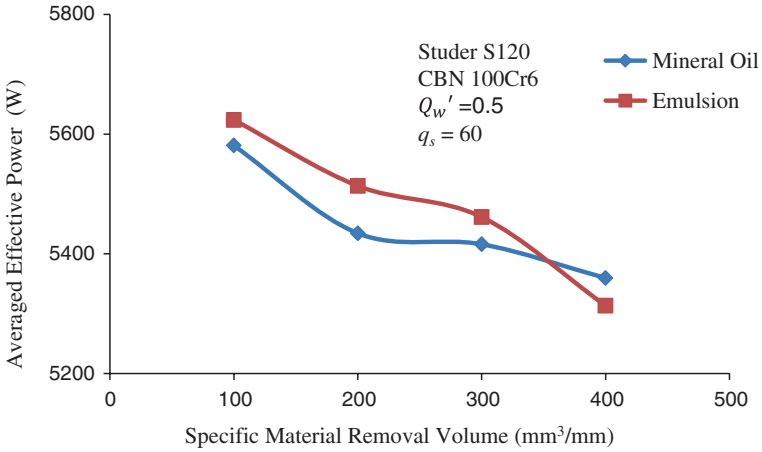

Fig. 4.16 Screening results: coolant type

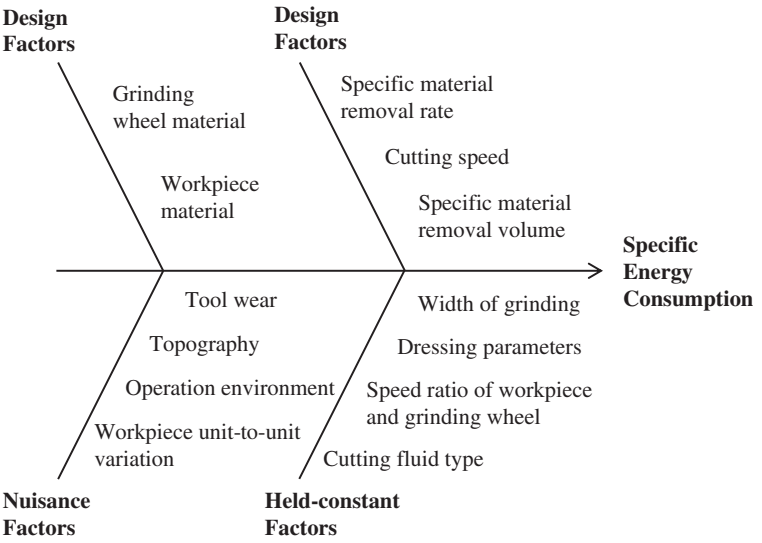

Fig. 4.17 Ishikawa diagram for tested grinding processes

After factor-screening, all the involved factors were classified into different groups as displayed in the Ishikawa diagram in Fig. 4.17.

As mentioned before, there are many constraints for defining the levels of process variables. Instead of using RSM for design of experiments, the full factorial experiments were used in the case of grinding. For most of the factors, the range of variance is very limited. From the test of turning and milling process, the material removal rate has been proved as a key factor (Sects. 4.1 and 4.2). Previous

Table 4.14 The levels of tested factors for grinding processes

Factors	Variable levels					
Workpiece	100Cr6			16MrCr5		
Grinding wheel	CBN B 126 M 8 VD 49			Al_2O_3 A 120 K 9 V 3		
Cutting speed, V (m/s)	60			40		
Specific material removal rate, Q'_w (mm^3/mm·s)	0.50	0.75	1.00	0.25	0.50	0.75
	1.25	1.50	1.75[a]	1.00		
Specific material removal volume, V'_w (mm^3/mm)	100	200	300	50	100	150
	400	500[a]		200		

[a]The extreme levels were only tested on the Studer S120

researches about grinding forces also showed the decisive impacts of Q'_w on specific grinding energy (Malkin 1975). Thus, the levels of variable Q'_w were maximized. Table 4.14 lists the levels of each design factor for the tested grinding machine tools.

4.3.3 Experiment Details

The experiment for grinding process was kept simple and straightforward. The power curve of an exemplary run was shown in Fig. 4.18.

The first power peak reflects the acceleration of the grinding wheel spindle. At the same time, the grinding wheel rapidly travelled towards the workpiece until reaching the safety distance, then slowed down to the same speed as actual grinding. In practice, the safety distance is kept minimal, because it refers to a non-value-adding period. Nevertheless, the safety distance was kept relatively long in this research to help the data analysis by separating the energy consumed during the grinding period. The instantaneous power started to increase once the grinding wheel contacted with the workpiece surface. Then the power consumption decreases along the grinding process due to the topography change of the grinding wheel. In each run, 100 mm^3/mm or 50 mm^3/mm of workpiece materials were removed by the CBN wheel or Al_2O_3 respectively. After repeating the procedure for three or four times, the grinding wheel was dressed with a fixed dressing parameter. During the experiments, a mineral oil based emulsion was employed as coolant. The emulsion had a concentration of 8.0 % and kinematic viscosity of 1.1 m^2/s at 40 °c. The coolant was delivered as a flood through a tangential nozzle into the contact zone.

4.3.4 Regression Results

First, the power demand during the grinding period was separated from the raw data file, as shown in Fig. 4.18a. The SEC then can be calculated according to Eq. 4.9.

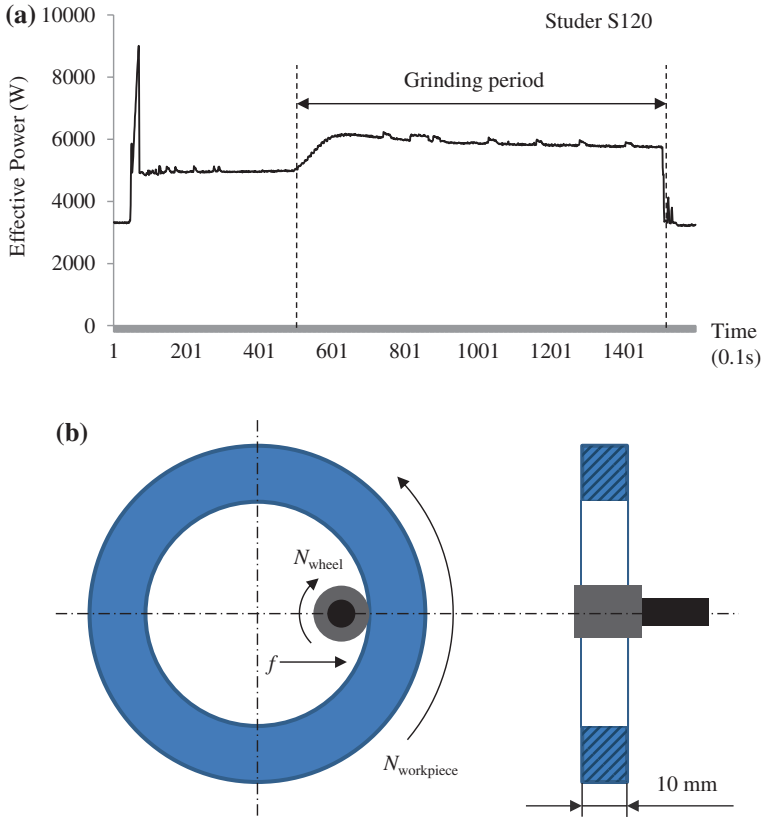

Fig. 4.18 Exemplary power curve of one grinding experiment and illustrations of internal grinding operations. **a** Exemplary power curve of one grinding experiment. **b** Schematic illustration of internal grinding operations

$$SEC = \frac{E}{Q} = \frac{\int P_i \cdot d_t}{V'_w \cdot w} \tag{4.9}$$

Then, each design factor was processed with curve-estimation in relation to SEC. The material removal rate (MRR) was used instead of specific material removal rate, since MRR is a more comparable process parameter. Other indirect process parameters have also been tested, such as the rotation speed of grinding wheel spindle (N_s, rpm), the feed speed of grinding wheel (v_{fr}, mm/min), and the feed length of grinding wheel (l_{fr}, mm). Similar to turning and milling, the MRR has showed the highest R-square value comparing to the other factors.

However, different model shapes have achieved R-square value over 0.9. This is mainly due to the limited range of material removal rate. Unlike turning or milling process, the observed data for grinding can only plotted in a segment of the curve

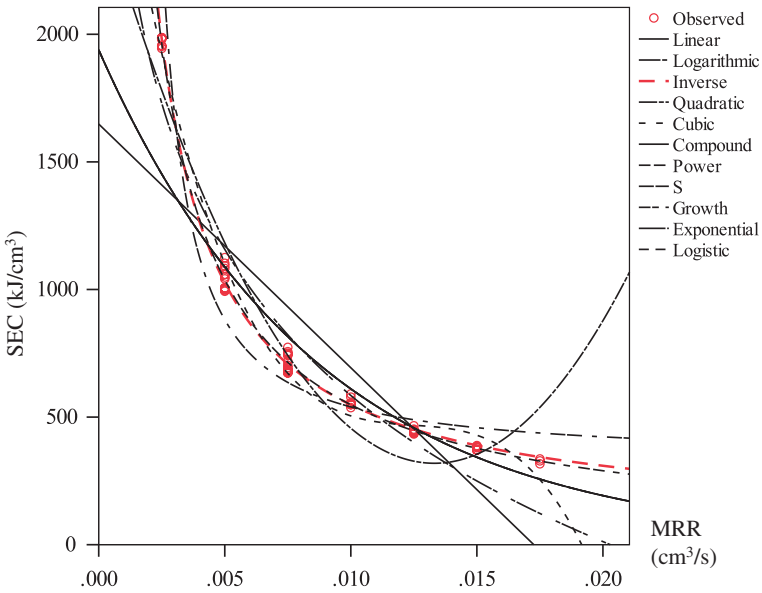

Fig. 4.19 Model plot between MRR and SEC for the Studer S120

in which a number of models can fit well. The high steepness of the curve can even be approximated as a linear line.

Regardless, the inverse model still has resulted in the highest *R*-square value and the largest *F*-value among all the 11 available models. The statistical results have suggested that the inverse model is the best-fit model after curve-estimation. The model plot and statistical results for the Studer S120 are presented in Fig. 4.19 and Table 4.15 respectively. The ANOVA analysis of inverse model and model plots for the other tested machine tools can be found in Appendix 3.

The residual analyses of the inverse models show mixed results. The residuals plot for the Reinecker ISA 110 shows an unclear trend (Fig. 4.20), whereas there is an arrow shape in the one for the Studer S40 (Fig. 4.21). Thus, stepwise multiple-linear regression was performed afterwards.

All the collected data was processed for a stepwise multiple-linear regression. As listed in Table 4.16, the model for the Reinecker only accepts MRR as a significant factor, whereas the models for other two machines disagree with each other. The *R*-square values were only increased by less than 2 % after introducing new factors. Therefore, the other process parameters can be concluded negligible for estimating SEC.

Based on above statistical analysis, the SEC model for tested internal cylindrical grinding processes can be summarized in Table 4.17. The grinding SEC models join the same shape with the ones for turning and milling processes, as shown in Eq. 4.4.

Table 4.15 Model summary of curve-estimation between MRR and SEC for the Studer S120

Model type	Model summary					Equation
	R^2	F-value	DF_1	DF_2	P-value	
Linear	0.718	165.575	1	65	0.000	$y = 1648 - 95509x$
Logarithmic	0.921	754.243	1	65	0.000	$y = -3220 - 826 \ln x$
Inverse	0.996	17,335.020	1	65	0.000	$y = 70 + 4.8/x$
Quadratic	0.934	452.098	2	64	0.000	$y = 2534 - 332868x + 1.2 \times 10^7 \cdot x^2$
Cubic	0.986	1508.654	3	63	0.000	$y = 3279 - 6.6 \times 10^5 \cdot x + 5.3 \times 10^7 \cdot x^2 - 1.4 \times 10^9 \cdot x^3$
Compound	0.916	705.686	1	65	0.000	$y = 1939 \times 6.7^{-0.051 \cdot x}$
Power	0.995	14,352.768	1	65	0.000	$y = 7.9 \cdot x^{-0.92}$
S	0.913	681.122	1	65	0.000	$\ln y = 5.8 + 0.005/x$
Growth	0.916	705.686	1	65	0.000	$\ln y = 7.6 - 115.5x$
Exponential	0.916	705.686	1	65	0.000	$\ln y = \ln 1939 - 115.5x$
Logistic	0.916	705.686	1	65	0.000	–

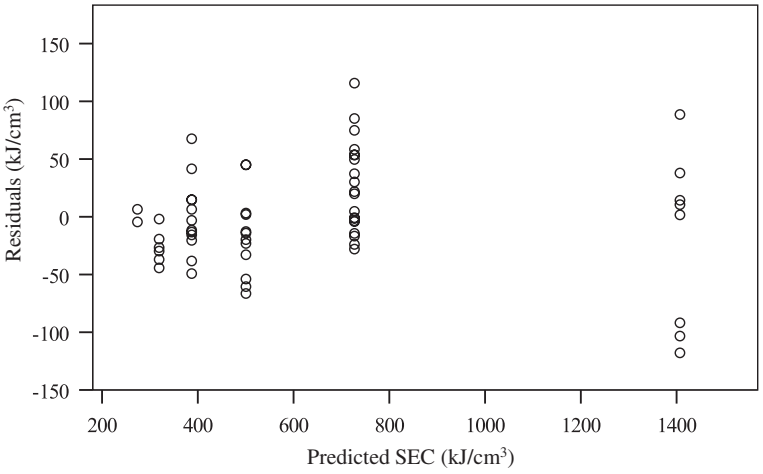

Fig. 4.20 Residuals plot of the inverse model for the Reinecker ISA 110

4.3.5 Model Validation

During the validation experiments, additional sets of grinding parameters were used to assess the discrepancy between the predicted and measured energy consumption. The validation runs were conducted on different grinding wheels and workpiece materials. Table 4.18 lists the results of few validation runs; and, the

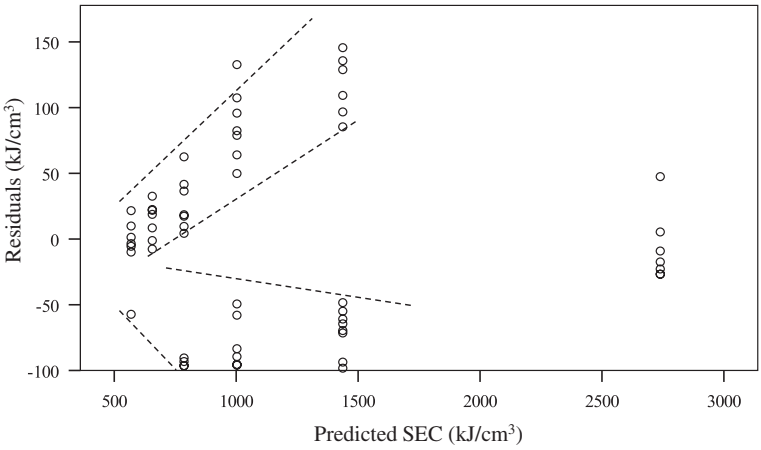

Fig. 4.21 Residuals plot of the inverse model for the Studer S40

Table 4.16 Results of stepwise multiple-linear regression for tested grinding processes

(g) Reinecker ISA 110		
Step	R^2	Equation
1	0.983	$y = 47 + 3.4/MRR$
(h) Studer S120		
Step	R^2	Equation
1	0.996	$y = 70 + 4.8/MRR$
2	0.998	$y = -105 + 4.9/MRR + 0.006N_s$
3	0.998	$y = -78 + 4.8/MRR + 0.007N_s - 0.188v_{fr}$
(i) Studer S40		
Step	R^2	Equation
1	0.988	$y = 135 + 6.5/MRR$
⋮	⋮	⋮
4	0.998	$y = -83 + 6.7/MRR + 456l_{fr} + 0.836HRC - 152v_{fr}$

N_S refers to spindle rotation speed (rev/min); v_{fr} refers to feed speed (mm/min); *HRC* refers to Rockwell hardness; l_{fr} refers to feed length (mm)

Table 4.17 Summary of SEC models for tested grinding processes

Machine	*R*-square	SEC model
Reinecker ISA 110	0.983	$\text{SEC} = 47.269 + \frac{3.399}{\text{MRR}}$
Studer S120	0.996	$\text{SEC} = 70.240 + \frac{4.781}{\text{MRR}}$
Studer S40	0.988	$\text{SEC} = 135.103 + \frac{6.510}{\text{MRR}}$

Table 4.18 Validation of SEC model for tested grinding processes

Machine	Reinecker ISA 110	Studer S120	Studer S40
Grinding wheel	CBN	Al_2O_3	CBN
Workpiece	100Cr6	100Cr6	16MnCr5
w (mm)	10	10	10
Q'_w (mm^3/mm·s)	0.8	0.4	1.2
V'_w (mm^3/mm)	250	120	250
MRR (cm^3/s)	0.008	0.004	0.012
Q (cm^3)	2.5	1.2	2.5
Predicted SEC (kJ/cm^3)	472.14	1265.49	677.60
Predicted E (kJ)	1180.36	1518.59	1694.01
Measured E_i (kJ)	1132.67	1498.04	2510.11
Difference (%)	4.21	1.37	3.52

complete results are presented in Appendix 4. As the results show, the errors of the predictions remained less than 10 % of the total energy consumption. Therefore, the derived SEC models have been validated with a high accuracy.

4.4 Energy Efficiency Characterization for Injection Molding Processes

4.4.1 Background

Injection molding is one of the most commonly used thermoplastic processes. It refers to the process of manufacturing plastic parts, where the plastic pellets or powders are firstly melted and then forced into a cavity to form a desired shape. This process is favored by designers and engineers for its inherent ability to manufacture parts using a variety of materials, shapes and sizes. In many cases injection molding is the only viable option for the manufacture of high-volume components due to a short cycle time and high levels of repeatability and accuracy (Rosato 2000). Numerous products such as mobile phones, computers and automobiles contain injection molded parts.

The injection molding machine tools generally consists of four units; heating unit, clamping and injection unit, and cooling unit. According to the type of driving systems, the machines can be classified into hydraulic, hybrid and all-electric types. A typical hydraulic type machine is illustrated in Fig. 4.22, which converts electricity into heat and hydraulic pressure for performing the injection molding process.

This research selected three different hydraulic-type injection molding machines for developing energy consumption models. They cover a wide range of age, size, and control system, as displayed in Fig. 4.23. The German-made

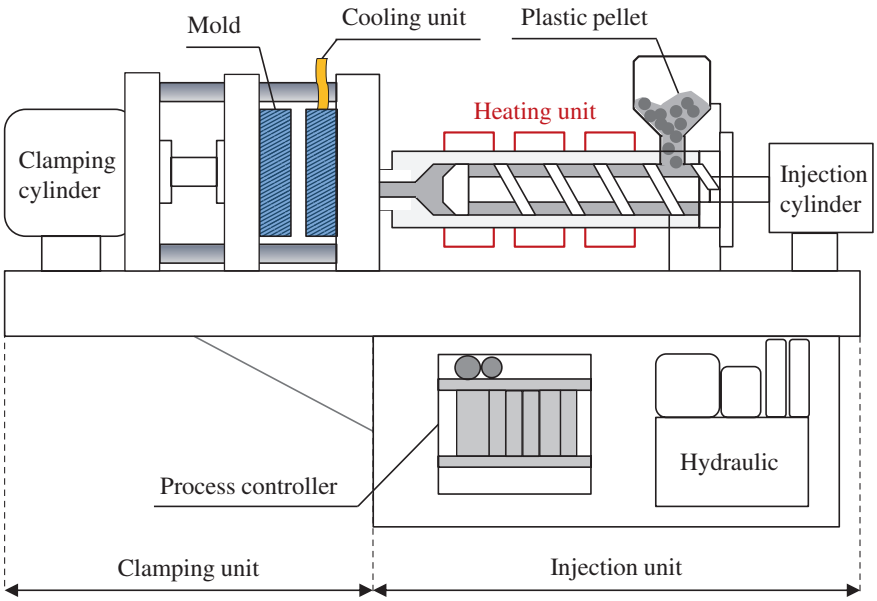

Fig. 4.22 Illustration of a hydraulic-type injection molding machine

BOY 15S was located in the manufacturing laboratory of School of Mechanical and Manufacturing Engineering, the University of New South Wales. An older and smaller version, BOY 15, and a CNC injection molding machine Battenfeld BA500CD were investigated in Sydney City TAFE.

4.4.2 Design of Experiments

Unlike the metal machining processes, there are several stages involved in one injection molding cycle; they include plasticization, filling, packing, cooling, and part ejection (Rees 2002). First, the plastic granules or pellets are melted in a heated chamber in which several heaters are switched on and off to maintain the desired temperature; then, the molten plastic is injected into the cavity, while material shrinks naturally; thus, the additional space in the cavity is filled during packing stage; once the cavity is filled completely, the molten plastics solidify with the help of a cooling system; finally, the part is ejected from the mold. There are numerous factors affecting the process, which can be grouped into the following categories:

- Type of material: generally referring to melting temperatures and density;
- Mold design: i.e. shape, size, number of cavities, wall thickness, etc.;
- Plasticizing unit: number of heaters, temperatures, decompression pressure and speed, etc.;

BOY 15S
Year: 1978
Max Pressure: 140 bar

BOY 15
Year: 1976

BattenfeldBA500CD
Year: 1990s
Max Pressure: 1484 bar
Clamping force: 500 kN

Fig. 4.23 Photograph of tested injection molding machines

- Injection and holding unit: i.e. injection pressure and speed, holding pressure, etc.;
- Clamping unit: i.e. clamping pressure, mold close and open speed;
- Cooling unit: cooling water flow rate;
- Ejecting unit: ejection speed and pressure;
- Timers: injection and holding time, cooling time, and dwell time;
- Operation environment: i.e. temperature, humidity, etc.

Correspondingly, there are a large number of control options to configure the above mentioned process parameters. Figure 4.24 shows an example of BOY 15S. The switches for pressures and speeds set a certain percentage of the maximum value. The timer can numerically configure the injection and holding time, the cooling time, and the dwell time.

Different materials feature different melting temperature and heat capacity. From the energy point of view, the energy consumption of heating units would correspond to the use of different materials. Normally, the heaters are set at the lowest possible temperature to melt the plastics while achieving adequate viscosity. Moreover, different heat capacity results in different time for melting and cooling the material. Thus, the material type was initially determined as a design factor, and the temperature was coupled with it.

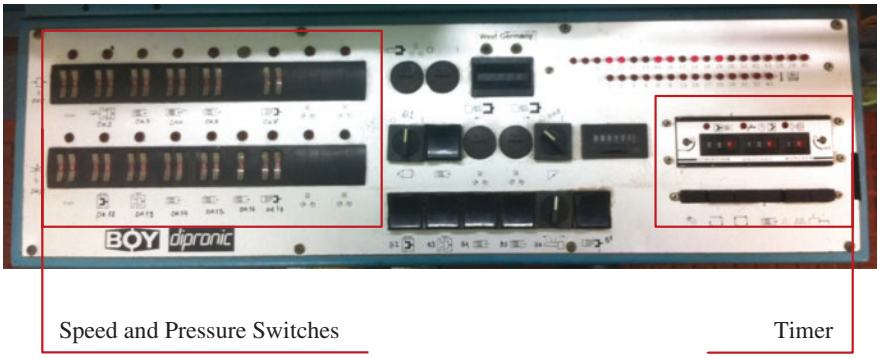

Fig. 4.24 Photograph of the control panel of BOY 15S

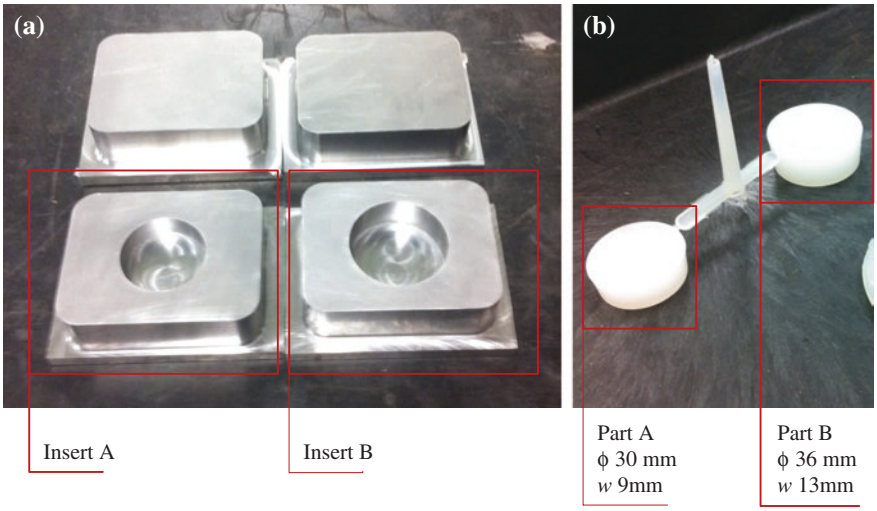

Fig. 4.25 Photograph of the inserts and injected parts on the BOY 15S. **a** Photograph of inserts. **b** Photograph of parts (Li et al. 2015)

The mold design also has a significant impact on this process (Rees 2002). The volume, wall thickness (w), cavity numbers were suggested to limit the selection of pressures, speeds, as well as the cycle time. However, mold making is an expensive and time-consuming process due to the high requirements of surface finish and dimensional accuracy. CNC machining is currently the main means of making the molding tools, owing to the accuracy and flexibility of the machine tools. For the molds with complex shape, electrical discharge machining (EDM) is also used. All the tested machines featured a two-cavity, two–plate mold. Two inserts were designed for this research, as shown in Fig. 4.25. They featured a basic round shape with different diameters and thickness (w). This design allowed the experimenters to change the volume of injected material. When both two inserts were

installed normally, the maximum injection volume was achieved. The cavity can also be blocked in order to change the injection volume.

The cycle time is another important indicator which is used to assess the productivity and economic performance of the process. It generally consists of three elements: injection and holding time, cooling time, and dwell time. Ideally, the total cycle time should be reduced to a minimal level. Thus, the dwell time, which is the pausing period between two cycles, was kept constant as 2 s throughout the experiments. The other two elements determine the total cycle time. Therefore, the injection and holding time and cooling time were considered as design factors.

There are a number of parameters for different speed and pressure. Obviously, it is inefficient to change each one of them. Some of the parameters are kept constant in practice, such as ejection speed and pressure, mold open and close speed, etc. Those parameters are set at the maximum value in order to minimize the cycle time. However, it was difficult to screen all the other parameters relating to the speed and pressure (Qureshi et al. 2012). This was due to the power consumptions of the three heaters, which switch on and off at a different pace. As a result, the accuracy of the analysis was influenced significantly. Alternatively, the speed and pressure parameters were combined as one factor. It was reasonable to assume that the higher speed and pressure may require more energy; and the combined factor would result even more significant trend. For example, if higher injection speed or higher clamping pressure require more power individually, setting both parameters at the high level would consumes much more power. Therefore, the involved factors can be summarized in an Ishikawa diagram, see in Fig. 4.26.

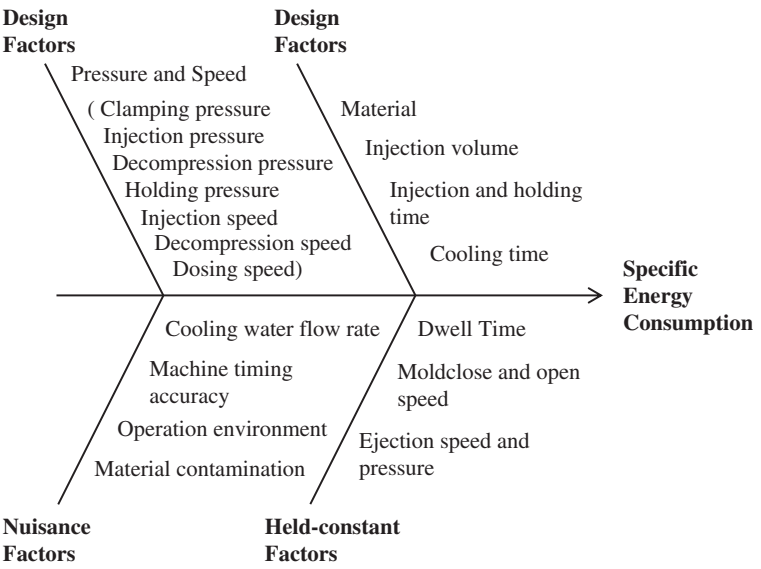

Fig. 4.26 Ishikawa diagram for tested injection molding processes

As mentioned before, the plastics have firstly been melted and then solidified. The shrinkage during the cooling stage is normal and expected. This drawback has attracted intensive research to predict and manage this phenomenon (Fischer 2003). Since this research needs observed data for input, it is impractical to measure the volume change. Alternatively, the mass of the processed material (m) is constant throughout plasticization and solidification. The injected part can be easily weighted as shown in Sect. 3.1.4. Therefore, the model response SEC for injection molding process is the total energy consumption of producing 1 g of part (kJ/g); see the equation in Eq. 4.10.

$$SEC = \frac{E}{m} = \frac{\int P_i \cdot d_t}{m} \tag{4.10}$$

Throughput rate is another important indicator for injection molding process, which suggests the process productivity. It can be considered as similar to MRR for material removal processes. The calculation of throughput rate ($\dot{m}$, g/s) is straight forward as Eq. 4.11.

$$\dot{m} = \frac{m}{T} = \frac{m}{t_i + t_c + t_d} \tag{4.11}$$

where t_i refers to the injection and holding time; t_c refers to the cooling time; and, t_d refers to the dwell time between two cycles.

After a few trial runs, the levels of each design factor were determined accordingly for the three tested materials, as shown Table 4.19. The possible wide range has been obtained in which the injected parts were neither incomplete nor with excessive flushes. Similar to the other processes, the experiment schedules were generated through the use of MiniTab®.

4.4.3 Experiment Details

From the empirical modelling point of view, each combination of process variables should be repeated several times. Hence, the machines were running at automatic mode, and produced at least 10 parts with each process configuration. Figure 4.27 shows an exemplary power curve over 11 cycles. Each cycle has then been separated and processed to calculate the SEC according to Eq. 4.10.

4.4.4 Regression Results

The similar statistical analysis was conducted here. Each process parameter was processed with curve-estimation. Similar to the results of material removal processes, the throughput with an inverse model has resulted in the highest R-square value and largest F-value. Figure 4.28 and Table 4.20 presents the model plot

Table 4.19 The levels of tested factors for injection molding processes

Factors		Variable levels								
Volume (cm^3)		6.03			18.45					
Material		High density polyethylene (HDPE)			Low density polyethylene (LDPE)			Polystyrene (PS)		
Heating unit	Zone 1 °C	260			160			120		
	Zone 2 °C	300			200			160		
	Nozzle %	30			70			0		
Timer	t_i (S)	2	6	9	2	6	9	1	5	9
	t_c (S)	20	40	60	20	60	100	8	34	68
Pressure and speed (%)	Clamping pressure	50	75	99	65	82	99	99	99	99
	Injection pressure	45	72	99	65	82	99	50	75	99
	Holding pressure	40	50	60	50	55	60	30	55	80
	Decompression pressure	10	55	99	10	25	40	20	30	40
	Injection speed	10	55	99	20	60	99	20	60	99
	Decompression speed	8	14	20	12	16	20	15	25	35
	Dosing speed	2	6	9	2	6	9	2	6	9

and the model summary for the BOY 15S respectively. The ANOVA analysis of inverse model and model plots for the other tested machine tools can be found in Appendix 3.

The residual analysis also suggest that the inverse model is a good one, since there is no clear trend observed in the residuals plot, see Fig. 4.29.

Based on above statistical analysis, the SEC model for injection molding process can be written in a form as Eq. 4.12. The values of coefficient c_0 and c_1 for the tested injection moulding processes are summarized in Table 4.21.

$$SEC = c_0 + \frac{c_1}{\dot{m}} \tag{4.12}$$

4.4.5 Model Validation

Despite the strong statistical evidence, additional runs were conducted on BOY 15S to further validate the derived model. Since the models require throughput rate as input, the mass of injected parts should be estimated. This can be done by multiplying the volume of cavities with material density. The cycle time can be

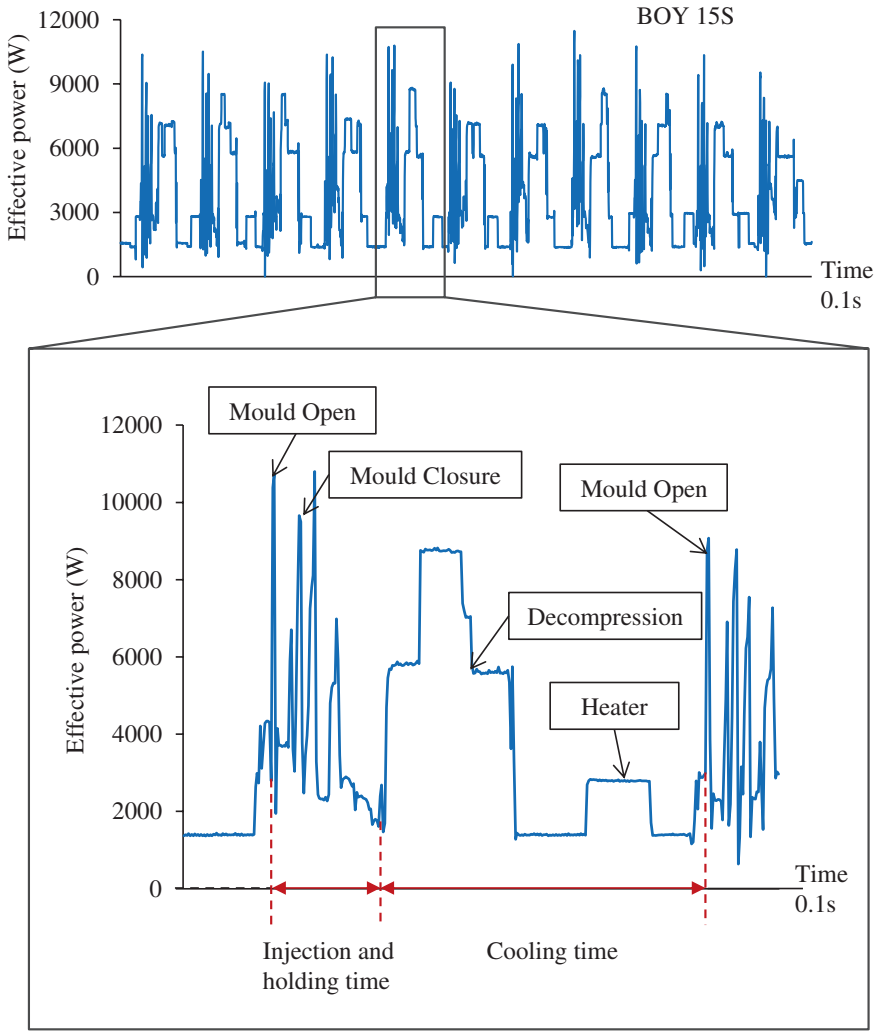

Fig. 4.27 Exemplary power curve of the tested injection molding process (Li et al. 2015)

easily estimated based on the configuration of injection and holding time, cooling time and dwell time. It should be noted that the estimation of throughput contains errors, which assumes that there is no shrinkage or flush of the injected part, and the machine timing is accurate. For the validation runs, the insert A (see in Fig. 4.25) was turned over in order to block one cavity, so the volume of injected part was different than the ones for model development. The results are listed in Table 4.22.

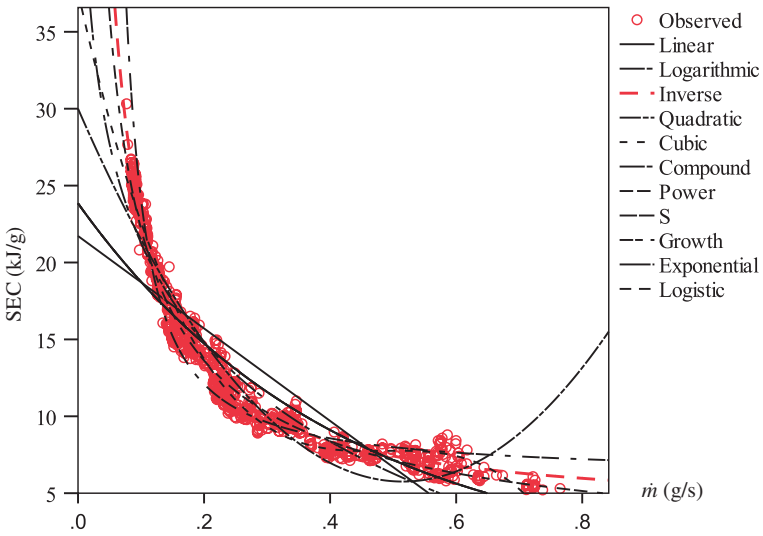

Fig. 4.28 Model plot between throughput and SEC for the BOY 15S

Table 4.20 Model summary of curve-estimation between throughput and SEC for the BOY 15S

Model type	Model summary					Equation
	R^2	F-value	DF_1	DF_2	P-value	
Linear	0.72 h	2585.25	1	998	0.000	$y = 21.7 - 30.1x$
Logarithmic	0.917	11,004.06	1	998	0.000	$y = -0.18 - 9.3 \ln x$
Inverse	0.982	54,054.51	1	998	0.000	$y = 3.6 + 1.9/x$
Quadratic	0.917	5529.60	2	997	0.000	$y = 30 - 94x + 91x^2$
Cubic	0.970	10,714.44	3	996	0.000	$y = 38 - 186x + 383x^2 - 263x^3$
Compound	0.860	6136.48	1	998	0.000	$y = 24 \times 0.09^x$
Power	0.971	33,647.59	1	998	0.000	$y = 4.4 \cdot x^{-0.703}$
S	0.928	12,887.542	1	998	0.000	$\ln y = 1.8 + 0.138/x$
Growth	0.860	6138.48	1	998	0.000	$\ln y = 3.2 - 2.4x$
Exponential	0.860	6138.48	1	998	0.000	$\ln y = \ln 24 - 2.4x$
Logistic	0.860	6138.48	1	998	0.000	–

The discrepancy between predicted and measured energy consumption were under 10 % of the actual amount. Therefore, the models have been validated, which are capable of predicting energy consumption with an accuracy of over 90 %.

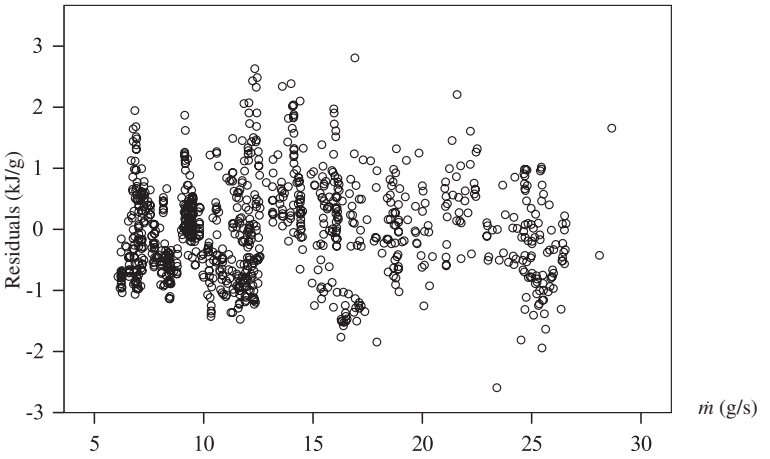

Fig. 4.29 Residuals plot of the inverse model for the BOY 15S

Table 4.21 Summary of SEC models for tested injection molding processes

Machine	*R*-square	SEC model
BOY 15S	0.982	$\text{SEC} = 3.552 + \frac{1.933}{\dot{m}}$
BOY 15	0.961	$\text{SEC} = 2.201 + \frac{2.239}{\dot{m}}$
Battenfeld BA500CD	0.966	$\text{SEC} = 1.582 + \frac{3.816}{\dot{m}}$

The unit of SEC is kJ/g; the unit of $\dot{m}$ is g/s

Table 4.22 Validation results of SEC model for the BOY 15S

Material	HDPE	LDPE	PS
Density (g/cm^3)	0.941	0.920	1.05
Injection volume, Q (cm^3)	12.42	12.42	12.42
Cycle time (s)	80	70	25
Mass, m (g)	11.69	11.43	13.04
Throughput rate, $\dot{m}$ (g/s)	0.146	0.163	0.522
Predicted SEC (kJ/g)	16.8	15.4	7.3
Predicted E (kJ)	196.15	175.90	94.65
Measured E_i (kJ)	209.251	184.15	98.25
Difference (%)	6.26	4.48	3.67

4.5 Energy Efficiency Characterization for Electrical Discharge Machining (EDM) Processes

4.5.1 Background

Electrical discharge machining (EDM) is one of the earliest non-conventional material removal processes, which has been widely used to machine hard materials or to achieve complicated shapes. It is a non-contact machining process where a series of discrete sparks are generated between the workpiece and the electrode to melt the material in a dielectric fluid. (Ho and Newman 2003). Although the origin of EDM can be traced back as far as 1768, the first EDM machine was presented almost two centuries later in 1955. With the advancement of introducing computer numerical control (CNC) in the 1980s, industries have widely used EDM for machining geometrically complex or hard material parts. Since then, numerous efforts have been made to control EDM processes more efficiently. According to Ho and Newman's review, the research interests were mainly about improving performance measures (e.g. surface quality), optimizing the process variables, monitoring and control the sparking process, simplifying the electrode design and manufacture. Abbas et al. (2007) reviewed recent research trends in EDM including ultrasonic vibration, dry EDM machining, EDM with powder additives, EDM in water, etc. Those research outcomes play an essential role to enhance the capability and stability of EDM processes, however the energy efficiency of EDM processes remains untouched.

As mentioned in Sect. 2.1.3, initial exergy study by Gutowski et al. (2006) has suggested that the EDM process is much more energy intensive comparing to other conventional material removal processes. Owing to the stochastic nature of EDM processes, theoretical models fail to practically predict the energy consumption and material removal rate (MRR) of EDM processes (Abbas et al. 2007). In addition, the auxiliary components such as cooling unit consume a significant share of energy. Therefore, the EDM processes are selected to further test the validity of the proposed methodology.

There are a number of machine variations based on the general process mechanism of EDM. Two main types are ram EDM (or called die-sinking EDM) and wire-cut EDM. The ram EDM is the process which the form of the electrode is mirrored in the workpiece. The wire-cut EDM uses a thin continuously travelling wire feeding through the workpiece to generate complicated shapes. In this research, two ram EDM machines were used to characterize their energy efficiency as shown in Fig. 4.30. Both machine tools were located in Sydney City TAFE. One is a SODICK A3R manufactured in 1997, which is a CNC machine with a set of integrated programs. The other machine is an AGIE TRON 30 L, which is a manual command type with a capacity of 30 A.

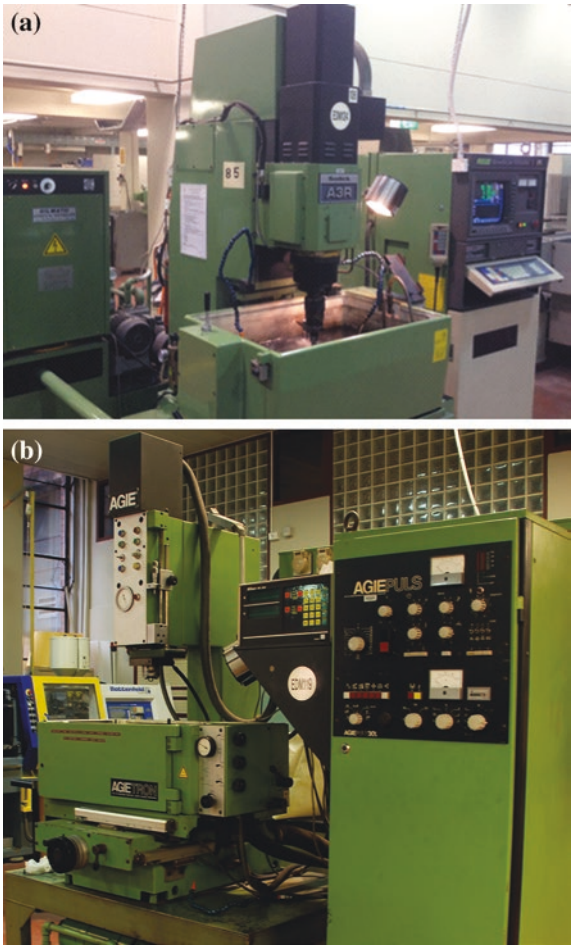

Fig. 4.30 Photograph of tested ram EDM machines. **a** SODICK A3R. **b** AGIE TRON 30L

4.5.2 Design of Experiments

The EDM machining is a complex combination of electrical, fluidic and mechanical process. A number of controllable and uncontrollable process parameters can potentially affect its energy efficiency. These factors can be generally classified into following five groups:

- Tool parameters: material, geometry, electrode polarity, electric conductivity, tool wear, potential arcing, etc.;
- Workpiece parameters: material, melting temperature, electric conductivity, thermal expansion, calorific capacity, etc.;
- Machining parameters: discharge peak current, on-time, off-time, no-load voltage, working voltage, up and down movement, feed speed, etc.;

- Dielectric fluid parameters: electric conductivity, capacitance, viscosity, calorific capacity, etc.;
- Other parameters: servo-voltage; arc detection level, spark gap, discharge stability, process arc control reaction, etc.

Due to the large number of variable factors, a combination of quantitative and qualitative screening approach was applied for the EDM case. Firstly, previous analytical and empirical studies suggested that the machining parameters have a significant impact on MRR; so, these parameters have been directly grouped as design factors. The tested machines only use mineral based oil as dielectric fluid, so the dielectric fluid related parameters were held constant for this research. Some other factors were unclear and a quantitative screening test was conducted to determine its main effect on SEC and MRR, for example, electrode geometry. Two different shapes of graphite electrodes were used for the screening test. The t-test suggested that the effect of electrode geometry on SEC cannot be neglected at this stage. Thus, the electrode geometry was grouped as design factors. After completing the screening tests, all the process parameters were grouped into four types as shown in Fig. 4.31.

The levels of variances were further determined according to the recommend process parameter table by AGIE® and the provided code by SODICK®. Two different types of electrode, electrode geometry, and workpiece material were

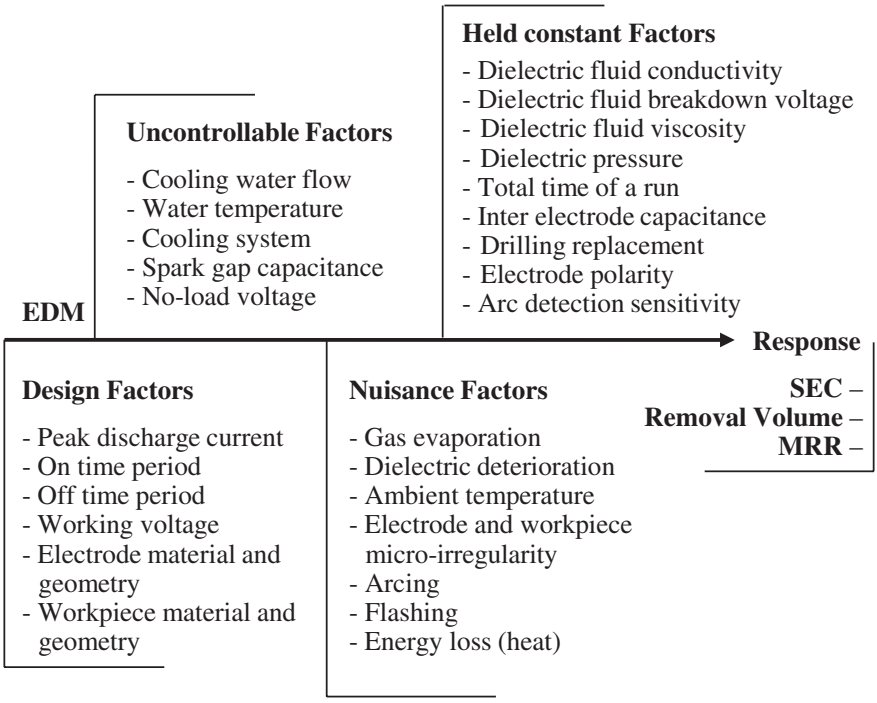

Fig. 4.31 Ishikawa of EDM processes

Table 4.23 The levels of tested factors for EDM processes

Factors	Variable levels						
Electrode material Electrode shape Workpiece material	Graphite Square 10 × 10 mm Mild steel				Copper Cylindrical ϕ10 mm Aluminum		
Peak discharge current (A)	2	4	5	8	10	12	16
	17	20	30	37			
No-load voltage (V)	12	90	120	180	280		
On time (μs)	4	20	40	60	80	100	150
	180	210	550				
Off time (μs)	6	30	40	60			

tested. Since each design factor has different levels of variances, a full factorial experiment design was used in this case. Each combination of process parameters were repeated for 5 times. Table 4.23 lists the tested levels of variances.

4.5.3 Experiment Details

The experiments were conducted according to the experiment schedule derived in Sect. 4.5.2. Figure 4.32 shows an exemplary experiment with square graphite electrode on SODICK A3R.

The energy consumption of the entire machine including the cooling system was recorded during each experiment. The energy profile of the SODICK A3R is shown as an example in Fig. 4.33.

As the Fig. 4.33 shows, the cooling system was switched on and off regularly during the entire time. A clear power increase was observed whenever the cooling system was activated. In comparison, the machining power was only fluctuated with a very small magnitude. This trend is due to that the metering point is at the main bus of the entire machine tool, and individual electrical discharge (spark) is not visible at this level. Normally, the spark is generated by the power supply unit where the AC power is converted to DC power, and a capacitor is used to precisely

Fig. 4.32 Photograph of one EDM experiment

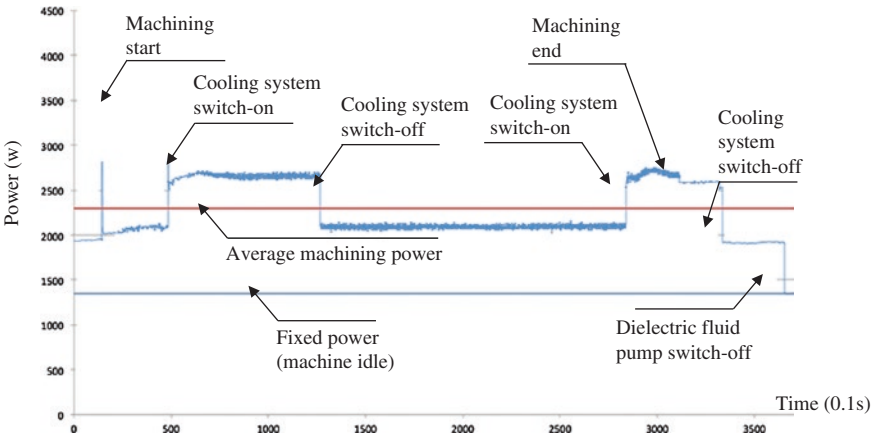

Fig. 4.33 The power profile of SODICK A3R (Li and Kara 2015)

control the power and duration of each pulse. The total machining energy consumption is calculated as Eq. 4.13.

$$E_{total} = P_{Ave.Mach} \times (t_1 - t_0) \tag{4.13}$$

where $P_{Ave.Mach}$ is the average machining power; t_0 is the machining start time; and, t_1 is the machining end time.

As mentioned before, each run of experiment has been kept constant for 5 min, and the final depth-of-cut has also been precisely recorded. Then, the total material removal volume, Q_{volume} can be calculated depending on the shape of electrode and the final depth-of-cut. Hence, the SEC and MRR of each experiment run can be derived according to Eqs. 4.14 and 4.15.

$$SEC = \frac{E_{total}}{Q_{volume}} P_{Ave.Mach} \tag{4.14}$$

$$MRR = \frac{Q_{volume}}{t_1 - t_0} \tag{4.15}$$

Notably, the cooling system and the dielectric fluid pump remained active after the end of machining process. It took approximately 1 min until the power was back to the fixed level. The amount of energy consumption due to this reason was almost constant disregarding the duration of machining processes or the material removal volume. In other words, it is independent from the design factors. Therefore, this share of energy consumption was purposely excluded for the modelling stage in Sect. 4.5.4. Alternatively, it should be added as a fixed amount for each machining process.

4.5.4 Regression Results

At this stage, all the observed SEC and MRR values were processed with SPSS® for modelling and regression analysis according to the proposed methodology in Chap. 3.

Firstly, the relationship between SEC and process parameters was analyzed by using the curve estimation. This analysis investigates the main effect of each process parameter or a combined process parameter, and it determines the best-fit model among the 11 available model types. All the design factors showed a poor ability to individually describe the variance of SEC. The R^2-value for these models is less than 0.3. Like conventional material removal processes, the MRR, a combined process parameter, has a decisive influence on the SEC of EDM processes. As shown in Fig. 4.34, the inverse model is the best-fit between the observed SEC and MRR on SODICK A3R, whose R^2-value is 0.99. The same trend has been observed for the AGIE TRON 30L. The derived SEC models are summarized in Table 4.24.

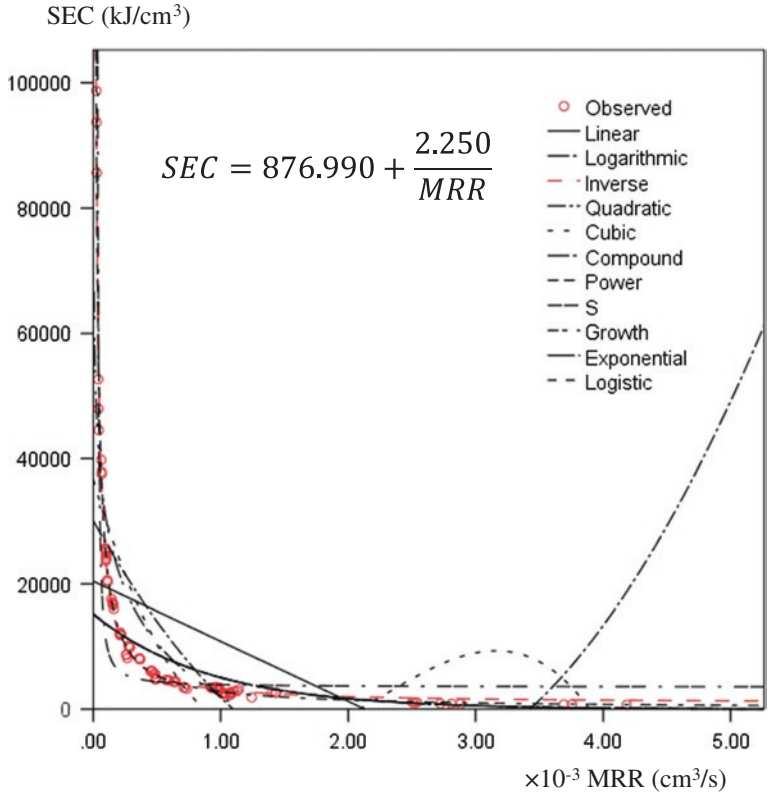

Fig. 4.34 The curve estimation between SEC and MRR of SODICK A3R (Li and Kara 2015)

Table 4.24 Summary of SEC models for tested EDM processes

Machine	*R*-square	SEC model	Fixed power
SODICK A3R	0.990	$SEC = 876.990 + \frac{2.250}{MRR}$	1.4 kW
AGIE TRON 30L	0.989	$SEC = 1255.974 + \frac{2.111}{MRR}$	1.26 kW

The unit of SEC is kJ/cm^3; the unit of MRR is cm^3/s

Since the MRR has been proved as a decisive factor for SEC models, the prediction of MRR becomes equally important in order to predict energy consumption of EDM processes. Owing to the stochastic nature of EDM processes, it is challenging to derive models for predicting the MRR. While previous researches were mainly focused on maximizing MRR, a number of modelling efforts have been mentioned by Hinduja and Kunieda (2013). For example, Yahya and Manning (2004) derived a mathematical MRR model by using dimensional analysis; Wang and Tsai (2001) provide a semi-empirical model to predict the MRR of work and tool; Torres et al. (2015) provided an empirical MRR model of machining hard-to-machine alloys. However, the model form appears different among those approaches, and the derived empirical coefficients are limited to the tested combination of electrode and workpiece material. Therefore, the observed MRR through the experiments were used again to further characterize the relationship between MRR and process parameters.

The process parameters (e.g. peak discharge current, on-time, etc.) were first used to describe the observed MRR. The curve estimation suggests that there is a significant correlation between the process parameters and the MRR. However, the *R-square* value is low which means the MRR is affected by a number of process parameters. Alternatively, two theoretical MRR models from previous analytical studies were selected to test the model validity, and to derive coefficients for prediction purpose. The theoretical model 1 is based on Yahya and Manning's dimensional analysis (2004), whereas the theoretical model 2 was based on the semi-empirical study by Wang and Tsai (2001). The observed MRR and process parameters were then processed with ANOVA analysis by SPSS®, as summarized in Table 4.25.

As the *R-square* value suggests, both MRR models are capable of describing the observed variance. The theoretical model 2 has a higher *R-square* value, which is mainly due to the consideration of a higher order of process variables. However, the coefficients of the theoretical model 2 appear less logical than the ones of the theoretical model 1. For example, the aluminum workpiece, comparing to mild steel, is easier to machine and has a lower melting temperature. The experimental results confirmed that the MRR of machining aluminum is higher than mild steel. The coefficient A_1 in the theoretical model 1 agrees with the trend, whereas the one in the theoretical model 2 shows an opposite trend. In addition, the *R-square* difference between model 1 and 2 is marginal. Therefore, the theoretical model 1 is preferred which is also more practical.

Table 4.25 Derived MRR models for the tested combinations of electrode and workpiece materials

Theoretical model 1	$MRR = A_1 \cdot U \cdot I \cdot t_{on} \cdot F$			
Electrode	Copper		Graphite	
Workpiece	Steel	Aluminum	Steel	Aluminum
A_1	1.660×10^{-8}	4.993×10^{-8}	2.429×10^{-8}	5.707×10^{-8}
R-square	0.936	0.964	0.897	0.976
Theoretical model 2	$MRR = A_1 \cdot \left(A_2 + A_3 \cdot t_{ratio} + A_4 \cdot t_{ratio}^2 + A_5 \cdot t_{ratio}^3\right) \cdot U \cdot I \cdot t_{on} \cdot F$			
Electrode	Copper		Graphite	
Workpiece	Steel	Aluminum	Steel	Aluminum
A_1	1.415×10^{-9}	3.539×10^{-10}	0.078	0.003
A_2	9.371	301.525	0.026	−1.445
A_3	−0.815	−180.250	−0.080	4.478
A_4	0.690	50.911	0.077	−4.334
A_5	−0.065	−3.625	−0.023	1.300
R-square	0.988	0.979	0.963	0.982

A_i refers to the model coefficient; U refers to the no-load voltage (in the unit of V); I refers to the peak discharge (in the unit of A); t_{on} refers to the on time (in the unit of μs); F refers to the frequency; t_{ratio} refers to the ratio between on time and off time; the unit of MRR is mm^3/min

4.5.5 Model Validation

Besides the statistical proofs presented in Sect. 4.5.4, additional runs were conducted on both tested machines to further validate the accuracy of derived empirical models. Comparing to the process parameters used in the stage II, two different settings were used with five repetitions. The MRR was estimated according the theoretical model 1 (see in Table 4.25). The predicted SEC was compared with the measured average SEC as listed in Table 4.26. The error margin of the energy consumption prediction is calculated, which is less than 10 % for all the validation tests. Therefore, the derived SEC and MRR models are accurate enough for predicting the energy consumption of EDM processes.

4.6 Summary

This chapter has validated the proposed methodologies to characterize the energy efficiency on variant manufacturing processes including turning, milling, grinding, injection molding and electrical discharge machining. Among all the tested cases, a reverse trend has been consistently observed between the specific energy

Table 4.26 Model Validation on two tested EDM machine tools

Machine name	SODICK A34	
Run number	Run 1	Run 2
Electrode/workpiece	Copper/steel	Copper/steel
Predicted MRR (mm^3/min)	37.448	9.358
Measured SEC (kJ/cm^3)	4624.01	16,817.61
Predicted SEC (kJ/cm^3)	4484.38	15,313.62
Error[a]	3.1 %	9.8 %
Machine name	AGIE TRON 30L	
Run number	Run 3	Run 4
Electrode/workpiece	Graphite/steel	Graphite/steel
Predicted MRR (mm^3/min)	1.2620	0.3785
Measured SEC (kJ/cm^3)	2909.99	6326.46
Predicted SEC (kJ/cm^3)	2928.76	6833.64
Error[a]	0.6 %	7.4 %

[a] $Error = \frac{|SEC_{prediction} - SEC_{actual}|}{SEC_{actual}} \times 100\,\%$

Table 4.27 List of observed data for tested machine tools (Access via http://extras.springer.com)

Machine name
Colchester Tornado A50
MoriSeik NL2000 MC/500
MoriSeiki SL15
Nukamara TMC-15
IKEGAI AX20
MoriSeiki DuraVertical 5100
Fadal VMC4020
DMU 60P
Reinecker ISA 110
Studer S120
Studer S40
BOY15S
BOY15
Battenfeild BA500CD

consumption and process rate (e.g. material removal rate and throughput). The derived SEC models offer a great ability to predict energy consumption of a given process with an accuracy of over 90 %. The observed data as listed in Table 4.27 can be accessed via the link (http://extras.springer.com).

References

Abbas NM, Solomon DG, Bahari F (2007) A review on current research trends in eletrical discharge machining. Int J Mach Tools Manuf 47:1214–1228

Armarego EJA, Wiriyacosol S (1978) Oblique machining with triangular form tools—I. Theoretical investigation. Int J Mach Tool Des Res 18(2):67–80

Fischer JM (2003) Handbook of molded part shrinkage and warpage, 1st edn. William Andrew, Norwich

Gutowski T, Dahmus J, Thiriez A (2006) Electrical energy requirements for manufacturing processes. In: 13th CIRP international conference on life cycle engineering. Leuven

Hinduja S, Kunieda M (2013) Modelling of ECM and EDM processes. CIRP Ann Manuf Technol 62(2):775–797

Ho KH, Newman ST (2003) State of the art electrical discharge machining (EDM). Int J Mach Tools Manuf 43:1287–1300

Kalpakjian S, Schmid SR (2005) Manufacturing engineering and technology, 5th edn. Prentice Hall, Englewood Cliffs

Kara S, Li W (2011) Unit process energy consumption models for material removal processes. CIRP Ann—Manuf Technol 60(1):37–40

Li W, Kara S (2011) An empirical model for predicting energy consumption of manufacturing processes: a case of turning process. In: Proceedings of the Institution of Mechanical Engineers, Part B. J Eng Manuf 225(9):1636–1646

Li W, Kara S (2015) Characterising energy efficiency of electrical discharge machining (EDM) processes. Procedia CIRP 29:263–268

Li W, Kara S, Qureshi F (2015) Characterising energy and eco-efficiency of injection moulding processes. Int J Sustain Eng 8(1):55–65

Malkin S (1975) Specific energy and mechanisms in abrasive processes. In: Proceedings of third North American metalworking research conference. Carnegie Press, Lancaster

Malkin S, Guo C (2008) Grinding technolog—theory and applications of machining with abrasives, 2nd edn. Industrial Press, New York

Oxley PLB (1998) Development and application of a predictive machining theory. J Mach Sci Technol 2(2):165–189

Qureshi F, Li W, Kara S, Herrmann C (2012) Unit process energy consumption models for material addition processes: a case of the injection molding process. In: 19th CIRP international conference on life cycle engineering. Berkeley

Rees H (2002) Mold engineering, 2nd edn. Hanser Gardner Publications, Cincinnati

Rosato DV (2000) Injection molding handbook, 3rd edn. Springer, Berlin

SECO® Tools (2009) MN2009-turning: the machining navigator catalogue

Sreejith PS, Ngoi BKA (2000) Dry machining: machining of the future. J Mater Process Technol 101(1):287–291

Torres A, Puertas I, Luis CJ (2015) Modelling of surface finish, electrode wear and material removal rate in electrical discharge machining of hart-to-machine alloys. Precis Eng 40:33–45

Wang PJ, Tsai KM (2001) Semi-empirical model on work removal and tool wear in electrical discharge machining. J Mater Process Technol 114:1–17

Yahya A, Manning CD (2004) Determination of material removal rate of an electro-discharge machine using dimensional analysis. J Phys D Appl Phys 37:1467–1471

Chapter 5
Eco-efficiency of Manufacturing Processes

With the proposed methodology in Sect. 3.2, this chapter further characterizes the manufacturing processes in terms of their eco-efficiency. The characterization starts with processes where the main energy and resource consumption is only electricity, such as turning, milling, and injection molding. Then, a grinding case is presented to demonstrate and validate the proposed methodology for a more complicated case.

5.1 Eco-efficiency of Material Removal Processes

5.1.1 The Value of Material Removal Processes

As the name suggested, the primary objective of material removal processes is removing material from the workpiece. Thus, the process value can be easily defined as the removal of volume. This is true for most of the turning and milling processes, where the surface finish is less important. However, in machining for finishing purposes, the desired surface roughness needs to be achieved; otherwise, the part will be rejected. In that case, the surface roughness becomes more important, and thus should not be ignored. In order to achieve a high surface finish, a small feed rate or depth of cut is normally applied resulting in a slow material removal rate. Consequently, the energy consumption for removing the same amount of material would be relatively high according to the derived SEC models.

Besides limiting the range of material removal rate, the additional requirements of surface roughness does not further affect the process. Therefore, the surface finish of turning and milling process can be initially ignored. The following analysis is based on turning and milling processes with a general machining purpose; and, the process function is defined as removing 1 cm^3 of material.

W. Li, *Efficiency of Manufacturing Processes*, Sustainable Production,
Life Cycle Engineering and Management, DOI 10.1007/978-3-319-17365-8_5

5.1.2 The Associated Environmental Impact of Material Removal Processes

As discussed in Sect. 3.2, the associated environmental impact of turning and milling processes consists of three parts, electricity energy consumption, usage of cutting tool, and the loss of cutting fluid during the process.

Preliminary environmental studies for machine tools used in discrete part manufacturing (e.g. turning and milling) indicate that more than 99 % of the environmental impacts are due to the consumption of electrical energy (Cecimo 2009). The derived SEC model describes the dynamic behavior of unit process in terms of energy consumption. As mentioned in Sect. 3.2.3, the environmental impact due to electricity generation is location specific. For example, the CO_2 emissions from electricity and heat generation for Australia and Brazil are 853 and 64 g/kWh in 2009 respectively (International Energy Agency 2011). This huge difference is due to the use of primary energy resource; Australia relies on coal for electricity generation, whereas Brazil mainly uses hydro energy which is free of CO_2 emissions. By using the derived SEC models, the energy induced CO_2 emissions can easily be calculated by multiplying the carbon intensity of electricity generation in a specific region. Therefore, the SEC model provides generic information, and enables further analysis of environmental impacts due to electricity consumption.

The environmental impact due to tool consumption can be initially neglected due to the long tool life. Gu et al. (1999) explored the tool wear mechanism of uncoated and coated milling inserts by cutting 4140. According to their results, the correct selection of tool material can dramatically improve the tool life. In practice, an insert can normally last for a few months to a year, thus the environmental impact due to the use of tool becomes negligible for removing 1 cm^3 of material.

The negative environmental impacts of cutting fluid are discussed in Sect. 3.2.3. In order to overcome those drawbacks, dry machining is currently promoted by a number of researchers (Stanford and Lister 2002; Graham 2000; Sreejith and Nogi 2000). They suggested different approaches to apply dry cutting whilst enhancing surface finish, accuracy, stability, chip-breaking characteristics and promoting chip transport. One of these is through the optimization of cutting tools, for instance the use of new coatings, which is claimed to reduce the thermal load on the tip as well as reducing the sliding friction on the tool chip contact face. Dry machining has been practiced in different turning and milling processes in industry. Therefore, the eco-efficiency evaluation is limited to dry machining environment; thus, the environmental impacts of cutting fluids is excluded in this case.

5.1.3 The Interrelationship Within the Material Removal Processes

According to above analysis, only the electricity consumption is included in the eco-efficiency evaluation. Therefore, the SEC model can be directly used for

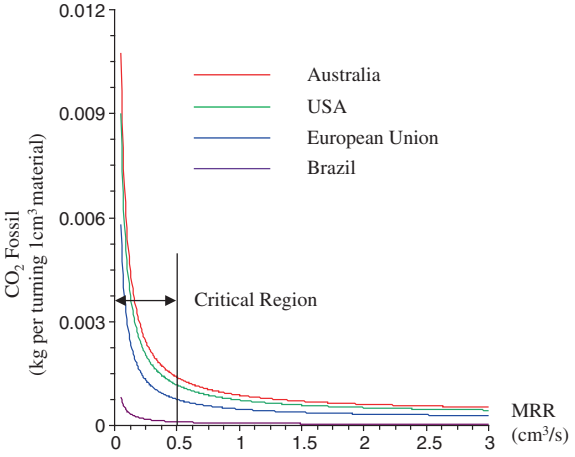

Fig. 5.1 Environmental impact (CO_2 Fossil) against MRR (Colchester Tornado A50)

evaluating eco-efficiency of material removal processes. If the process is located in the European Union, 1 kJ of electricity consumption equals to 0.000128 kg fossil fuel CO_2 emissions ('CO_2 Fossil') according to Ecoinvent database Version 2.2 (2010). The value for Australia, USA, and Brazil is 0.000237, 0.000199 and 0.000018 kg CO_2 Fossil emissions per 1 kJ of electricity consumption. Eco-efficiency evaluations for the Colchester Tornado A50 in different regions are compared in Fig. 5.1.

As shown in the Fig. 5.1, the curve of CO_2 emissions is just an offset of the SEC model. Due to the high carbon intensity of electricity generation, Australia results in the highest CO_2 Fossil emissions among other countries. Brazil performs better than other major industrial countries due to the use of hydro energy. Notably, if the electricity energy is completely generated from renewable resources, the environmental impact of the material removal process would be close to zero emission. However, current electricity generation still relies on coals and other none-renewable resources. Thus, the electricity consumption still dominates the environmental impacts in most of the world. In addition, reducing MRR within the range from 0 to 0.5 cm^3/s would result a dramatic increase of CO_2 Fossil emissions. Thus, this critical region should be avoided if possible.

5.2 Eco-efficiency of Injection Molding Processes

5.2.1 The Value of Injection Molding Processes

As mentioned in Sect. 3.2.2, the value of injection molding processes can be measured by the weight of injected part. This simple measurement is found efficient as the measured weight can be compared with the weight of a standard part; thus, the major defects such as flash and short shots can be quantified by the weight

difference. Of course, other quality measures are important for injection moldings, such as surface finish, shape complexity, and dimensional accuracy. However, these measures are product specific, and it is difficult to be objective when comparing among different products. Moreover, these measures are mainly relying on the mold design and production. From a unit process point of view, theses quality measures are not comparable among different injected parts. Thus, these measures cannot be compared equally. Alternatively, it would be helpful to develop a matrix for evaluating the value of the process including above mentioned requirements, meanwhile each measure can be weighted according to customer's preferences. To develop such a matrix requires comprehensive surveys about the capacity of the injection molding processes, the general customer requirements, the variety of injected parts, etc. At this stage, the weight is used for representing the value of the injection molding processes. For a given shape of injected part, the value of injection molding process can be increased by maximizing the parts per injection cycle. In that sense, the total weight of injected parts per cycle is maximized, so is the value of the process.

5.2.2 The Associated Environmental Impact of Injection Molding Processes

As reviewed in Sect. 2.2.2, Thiriez and Gutowski conducted environmental analyses of injection molding process. However, they only included the environmental impacts during the production of plastic pellets into their analysis. Consequently, the environmental impacts of injection molding process itself became insignificant. The results have emphasized the importance of material production or the selection of material, but they do not reflect the real energy and eco-efficiency of the injection molding process itself since an averaged specific energy consumption of the injection molding process was used for their analyses.

Unlike the pervious tested metal machining processes, there is no cutting tool or other additional resources consumed during the process. Although the production of mold may require some energy-intensive processes such as EDM, the mold can be used for a long period with the careful selection of mold material and manufacturing methods. Thus, the energy consumption and the associated environmental impact due to mold production can be shared with a large number of produced parts; and, it can be ignored from an injection molding process point of view.

Injection molding machine tools solely use water in the cooling system. The water flow is supplied by either a pump motor or a centralized water circulating system. In many parts of the world industrial water use is an important concern due to local or regional water scarcity, e.g. Australia; however, since most injection molding processes use closed cooling channels, the amount of evaporated water is believed to be negligible. Therefore, in this research, the environmental impacts due to the use of cooling system can be simplified as add-on electricity consumptions to the derived SEC models.

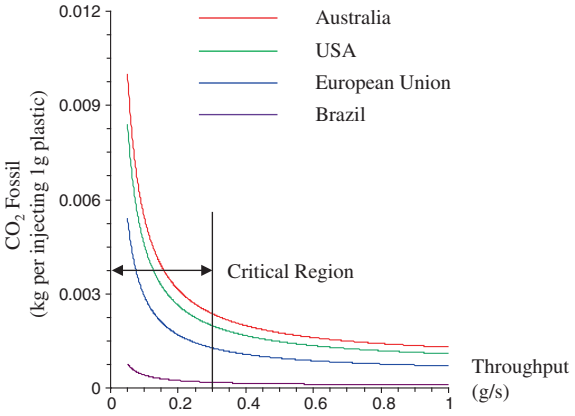

Fig. 5.2 Environmental impact (CO_2 Fossil) against throughput (BOY 15S) (Li and Kara 2015)

Therefore, the environmental impacts of injection molding processes are mainly due to the use of electricity. The derived SEC models for injection molding process actually are the energy consumption for processing 1 g of plastics. Since the value of injection molding process can be measured by the weight, the inverse of the SEC represents the eco-efficiency of injection molding processes. In general, the higher the throughput rate, the more plastics processed during a unit time; hence, the process consumes less energy, resulting less environmental impacts. Similar to the case as turning and milling, the environmental impacts of the process became location specific, where the resources for electricity generation determines the CO_2 emissions of 1 kWh used electricity. Figure 5.2 shows the relationship between CO_2 Fossil emissions per 1 g processed material and throughput rate in different regions. The figure is similar to the one for the turning machine (Fig. 5.1), where Australia results in the highest CO_2 emissions due to high carbon intensity of electricity generation. In addition, a critical region has been also identified. Increasing throughput in the range from 0 to 0.3 g/s would result in a considerable reduction of CO_2 Fossil emissions.

5.3 Eco-efficiency of Grinding Processes

5.3.1 The Value of Grinding Processes

Unlike turning and milling processes, the surface integrity has the highest priority for grinding processes. Thus, the surface roughness should be included to value this process, which is also extremely sensitive to the topography of the grinding wheel or any changes of process parameters (Jawahir et al. 2011). The surface roughness R_z was monitored during the additional grinding experiments with HOMMEL-ETAMIC® T1000 basic, as shown in Fig. 5.3.

The additional experiments were conducted on the Studer S120 under different material removal rate and different material removal volume. The experiment

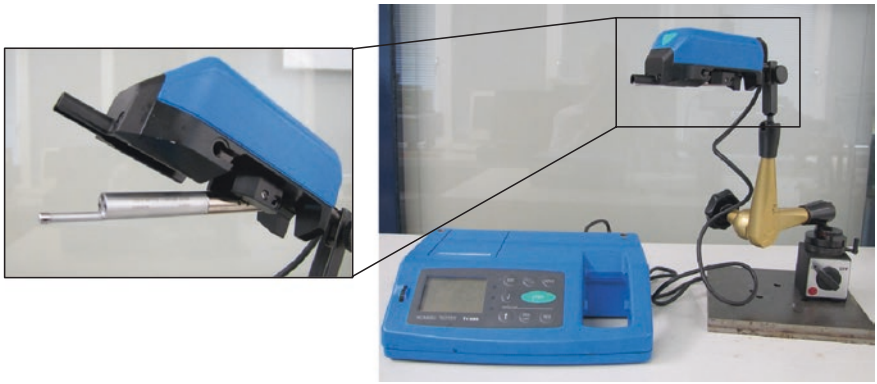

Fig. 5.3 Photograph of surface roughness measurement device

procedure was very similar to the experiments during model development, as presented in Sect. 4.3. Both CBN and Al_2O_3 wheels were tested to grind 100Cr6. The surface roughness R_z (μm) was measured at four different points at the work piece. The measured surface roughness was plotted over the energy consumption trend in Figs. 5.4 and 5.5 for CBN and Al_2O_3 respectively. As shown in both figures, the surface roughness measurement after grinding the first 100 mm^3/mm remains relatively constant due to the effective dressing process (the lower dash line). However, there is a general trend that the surface roughness worsens as MRR increases, especially when grinding with Al_2O_3 grinding wheels. It clearly shows a trade-off between energy consumptions and surface roughness.

For a given MRR, increasing specific material removal volume (V'_w) also degrades the surface roughness. As shown in the Figures, the longer color bar indicates the requirement for more frequent dressing in order to maintain constant surface finish. The relationship between surface roughness (R_Z) and process parameters (V'_w and Q'_w) were given empirically as shown in Eq. 5.1 ($R^2 = 0.908$).

$$R_Z = \beta_0 + \beta_1 \cdot Q'_W \cdot V'_W \tag{5.1}$$

According to the trade-off analysis, there is a cross region resulted in the Figs. 5.4 and 5.5. It suggests that when MRR is around 0.01 cm^3/s, grinding with CBN wheel will result in low energy consumption, high surface finish and relatively low tool wear rate. A similar point was found for Al_2O_3 grinding wheels as 0.0075 cm^3/s. They can be recommended as the first-choice of material removal rate.

5.3.2 The Associated Environmental Impact of Grinding Processes

Besides the electrical energy consumption during the grinding process, it requires dressing process to keep the sharpness of the grinding wheel. As the color bar in Figs. 5.4 and 5.5 shows, the grinding wheel lost the prefect sharpness during

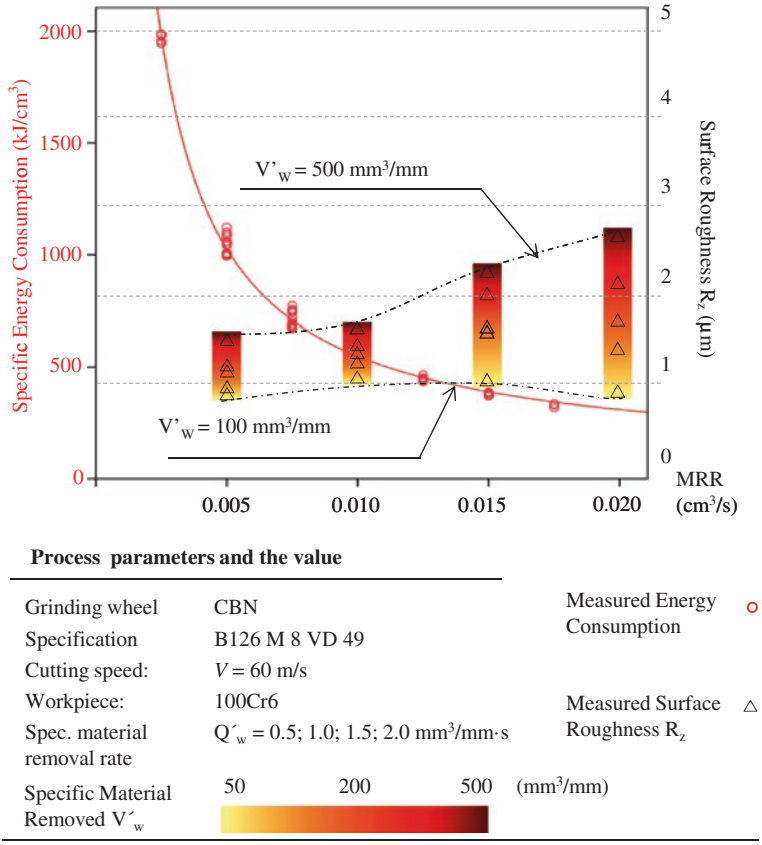

Fig. 5.4 Trade-off between energy consumption and surface roughness (CBN wheel on the Studer S120)

the abrasive machining process. Once the surface roughness exceeds the desired requirement, the dressing process should be performed, which consumes electricity, coolant, grinding wheel and dresser. During the additional experiments, the radial grinding wheel wear Δr_s was also measured. After each infeed, the grinding wheel was ground in a thin steel plate (0.25 mm); then, the grinding wheel profile was measured through the thin steel plates with a measuring probe, as shown in Fig. 5.6.

The empirical relationship between dressing amount (Δr_s) and process parameters were derived and displayed in Eq. 5.2 ($R^2 = 0.904$).

$$\Delta r_s = \alpha_0 + \alpha_1 \cdot Q'_W \cdot V'_W \tag{5.2}$$

The information can be used to determine the amount of grinding wheel to be removed during dressing process. It can be considered as the tool consumption of the unit process. Thus, tool consumption can be theoretically included for the eco-efficiency evaluation.

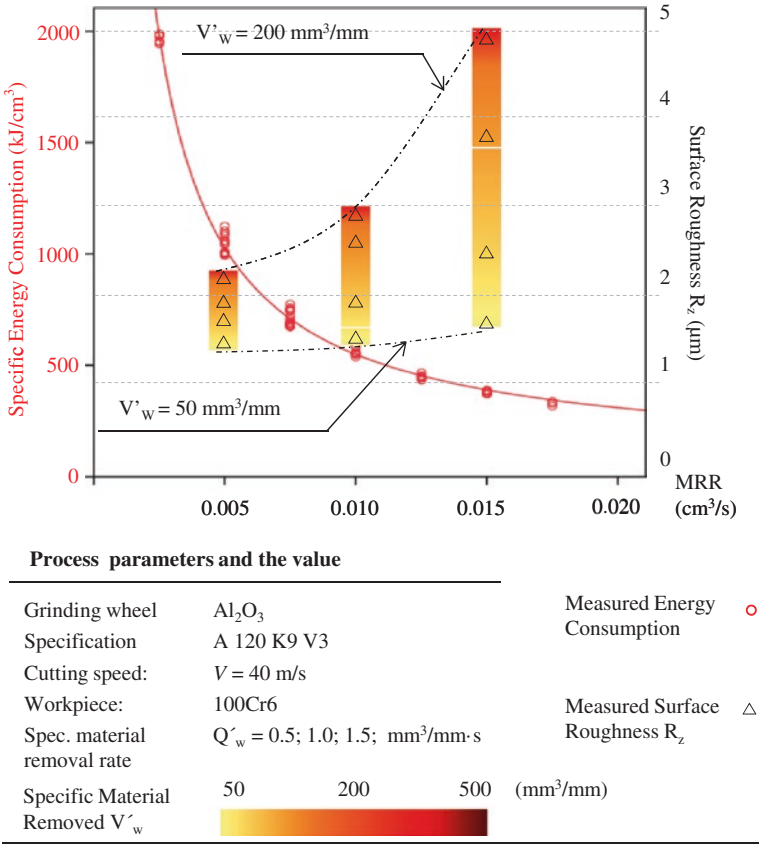

Fig. 5.5 Trade-off between energy consumption and surface roughness (Al_2O_3 wheel on the Studer S120)

A screening Life Cycle Assessment (LCA) was conducted to assess the environmental impacts of grinding wheels, including 4 steps: goal and scope, inventory analysis, impact assessment, and interpretation.

The functional unit of this analysis was defined as "raw materials and disposal of 1 kg of CBN and Al_2O_3 grinding wheel". Owing to the limited information, the analysis was only focusing on the raw material and end of life stage. Since the use phase of grinding wheel is the grinding process and dressing process, the electricity consumption has already been considered from the unit process point of view, thus it was excluded for the grinding wheel analysis.

The CBN grinding wheel mainly consists of the cubic form of boron nitride, or called as β-BN. Other material and elements are added to change its color, conductivity and toughness, such as Li_3N, Be, Si, C, or P (Wentorf 1961; Greim and Schwetz 2006). The β-BN was made from boron acid with urea through a hot-pressing process (4–6 GPa, 1400–1700 °C). The chemical reaction is listed below:

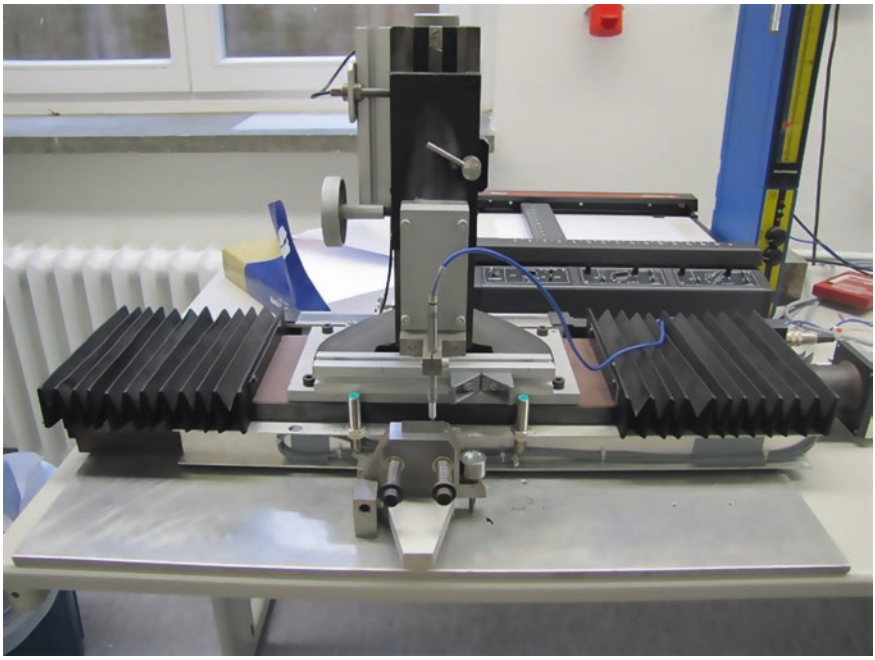

Fig. 5.6 Photograph of the device for measuring grinding wheel wear

$$B_2O_3 + CO(NH_2)_2 \xrightarrow{>1000\,^{\circ}C} 2BN + CO_2 + 2H_2O$$

According to the molecular weight, the amount of raw materials for producing 1 kg β-BN powder can be estimated as 1.4 and 1.2 kg for boron acid and urea respectively. The Al_2O_3 grinding wheel consists of 98 % of Al_2O_3, 1.5 % of TiO_2, and other bonding materials (Klocke and König 2005).

The production of grinding wheel generally requires 4 stages. The process begins with selecting and mixing precise quantities of abrasives, bond materials, and additives according to a specific formula. Then, the mixture is poured into a mold and pressed with a pressure in the range of 100–5000 psi. After molding, the vitrified grinding wheels are fired to temperatures between 927 and 1260 °C in order to melt the binder around the abrasives and to convert the wheels to a form that resist the heat and solvents encountered during grinding. Finishing was the last step to correct thickness or parallel wheel sides, or to create special contours on the side or circumference of the wheel (Borkowski and Szymański 1992; Marinescu et al. 2000). However, the current information is insufficient to quantify the energy requirements during the production stage. In addition, the use of problematic chemicals and the related emissions remains unidentified. Therefore, further investigation into the production of grinding wheels is recommended.

The removed abrasives and bonding materials are flooded away with grinding swarf. It is difficult and uneconomical to recycle the removed grinding wheels. Thus, the disposal of grinding wheel was assumed as 100 % land fill.

The inventory analysis produces the Life Cycle Inventory (LCI) results based on the above literature and the Ecoinvent 2.2 database. It includes the inputs and outputs of raw materials, emissions and wastes where results of the amount of carbon dioxide fossil emission have been extracted. A 7.94 and 1.81 kg fossil fuel CO_2 emission was calculated for the CBN and Al_2O_3 grinding wheel respectively.

Each dressing process only removes few micro meters of grinding wheel. For removing 1 kg of raw material, the loss of grinding wheel is in the range from 3 to 10 g (the density of CBN wheel is 3.48 g/cm^3). Comparing to the electricity consumption of grinding and dressing process, the environmental impacts of grinding wheel consumption appears to be relatively insignificant. This exclusion requires further validation once a full scale LCA of grinding wheels becomes available.

Unlike turning and milling processes, coolant is essential for grinding process due to the substantial amount of heat generated at the contacting zone. As discussed in Sect. 3.2, the environmental impacts of applying coolant are due to the electricity consumption for flow generation, as well as due to the coolant loss through the activities. Since the coolant pump requires constant power, the electricity consumption due to coolant pump can be easily estimated. The coolant loss mainly occurs along with the flood of grinding swarf, which is depending on the operation conditions. Assumptions are necessary to estimate the coolant loss during the grinding process. Comparing to the embodied energy of coolant other environmental impacts are also important, such as the fluid splashing, improper disposal, human health problem due to the exposure to the coolant, etc. As a consequent, there has been an occupational exposure limit (OEL) of 10 mg/m^3 for the sum of aerosol and vapor concentration of coolants with a flash point above 100 °C since 1996 (Schiefer 2000). Currently, air exhauster is essential for grinding machine tools to minimize the human exposure to the hazardous substances. However, the air exhauster cannot completely eliminate the hazardous substances (Dettmer 2006). In order to evaluate the human health related issues, the investigation of human exposure to coolant is recommended for future work.

In this research, the electricity due to the coolant pump was considered as the main environmental impact of applying coolant. In addition, the coolant loss was assumed to be between 5 and 30 % of the fill quantity (Clarens et al. 2008). The air exhauster was assumed to be functioning properly, thus human health related issues can be excluded. According to (Winter et al. 2012), 0.168 kg fossil fuel CO_2 is emitted to produce 1 kg mineral oil based emulsion; and, another 0.730 kg fossil fuel CO_2 is emitted during the end-of-life phase assuming a combustion in a hazardous waste incinerator (no credit was given for the recovered energy). Thus a rough estimation can be obtained for the CO_2 emissions due to the consumed coolant.

5.3.3 The Interrelationship Within the Grinding Processes

As discussed before, eco-efficiency of unit process requires considerations of process value and environmental impact concurrently when configuring the process parameters. Based on above analysis and existing database, the electricity and

embodied coolant energy induced environmental impact can be quantified and linked with process parameters and surface roughness for this grinding case.

The functional unit of this analysis is to grind 1 kg of 100Cr6 and maintain surface roughness under a given R_z value, with 10 mm cutting width and a mineral oil based emulsion (8 %) as coolant.

The total electricity consumption consists of three parts: grinding process energy consumption, dressing energy consumption, and coolant pump energy consumption. The first one is energy consumption due to grinding process (including the machine base load and the exhaust air filter), calculated based on the derived SEC model (Eq. 5.3).

The grinding process duration can be also computed as Eq. 5.4.

$$E_{grinding} = SEC \times Q = \left(c_0 + \frac{c_1}{MRR}\right) \times \frac{1\text{kg}}{Density} \tag{5.3}$$

$$T_{grinding} = \frac{Q}{MRR} \tag{5.4}$$

The second part is due to dressing process. The dressing period was estimated according to empirical results from last section. Since the surface roughness shares a similar model (Eqs. 5.1 and 5.2), the dressing amount can be written as a function of R_z, see in Eq. 5.5.

$$\Delta r_s = \alpha_0 + \alpha_1 \cdot \frac{R_z - \beta_0}{\beta_1} \tag{5.5}$$

Studer S120 consumes (ca. 5 kW) during dressing process, and the dressing speed (v_d) was kept constant during the study. The energy and time for dressing process can be calculated based on Eq. 5.6.

$$E_{dressing} = 5\text{kW} \cdot T_{dressing} = 5\text{kW} \cdot \frac{\Delta r_s}{v_d} \tag{5.6}$$

The third part is due to coolant pump (ca. 2 kW) throughout both grinding period and dressing period (Eq. 5.7).

$$E_{coolant} = 2\text{kW} \cdot \left(T_{grinding} + T_{dressing}\right) \tag{5.7}$$

Therefore, the total energy consumption for this functional unit can be written as a function of surface roughness and material removal rate (Eq. 5.8).

$$E_{total} = E_{grinding} + E_{dressing} + E_{coolant} = f(MRR, R_z) \tag{5.8}$$

If the production was assumed to be done in Europe, therefore 1 kJ of electricity consumption equals to 0.000128 kg fossil fuel CO_2 emissions (CO_2 Fossil) according to Ecoinvent database Version 2.2 (2010).

As discussed in Sect. 5.3.2, the coolant loss during the operation is assumed to be 30 % over a week time of production (5 L/day). And the CO_2 emissions due to the use of coolant are used to compare with the electricity consumption induced environmental impacts. Therefore, the results are represented in 3D curves for CBN and Al_2O_3 grinding wheel as shown in Fig. 5.7.

The red lines in Fig. 5.7 show an evenly decreasing trend of the CO_2 Fossil caused by an increasing MRR. This can be explained by the reduced process time; indeed the required process energy is higher but simultaneously the share of base load is reduced by the shorter process time. Chasing the high surface finish (low R_Z value) results in higher CO_2 Fossil. After a certain point, the environmental impact goes up exponentially. Therefore, a critical region has been defined as shown in Fig. 5.7.

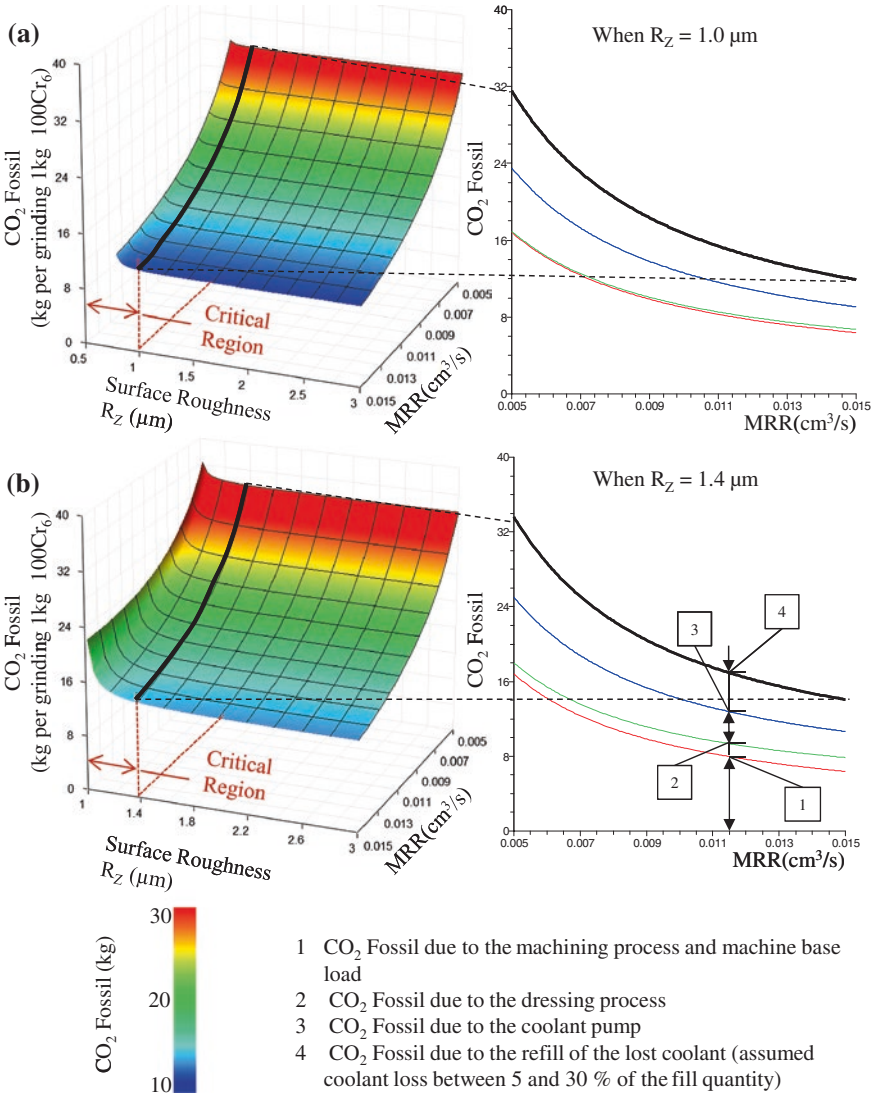

Fig. 5.7 Eco-efficiency evaluation of a selected grinding process (Studer S120) (Li et al. 2012)

Overall when comparing the plotted surface, the CBN grinding wheel shows much better capability for meeting high surface finishing requirements ($R_Z < 1.4$ µm). This can be explained by the higher micro hardness of the abrasive grains of the CBN grinding wheel. In comparison, the use of Al_2O_3 grinding wheel leads to significantly higher trend of CO_2 Fossil due to the increased MRR. This is caused by the higher wear and therefore the need for repeated dressing of the grinding wheel.

5.4 Summary

In this chapter, the energy efficiency of manufacturing processes has been extended with other aspects such as process value and environmental impacts, namely eco-efficiency. For the cases like turning, milling and injection molding, the energy efficiency can be easily converted into eco-efficiency since the environmental impacts are solely dependent on the electrical energy consumption. Comparatively, the case like grinding is more complicated, and shows a dynamic interrelationship among process parameters, process value and the associated environmental impacts. The characterized interrelationship can also be used for improving the eco-efficiency of the presented case.

Nevertheless, the current implementations of eco-efficiency face challenges to gather reliable data, such as LCI data for grinding wheel, coolant consumption/loss. This has showed the importance of improving the quality of LCI database. With derived SEC models in Chap. 4, another benefit from the model development is to supplement the LCI database and improve the reliability of existing datasets. This can be achieved easily, since the derived SEC models are highly transferable and applicable. With the help from machine tool builders, more machine specific information can be provided. Thus, the better environmental and life cycle analysis can be achieved.

References

Borkowski JA, Szymański A (1992) Uses of abrasives and abrasive tools. Ellis Horwood, Chichester

Cecimo (2009) Concept description for CECIMO's self-regulatory initiative (SRI) for the sector specific implementation of the directive 2005/32/EC. Available online. http://www.ecodesign-info.eu/documents/machin_tools_va_20oct09.pdf last visited 08/02/2010

Clarens AF, Zimmerman JB, Keoleian GA, Hayes KF, Skerlos SJ (2008) Comparison of life cycle emissions and energy consumption for environmentally adapted metalworking fluid systems. Environ Sci Technol 42(22):8534–8540

Dettmer GT (2006) Nichtwassermischbare Kühlschmierstoffe auf Basis nachwachsender Rohstoffe. PhD thesis in Technischen Universität Carolo-Wilhelmina zu Braunschweig, Germany

Graham D (2000) Going dry. Manufact Eng 124(1):72–78

Greim J, Schwetz KA (2006) Boron carbide, boron nitride, and metal borides. Ullmann's Encyclopedia of Industrial Chemistry, Wiley

Gu J, Barber G, Tung S, Gu R (1999) Tool life and wear mechanism of uncoated and coated milling inserts. Wear 225–229(1):273–284

International Energy Agency (IEA) (2011) CO_2 emissions from fuel combustion highlights. Online publication. http://www.iea.org/co2highlights/co2highlights.pdf last visited 01/03/2012

Jawahir IS, Brinksmeier E, M'Saoubi R, Aspinwall DK, Outeiro JC, Meyer D, Umbrello D, Jayal AD (2011) Surface integrity in material removal processes: recent advances. CIRP Ann Manufact Techonol 60(2):603–626

Klocke F, König W (2005) Fertigungsverfahren 2—Schleifen, Läppen. Springer Verlag GmbH, Berlin Honen

Li W, Kara S (2015) Characterising energy efficiency of electrical discharge machining (EDM) processes. Procedia CIRP 29:263–268

Li W, Winter M, Kara S, Herrmann C (2012) Eco-efficiency of manufacturing processes: a grinding case. CIRP Annals—Manufacturing Technology 61(1):59–62

Marinescu ID, Tonshoff HK, Inasaki I (2000) Handbook of ceramic grinding and polishing. William Andrew Publishing/Noyes, Norwich

Schiefer E (2000) Ökologische Bilanzierung von Bauteilen für die Entwicklung umweltgerechter Produkte am Beispiel spanender Fertigungsverfahren. PhD thesis in Technische Universität Darmstadt, Germany

Sreejith PS, Ngoi BKA (2000) Dry machining: machining of the future. J Mater Process Technol 101(1):287–291

Stanford M, Lister PM (2002) The future role of metalworking fluids in metal cutting operations. Ind Lubr Tribol 54(1):11–19

Wentorf RH (1961) Synthesis of cubic form of boron nitride. J Chem Phys 34(3):809–812

Winter M, Öhlschläger G, Dettmer T, Ibbotson S, Kara S, Herrmann C (2012) Using jatropha oil based metalworking fluids in machining processes: a functional and ecological life cycle evaluation. In: 19th CIRP international conference on life cycle engineering, Berkeley

Chapter 6
Implementation Towards Improving Energy and Eco-efficiency of Manufacturing Processes

The previous chapters have validated the results of the proposed methodology for characterizing the energy and eco-efficiency of unit processes. The characterization is around the development of unit process energy consumption models; because, the model response-SEC is the indicator of energy efficiency; and the associated environmental impacts of unit process are mainly due the consumption of electricity. The results among all the tested processes proved the reliability of the proposed methodology. However, due to the nature of empirical modelling, the meaning of the model coefficients remains to be answered.

World Energy Council (WEC) suggests that "*Energy efficiency improvements refer to a reduction in the energy used for a given service (heating, lighting, etc.) or level of activity*" (WEC 2008). The understanding of energy efficiency should evolve from a simple input/output ratio towards the global efforts for energy reduction. Therefore, the derived SEC models need to be used for developing energy efficiency strategies.

This chapter firstly explores the mechanism of model coefficients, by decomposing the SEC model. Then, a clustered model for material removal processes are presented and discussed. The following section discusses the challenges of characterizing energy efficiency in industries, and proposes a modified methodology with a case study in a biomedical products and services company. The derived energy consumption information is also compared with current LCI database in order to improve its quality. Finally, the strategies for improving energy efficiency are proposed from different perspectives.

W. Li, *Efficiency of Manufacturing Processes*, Sustainable Production,
Life Cycle Engineering and Management, DOI 10.1007/978-3-319-17365-8_6

6.1 Investigation into Model Coefficients

6.1.1 *Comparison Between Empirical Models and Exergy Framework*

As presented in Chap. 4 a variety of machine tools and manufacturing processes had been selected for developing energy consumption models, in order to evaluate the energy efficiency of the unit processes. Without exception, all the derived SEC models agree with a universal shape as Eq. 4.4. The model shape also agrees with exergy framework as reviewed in Sect. 2.1.3 (Gutowski et al. 2007). This similarity has raised an interesting question: are they identical? If the answer is positive, then the coefficient c_1 should equal to the idle power, or called fixed power which is the power demand during the machine stand-by mode. Table 6.1 lists the derived c_1 values and the corresponding fixed power demands for all the tested machine tools.

As shown in the table, there is a clear gap between the coefficient c_1 and fixed power demand. The c_1 value is constantly larger than the fixed power demand. In some cases, the fixed power is even less than the half of the coefficient value. Therefore, there is no evidence to suggest that c_1 is equal to the fixed power demand of the machine tool. In other words, the derived empirical models partially disagree with the exergy framework.

Exergy framework simply classifies the energy consumption of a machine tool into either for base load or process load (Gutowski et al. 2007). The base load refers to the energy for auxiliary components to ensure machine-readiness, while

Table 6.1 Comparison between c_1 and fixed power for the tested machine tools

Machine	c_1 (kW)	Fixed power P_f (kW)	$\frac{c_1}{P_f}$ (%)
Colchester Tornado A50	2.191	1.16	189
Mori Seiki NL200MC/500	2.445	1.58	155
IKEGAI AX 20	4.415	1.77	249
Mori Seiki SL-15	2.273	1.48	154
Nakamura TMC-15	2.349	1.54	153
Mori Seiki Dura Vertical 5100	1.344	1.02	132
Fadal VMC 4020	1.330	0.74	180
DMG DMU 60P	5.863	5.45	108
Reinecker ISA 110	3.399	2.16	157
Studer S120	4.781	1.69	283
Studer S40	6.510	3.69	176
BOY15S	1.933	1.41	137
BOY 15	2.239	1.02	220
Battenfeld BA500CD	3.816	3.26	117
SODICK A3R	2.250	1.40	161
AGIE TRON 30L	2.111	1.26	168

the process load is the amount of energy used for actual work. For the case of turning process, the total energy consumption should be the sum of fixed energy consumption and cutting energy at tool tip. However, this is an ideal situation. During the process, frictions and vibrations would generate heat, which results in a form of energy losses. In addition, the efficiency of the spindle drive motor and transmission system under dynamic loads is another complex topic. In short, the machine tools are complex systems; and the gap between empirical and theoretical models is mainly due to the over simplification of the system. In order to further understand the gap, model decomposition was conducted and presented in the following section.

6.1.2 SEC Decomposition

A turning case was selected for SEC decomposition owing to the simplicity of the process comparing to other tested manufacturing processes. The existing knowledge about turning process would also benefit the investigation. Dietmair and Verl (2008) used an approach in which they changed the operating conditions of a milling machine tool state by state in order to develop the energy consumption profile of each component. However, it is very difficult to differentiate between the energy consumed by the spindle drive motor and that consumed by the servo motors. It is also impractical to directly measure at the component level. Alternatively, this research decomposed the energy consumption based on different utilizations, and selected Colchester Tornado A50 to demonstrate the results.

When a machine is in stand-by mode or is idle, a fixed amount of power is required by the auxiliary components and unloaded components to ensure that the machine is ready for operation when required. In practice, an air cut is used to check the numerical control program; in this approach the spindle rotates and the cutting tool moves according to the program without contacting the workpiece. Thus, due to these essential operations there is an additional power requirement for an air cut compared to the fixed power required at stand-by mode. The power gap between the normal cut and the air cut is the energy utilized to remove material from the workpiece. However, this amount of energy is not the amount of energy used by the tool tip for material removal. Due to friction effects, some of this energy is converted into heat. Since the modelling response is SEC, the energy consumption is decomposed based on the operating period required to remove 1 cm^3 of material. Therefore, the SEC can be separated into the following four segments, as shown in Fig. 6.1.

- The specific fixed energy (SFE): this is the energy used to ensure that the machine is ready over the operating period required to remove 1 cm^3 of the workpiece.
- The specific operational energy (SOE): this is the energy used to enable the essential operations such as spindle rotation and cutting tool movement over the operating period required to remove 1 cm^3 of the workpiece.

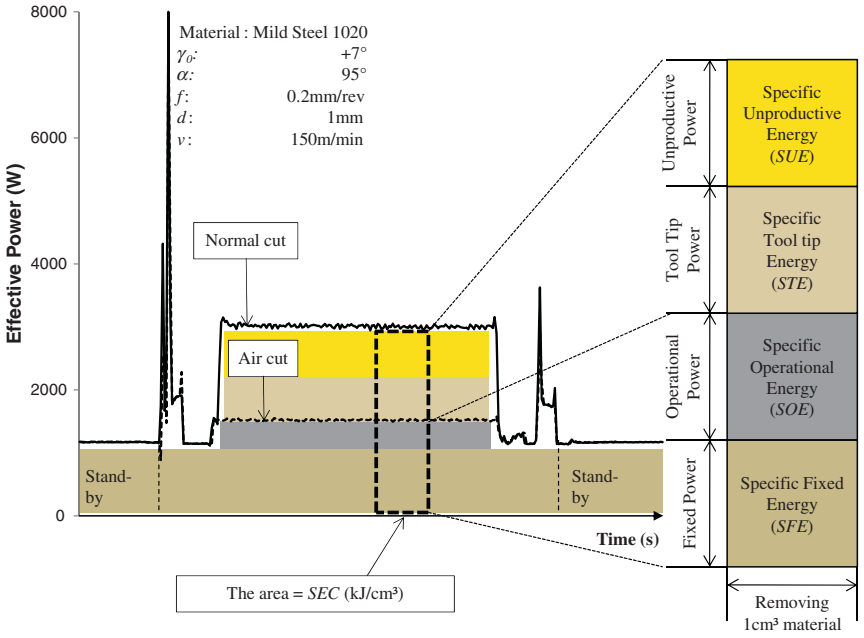

Fig. 6.1 SEC decomposition for the case of Colchester Tornado A50

- The specific tool tip energy (STE): this is the energy required by the tool tip to remove 1 cm^3 of the workpiece.
- The specific unproductive energy (SUE): this is the energy that is converted to heat or other form rather than cutting energy over the operating period required to remove 1 cm^3 of the workpiece.

The first two segments can be easily measured and separated from SEC based on power measurements of air cuts.

For the Colchester Tornado A50, the measured fixed power was 1.16 kW with a standard deviation of 0.003 kW. In the stand-by mode, the hydraulic pump motor is used to maintain the pressure level of the clamping system and the servo motors draw power to maintain their position. Also, the control system and other auxiliary components are activated to allow the machine to be ready for operation on request. During the cutting operations, these components remain at the same status except for the servo motors when extra cutting loads are allocated.

The machine tool requires supplementary power to perform the essential operations associated with the cutting process, such as rotating the spindle and moving the cutting tool along the programmed cutting path, which can be measured through the air cuts. Since the servo motors that control the X and Y axes motions are already enabled during the stand-by mode, the additional power required to move the cutting tool is insignificant. Hence, the required operational power

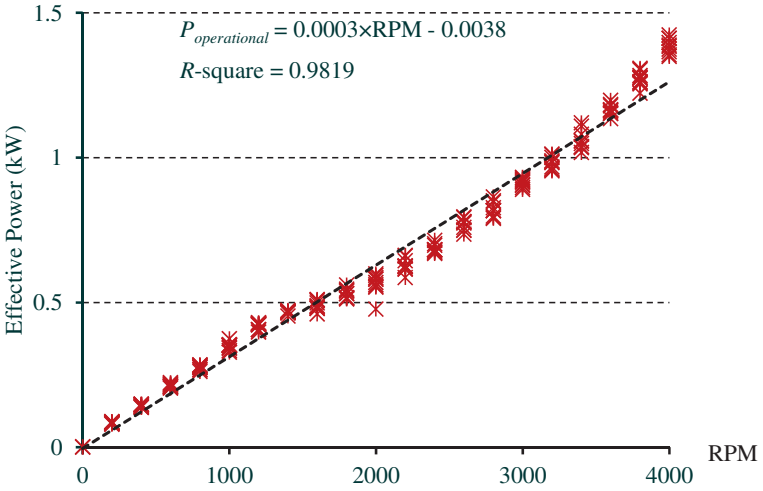

Fig. 6.2 Plot of operational power against rotational speed (Colchester Tornado A50)

is mainly due to the spindle drive motor, which is closely related to the rotation speed of the spindle. Since the power consumption of air cuts was additionally recorded, the SOE can be easily calculated and separated from SEC. As the tested machine tool has a relative small spindle drive motor (3.5 kW/4.7 HP), the operational power for spindle rotation only accounts for a small proportion of the total power demand, which follows a linear relationship with the rotational speed as shown in Fig. 6.2.

However, the other two segments, STE and SUE cannot be separated directly.

As discussed in Sect. 2.1, the tool tip energy consumption for turning processes can be estimated based on cutting forces. The comprehensive information available about tool geometries, material properties, and the formulas provided by SECO® Tools are used in this research (SECO® Tools 2009). The cutting forces can be obtained, according to Eq. 6.1, in terms of the specific cutting force k_c, the feed, and depth of cut. The specific cutting force is a function of the shear stress of the workpiece material ($k_{c1.1}$), the geometric properties of the cutting action (approach angle α, rake angle γ_0), and material exponent (mc).

$$F_c = k_c \cdot f \cdot d = \frac{1 - 0.01\gamma_0}{(f \sin \alpha)^{mc}} k_{c1.1} \cdot f \cdot d \tag{6.1}$$

In order to evaluate the accuracy of this equation the cutting forces were measured under different cutting conditions using a Kistler® Dynamometer. The observed cutting forces are compared with predicted values in Fig. 6.3. As Eq. 6.1 suggests, the shear zone, which is the product of the feed rate and depth of cut, has a linear relationship with the cutting force. Thus, the cutting forces are plotted against the share zone. While the accuracy of the predicted cutting force for the removal of aluminum is relatively high, the reliability decreases when harder materials are

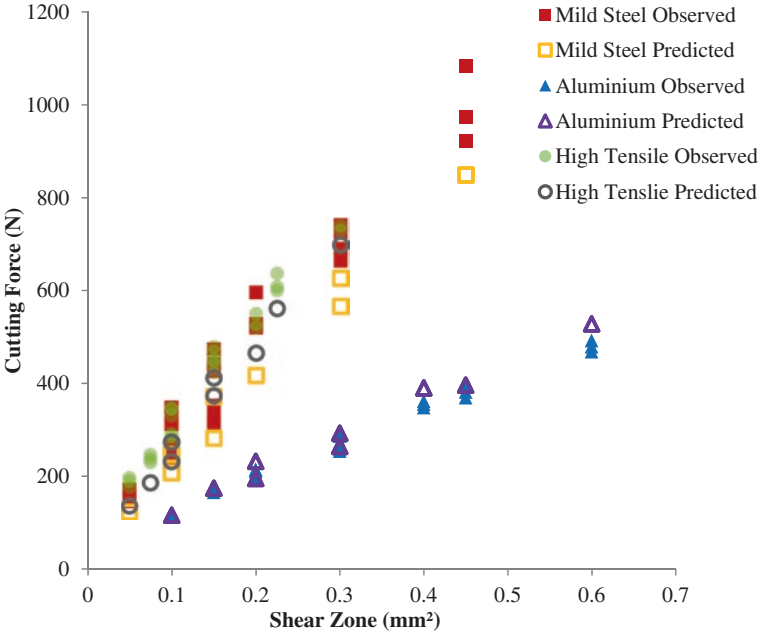

Fig. 6.3 Plot of measured cutting forces versus predicted cutting forces (Colchester Tornado A50)

considered. Thus, the cutting force model can only provide a rough estimate of the energy requirements of tool tip for material removal.

The unproductive energy is even more difficult to estimate. From a thermodynamic perspective the machine normally generates more heat than the levels expected due to the material removal process. The friction created at the bearing unit and transmission system could be additional sources of the unproductive energy (Altintas 2000). Jedrzejewski et al. (2005) suggested that the unproductive power in a machine system is due to a wide range of factors which result in a complex, dynamic, and non-linear state for the thermal equilibrium that is characterized by continuous changes in power losses, temperatures, and displacements. They developed a hybrid model which was combined with the finite element method and finite difference method to analyze the thermal performance of spindle and bearing units. Abele et al. (2010) presented a comprehensive review about spindle units including existing thermal models and they highlighted that the complexity and inherent limitations of these models make it unlikely that the reliance on experimental measurements will change in the near future. Direct measurement of generated heat is also inapplicable in this case. As an alternative approach this research uses the observed SEC values and subtracts the other segments SFE, SOE, and STE from SEC to estimate SUE. All the measured or estimated data has been processed with curve-estimation to characterize the relationship between MRR and each segment of SEC. Therefore, the SEC model decomposition was achieved. Figure 6.4 shows the results in a selected MRR range (0–1 cm^3/s).

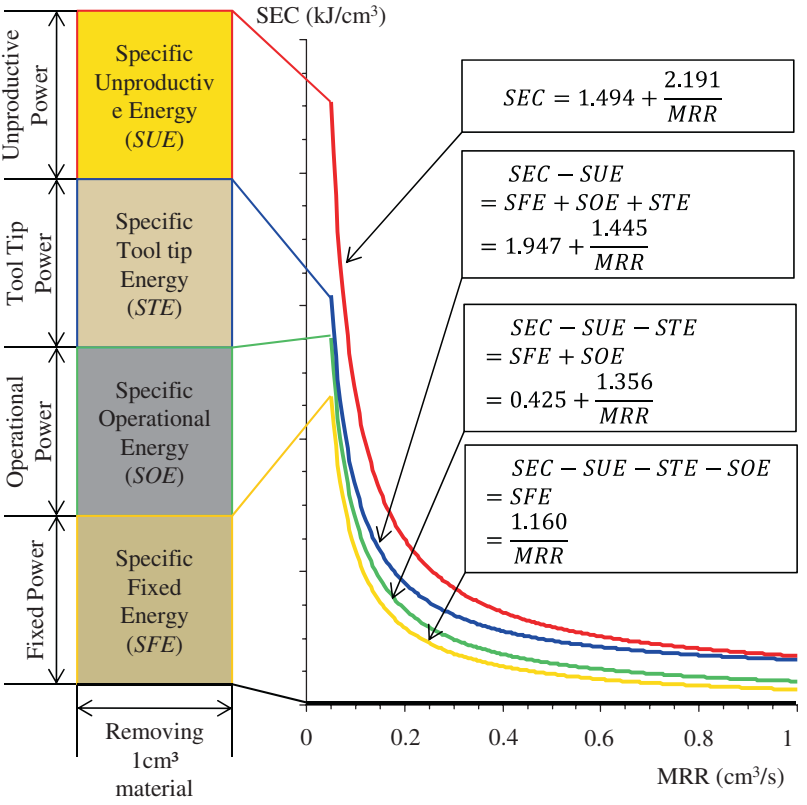

Fig. 6.4 Results of SEC decomposition for the Colchester Tornado A50 (Li and Kara 2011)

6.1.3 Coefficients c_0 and c_1

The above presented analysis shows the difficulty of estimating energy consumption of a machine tool from mechanical theories. Even obtaining the fixed power used in stand-by mode is dependent on measurements. The friction-generated heat and the energy converted to heat make the prediction of energy consumption more complicated and less applicable. More importantly, the total energy consumption of a machine tool is not only due to energy required for machine readiness and by the tool tip. The essential operations and friction effects also consume a proportion of the total energy. Thus, the coefficients c_0 and c_1 are not as the specific cutting energy and idle power suggested by the exergy framework (Gutowski et al. 2007).

Since the empirical approach considers the machine tool to be a single holistic system, it is difficult to precisely assign the factors or reasons for each coefficient in the model. However, the decomposition of SEC has shown several trends for each segment of energy consumption, which leads toward a qualitative definition of the factors in relation to coefficient c_0 and c_1.

As shown in Fig. 6.4, the empirical models for each segment of the energy consumption can be approximated to Eqs. 6.2–6.5.

$$SFE = \frac{1.16}{MRR} \tag{6.2}$$

$$SOE = 0.425 + \frac{0.196}{MRR} \tag{6.3}$$

$$STE = 1.522 + \frac{0.089}{MRR} \tag{6.4}$$

$$SUE = -0.452 + \frac{0.746}{MRR} \tag{6.5}$$

The fixed power consumption is the major components for SEC according to Fig. 6.4. The equation for SFE (see Eq. 6.2) also suggests that the fixed power is the main contributor for coefficient c_1. An investigation into fixed power consumption and the induced improvements would significantly reduce energy consumption during both stand-by and processing periods.

The SOE only counts a small proportion of the total SFE in the tested case. Since this share of energy consumption is mainly due to rotation of spindle drive motor, the size and the type of the motor would affect the proportion of SOE. Generally, the bigger the motor size the higher share of SOE. However, there are exceptions to this linear trend owing to the efficiency of the motors. Thus, the spindle motor characteristics affects the SOE so as the coefficient c_0.

The share of STE mainly contributes to the coefficient c_0 in SEC models. The tool tip energy mainly refers to the cutting energy during machining. Previously reviewed cutting force models have suggested that the involved factors include material, tool geometry and cutting parameters. In other words, coefficient c_0 is dynamic rather than a static value. However, a constant value for c_0 has been found adequate for the process mainly due to the trade-off between the operational and tool tip energy consumption. For example, removing aluminum requires a relatively low specific cutting force, but demands a high rotation speed resulting in a comparatively high operational energy. Correspondingly, a constant value for c_0 can still provide a reliable energy consumption prediction.

As shown in Fig. 6.4, the trend of SUE suggests that the lower the cutting load, the higher the unproductive energy. This refers to a close link between c_1 for SEC model and the motor and transmission efficiency of the machine tool. This behavior agrees with the feature of the induction motors, that the motor efficiency is very low when rotating at a slow speed or with small loads. The negative coefficient value in Eq. 6.5 is most likely due to the errors of the estimation. But the trend indicates that the unproductive energy become negligible when MRR reaches a certain point. This leads to the definition of a critical region in which decreasing MRR results in an exponential increase of SEC, and thus the region should be avoided if possible. In other words, the increase of MRR

outside the critical region would not result in a significant reduction of total energy consumption.

In summary, the coefficients c_0 and c_1 for the SEC models can be written as a qualitative function of above mentioned factors, see in Eqs. 6.6 and 6.7.

$$\begin{aligned} c_0 &= f(\text{spindle drive motor characteristics, cutting energy}) \\ &= f(\text{spindle drive motor characteristics, workpiece material,} \\ &\qquad \text{tool geometry, cutting parameters}) \end{aligned} \tag{6.6}$$

$$c_1 = f(\text{fixed power consumption, motor and transmission efficiency}) \tag{6.7}$$

6.2 Model Clustering for Metal Machining Processes

Chapter 4 presents the derived SEC models for a variety of machine tools and manufacturing process. Although the values of the coefficients for SEC models vary from machine to machine, they all agree with an inverse shape which enables the opportunity for model clustering and comparison. Since multiple material removal processes have been investigated, the results for turning, milling and grinding are further discussed.

The MRR features different range for different machining processes. For example, the turning process can remove metal with a MRR from 0.1 to 15 cm^3/s for finishing or roughing respectively; while, the MRR for grinding process is only limited in the range of 0.005–0.05 cm^3/s in order to achieve a high surface quality (Kalpakjian and Schmid 2005). If the MRR is assumed to have extreme values, the SEC models can be converted into Eqs. 6.8 and 6.9.

$$\lim_{MRR \to 0} SEC = c_0 + \frac{c_1}{0} = c_0 + \infty = \infty \tag{6.8}$$

$$\lim_{MRR \to \infty} SEC = c_0 + \frac{c_1}{\infty} = c_0 + 0 = c_0 \tag{6.9}$$

As above equation suggests, when MRR is very slow, the c_0's contribution to SEC becomes negligible. For instance, the MRR during grinding process is usually around 0.01 cm^3/s, resulting SEC above 1000 kJ/cm^3. Although the c_0 values for tested grinding process vary from 47 to 135, it accounts for less than 10 % of the total SEC. On contrary, when MRR exceeds certain point, the SEC only fluctuates within a limited range which can be approximate as a constant value. Therefore, it is possible to cluster all the tested material removal processes into one model.

All the observed data has been combined into one file and processed with curve-estimation, resulting in an inverse model with R-square value of 0.915, see in Eq. 6.10.

$$SEC = -5.530 + \frac{5.180}{MRR} \tag{6.10}$$

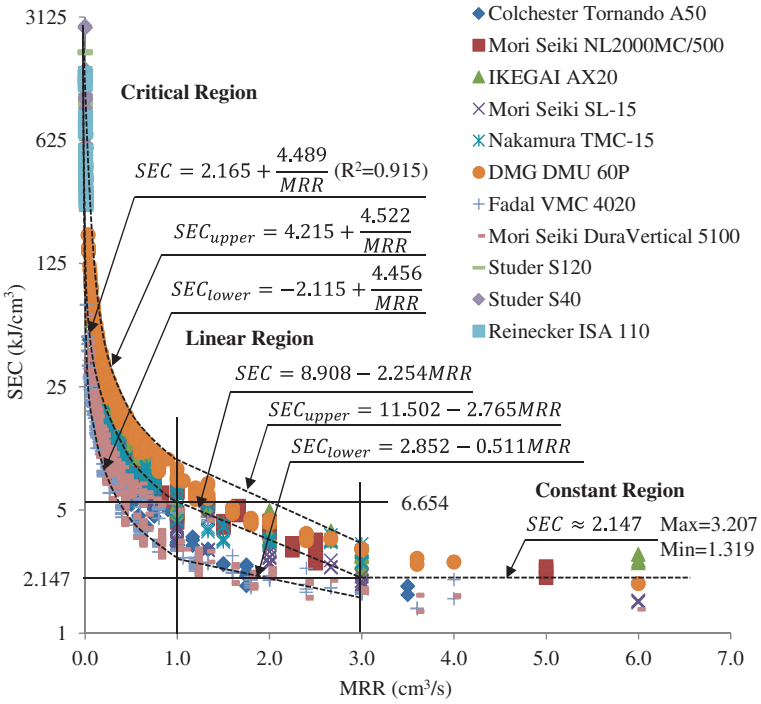

Fig. 6.5 SEC model clustering for metal machining processes

The negative value obtained for coefficient c_0 is mainly due to the variety of tested machine tools and the different ranges of MRR for different processes. As mentioned in Sect. 6.1.3, this value can help to define a critical region in which reducing MRR would result in an exponential increase of SEC. According to Eq. 6.10, when MRR is less than 1 cm^3/s, the SEC becomes positive, and increases significantly if further reducing MRR under 1 cm^3/s. Thus, a critical region of material removal rate for material removal processes is 0–1 cm^3/s, which should be avoided if possible.

Figure 6.5 plots all the observed data together. The curve-estimation has been repeated again for the data observed within the critical region. Besides the critical region, the trend of SEC turns to be constant when MRR is over 3 cm^3/s. This region (MRR > 3 cm^3) can be defined as a constant region, and thus the SEC can be approximated to the average value of the observed data. In addition, the area between critical and constant region can be simplified with a linear regression model. Therefore, a clustered model has been derived for material removal processes as shown in Eq. 6.11.

$$SEC = \begin{cases} 2.165 + \frac{4.489}{MRR} & |0 < MRR \leq 1 \\ 8.908 - 2.254MRR & |1 < MRR \leq 3 \\ 2.147 & |MRR > 3 \end{cases} \tag{6.11}$$

The clustered model is an ideal tool for rough estimation, since minimum input information is required for energy consumption estimation. It also provides a big picture over different machine tools and processes, which is helpful for obtaining energy efficiency measures at a unit process level. However, owing to the variety of the machine tools, the accuracy of the clustered model is not comparable with those machine specific models derived in Chap. 4. As shown in the linear region in Fig. 6.5, the variability is relatively high among different machine tools and processes. None of the 11 provided models by SPSS® can achieve *R*-square value over 0.3. Although the error remains high when MRR varies from 1 to 3 cm^3/s, the SEC can be limited in a relatively small range from 2.147 to 6.654 kJ/cm^3. More importantly, the clustered model can be safely used in the critical region and constant region, which is adequate enough for estimation during the early design stage.

6.3 Implementation the Methodology of Energy Efficiency Evaluation in an Industrial Environment

6.3.1 Challenges in Industries

As mentioned in Chap. 3, the empirical approach of developing energy consumption models for manufacturing processes requires series of experiments to filter different process parameters, as well as to characterize the relationship between process parameters and the energy consumption. More importantly, each tested parameter has to be varied in a relatively wide range, in order to capture the trends. Since the machine tools used in laboratories were highly flexible, researchers find little problem either to conduct a large number of experiments or to reach the limit of certain process parameters. However, it is unlikely to find this level of flexibility in industries.

First of all, experiments directly result in a significant expense, including operational costs, material costs, energy costs and labor costs. Prior to any experiments, an energy metering and monitoring system needs to be set up which normally requires a certified electrician to connect the meters to the tested machine tools. Disconnecting the metering system also needs to be done by the electricians. During the experiments, the output products might not be acceptable when changing the original process parameters. Consequently, the experiments become a waste of raw materials and production time. It is even worse for the process which requires a long time to reach production readiness, such as injection molding, extrusion, etc. Thus, the cost of experiments has to be considered with cautions.

In laboratories, machine tools can be isolated and studied individually. By contrast, the majority of machine tools or processes in industrial processes are closely related to the other ones in a production line. In other words, additional experiments on one process may have a significant impact on the whole process chain or even the entire factory, especially for the case of bottleneck processes. Hence, an appropriate schedule for the experiments is critical to obtain the approval from the industrial side.

The other important aspect for model development is the possibility to change process parameters. In industry, some machine tools are purpose built and run under specific process conditions. In these cases, it is preferable to apply the screening approach to obtain the energy profile of the machine tools. Conversely, industries commonly use one machine tool to produce different parts; corresponding, to different loads and cycle time result in different energy consumptions. These processes provide the opportunity to develop energy consumption models regarding dynamic loads but the process parameters are generally configured according to the quality requirements which limit the range of varying process parameters. Testing the extreme cases also places machine tools at risk of costly breakdowns. Therefore, the levels of variance for the process parameters need to be defined properly in order to meet the industrial requirements as well as to provide a sufficient range for model development.

Apart from the technical constraints, it is essential to obtain the management support. Ideally, the model development activities can be coupled with energy efficiency projects, since the models provide valuable information. As presented in Chap. 4, the derived SEC models have revealed the important relationship between the energy intensity of the process (i.e. energy consumption per unit volume/mass of processed materials) and the productivity of the process (e.g. throughput rate or material removal rate). The models also offer an accurate estimation and prediction of energy consumptions, which benefit the energy accounting activities in industries. Moreover, the energy efficiency aspect can be introduced to the stage of configuring process parameters. It is also possible to reduce the energy consumption whilst remaining at the same level of quality performances. Besides the benefits, industry support can be enhanced by minimizing the experimental costs and the interruption of the production. Therefore, the proposed methodology in Chap. 3 needs to be modified to meet industrial requirements.

6.3.2 Modified Methodology for Characterizing Energy-Efficiency in Industries

As suggested by Montgomery, DoE is the critical stage for any experimental work, but it is also time- and resource-consuming to filter out the insignificant factors (2009). The presented cases in Chap. 4 have proved that the production rate (e.g. material removal rate or MRR, throughput rate or $\dot{m}$) is the decisive factor for the SEC. In fact, both MRR and throughput rate are dependent variables. For example, the MRR of a turning process is the product of cutting speed, feed rate and depth of cut. The types of raw materials also affect the selection of MRR. Obviously, these independent factors have significant impacts on the energy consumption, and are normally classified as design factors during the DoE stage. However, it is a tedious procedure to statistically prove the significance or insignificance of each factor on energy consumption. Alternatively, the conclusion obtained from previous works can be adapted for the similar manufacturing processes. Instead of

testing the significance of each factor on energy consumption, the qualitative relationship between process parameter and production rate can be easily observed. For instance, drilling is similar to other conventional machining processes, such as turning and milling; and, the MRR is a function of driller diameter, feed rate and RPM (rotation per minute); other factors like workpiece materials and driller materials have an indirect impact on the MRR; so, these factors can be directly concluded as design factors for model development. As a result, the number of experiments can be reduced considerably.

As mentioned in Sect. 6.3.1, other issues need to be taken into account for experiment planning. The first question which needs to be answered is whether this process is suitable for empirical modelling or not. If all the process parameters of one process remain constant, a screening approach is more suitable for that process. Otherwise, the process can be considered for empirical modelling. Then, each factor is closely observed in conjunction with the production rate. If one factor has a significant impact on production rate, that factor needs to be targeted as design factor. Afterwards, the operational constraints need to be considered, which leads to an addition planning step prior to all the modelling work. Cost analysis, initial setup, scheduling issues and management support needs to be obtained during this step. Once the experiments are approved by industry, the remaining stages are similar to the original empirical approach, including physical experiments, statistical analysis and model validation. Therefore, the methodology can be modified as shown in Fig. 6.6.

6.3.3 Case Study: A Case of Sheet Extrusion Line

The presented case is derived from a biomedical products and services company in Australia. This company is continuously looking ways to improve their processes with environmental awareness. The company has strategic targets for substantially reducing energy and resource consumption as well as reducing its carbon foot-print. To achieve that goal, the company has invested on improving the transparency of its energy flows. Projects were formed to develop energy consumption models or to obtain energy profiles at unit process level.

The manufacturing plant in western Sydney specializes in producing sterilized IV and renal dialysis fluids. One of the key processes is the sheet extrusion line, which produces plastic sheeting to construct containers for IV solutions. A typical sheet extrusion line consists of an extruder, die, three roller stack, conveyor, pull rollers, and a winder. In general, the plastic pallets or powders are firstly melted and forced through the die by a screw. As the film is drawn out of the die, it passes through the roller stack which controls the cooling rate, final thickness and the surface of the sheet. The pull rollers are set to provide a uniform pressure, ensuring that the plastic does not slip between the rollers. At the end of the sheet line, a winder is normally used where the sheeting is stored.

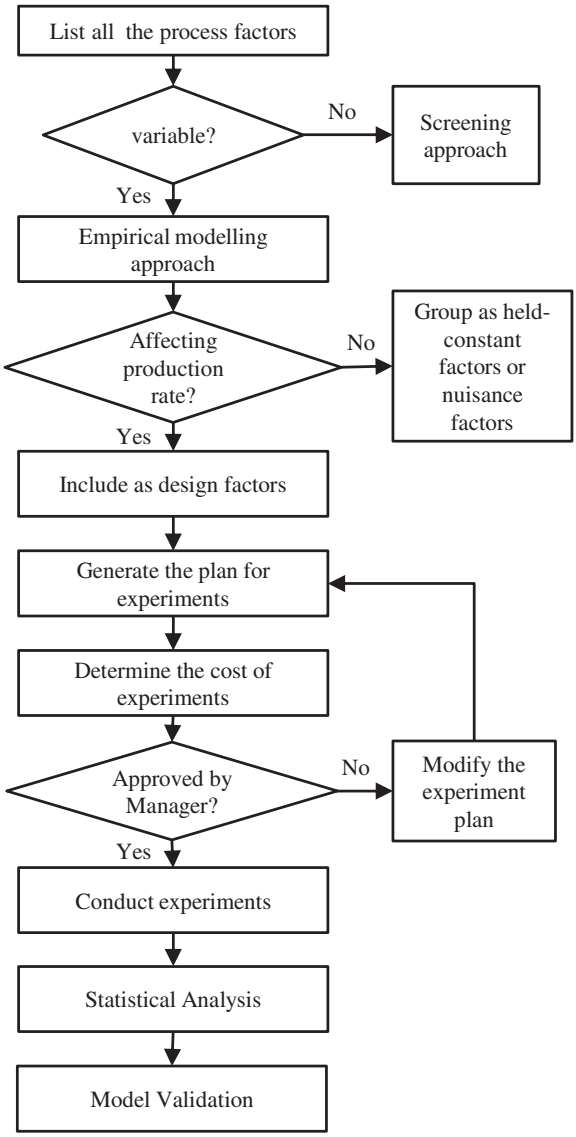

Fig. 6.6 Flow chart of the modified methodology for characterizing energy efficiency in industries (Li et al. 2013)

- **Design of Experiments**

According to Fig. 6.6, a complete list of factors was first identified for this plastic sheet extrusion line. The factors were categorized into four groups as shown in Fig. 6.7. Some factors, such as air humidity and temperature, can be concluded as uncontrollable factors. Other factors were further investigated in terms of their variance and impacts on production rate.

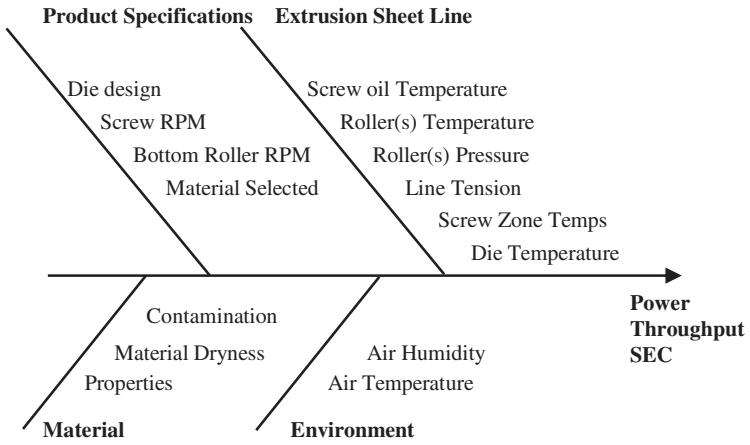

Fig. 6.7 Ishikawa diagram of the tested sheet extrusion

According to the production record, the tested sheet extrusion line produces different types of plastic sheets. Two types of raw materials are used, PVC and HDPE. The thickness of the plastic sheets also varies according to the size of the IV bag, which requires different settings for the process parameters. Therefore, it is useful and valuable to develop empirical models for this process.

The production rate of the process is measured by throughput rate, which is the mass of produced plastic sheet per unit time. There are two methods to measure the throughput of the tested process. The first method is to use the sensor which gauges the thickness. The material mass flow can be calculated in conjunction with the width and speed of the plastic sheet as well as the material intensity. The second method calculates an average throughput rate, dividing the total mass of one roll of plastic sheets by the production time. The first method is used to monitor the throughput rate during production. Figure 6.8 shows the throughput rate trend during the start-up period (after changing the filter). The results suggest that it requires at least 120 s for the mass flow to stabilize.

Figure 6.8 also suggested that the change of throughput rate is due to the increase of screw RPM from 6 to 100. The bottom roller RPM is adjusted accordingly to maintain the level of line tension. According to the operators, the screw RPM is normally set between 80 and 104. However, the theoretical range is much greater from 0 to 120. The production schedule also suggests that once the RPM is lower than 50, the demand cannot be met even if the process is running continuously. Therefore, the screw RPM was targeted and grouped as a design factor, the range of which is limited between 50 and 104.

Although different raw materials are used in production, the experiments with HDPE were rejected by the plant management, since the scrap of HDPE is not recycled onsite. Consequently, the tested material was limited to PVC, which is cheaper than HDPE. The production of PVC sheets accounts for a considerably

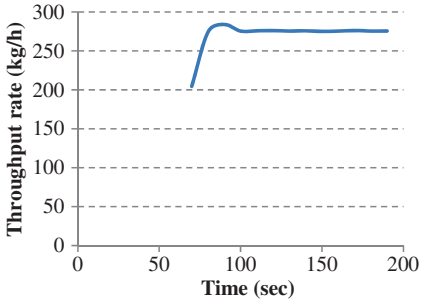

Fig. 6.8 Throughput rate change after filter change

higher proportion of the total output of this extrusion line. More importantly, the PVC scraps are shredded and reused for extrusion, which resulted in minimal material waste. Since the experiments were solely conducted with PVC, the temperatures were also held constant. Therefore, the design factors were narrowed down to the screw RPM.

In order to precisely characterize the relationship between power consumption and screw RPM, it is important to test multiple levels of this single design factor, since 2-level experiments initial assume the relationship would be linear. After discussion with the operators and plant manager, 6 levels of screw RPM would be used in the experiment allowing an increment of 10 RPM between each step from 50 to 100.

As discussed in Sect. 6.3.1, it is important to minimize the cost of experiments as well as the interruption of the normal production. Figure 6.8 suggests that the machine takes at least 120 s to stabilize. It was safe to allow 5 min for process stabilization, and another 10 min for data collection. The mass throughput can be manually recorded every 30 s, so 10-min experiments offers 20 samples at each level. The material cost was also estimated based on an average throughput rate. Since the machine is running 6 days a week, 24 h per day, the experiments were scheduled during one weekend, resulting in additional labor and operational cost. In addition, electrician was also ordered to connect the metering device. The overall cost was under the project budget with the highest proportion due to labor costs. Finally, the experiment plan was approved by the plant manager and the project manager.

- **Experiment details**

The tested extrusion sheet line is connected with different distribution boards and these distribution boards supply other processes. Thus, the extrusion line was separated into heating unit, screw unit, and the driving train unit (including the rollers, conveyer and the winder) and three Chauvin Arnoux®, C.A.8335 portable power analyzers were used to meter these units simultaneously with 1 s resolution.

Figure 6.9 shows the power consumption measurements of the screw unit. It clearly indicates the steps of the experiments, including an unexpected filter change during the process. The experiments steps were:

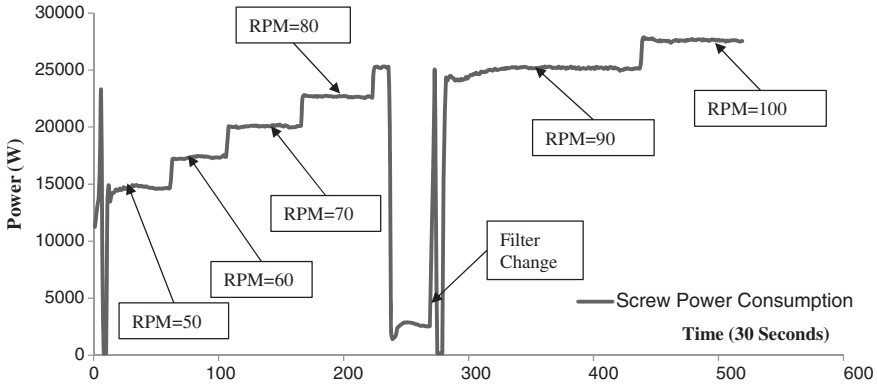

Fig. 6.9 Observed power consumption of the screw unit

– Once the process was at normal operating conditions the screw RPM was set to 50 and the drive train was set to keep the required tension on the line;
– The throughput of the process was observed for 5 min unit the process had stabilized;
– At the beginning of the experiment, the initial mass was measured. The throughput was recorded every 30 s for the duration of 10 min;
– After 10 min had elapsed, the total mass was measured again to calculate the average throughput rate;
– The screw RPM was increased to 60 and the drive train was adjusted accordingly;
– Step 2–5 were repeated and the screw RPM was increased to 70, 80, 90 and 100.

- **Statistical analysis**

A series of statistical analyses were conducted with a statistical package, MiniTab® version16.

The distributions of observed data at different levels were first analyzed. The heating unit power curve showed a similar pattern over the entire experiment. Two groups of measured heating power (screw RPM 50 and 100) were processed with a two-sample t-test. The null hypothesis had a p-value of 1.000, which suggests that both sets of observations belong to the same group and there is no variation present in the population. Another t-test was conducted on the variances between these two populations, which resulted in a p-value of 0.94. These two tests demonstrated that the power consumption of the heating unit remains constant during the operation. Therefore, the power consumption of the heating unit can be written as Eq. 6.12.

$$P_{heating} = 4.8699 + \varepsilon \tag{6.12}$$

Unlike the power consumption of heating unit, other observed data shows an obvious difference when the screw RPM changes. At each level of screw RPM, the

Table 6.2 Summary of the observed data

Design factor	Response means		
Screw RPM	Screw power (W)	Drive train (W)	Throughput (g/s)
50	14,636	9575	45
60	17,385	9657	48.6667
70	20,085	9671	56.6667
80	22,663	9691	65.6667
90	25,151	9714	73.3333
100	27,458	9856	81.3333

data sets were found to follow a normal distribution. The means of all the observed responses were listed in the Table 6.2.

The observed responses were then processed using linear regression. Figure 6.10 shows the fitted linear model against screw RPM for power consumption of screw unit, power consumption of the drive train unit, and throughput rate ($\dot{m}$) respectively. The models can be written as Eqs. 6.13–6.15.

$$P_{screw} = 1.479 + 0.2571 \times RPM + \varepsilon \tag{6.13}$$

$$P_{drive\_train} = 9.352 + 0.00456 \times RPM + \varepsilon \tag{6.14}$$

$$\dot{m} = 5.063 + 0.7562 \times RPM + \varepsilon \tag{6.15}$$

All of the derived linear models resulted in a high *R-square* value which indicates a high level of correlation between the observed responses and screw RPM. Notably, the lower R-square value for drive train power consumption is believed to be the lack of control of the process parameters at the related units. During the experiments, the drive train was adjusted to maintain the required line tension. The relationship between the roller speed and the screw RPM may not necessarily be linear. Nevertheless, the variance of drive train power consumption (from 9575 to 9856) is less significant than for screw power consumption (from 14,636 to 27,458). Hence, the linear model for the drain train power consumption is acceptable in this case.

The total energy consumption of the extrusion line can be then written as Eq. 6.16

$$P_{total}(\text{kW}) = 16.169 + 0.2617 \times RPM + \varepsilon \tag{6.16}$$

- **Model discussion and validation**

The power consumption model can be further converted into a SEC model as shown in Eq. 6.17 and Fig. 6.11. The SEC model also agrees with the ones for other manufacturing processes, which enables comparison among different manufacturing processes.

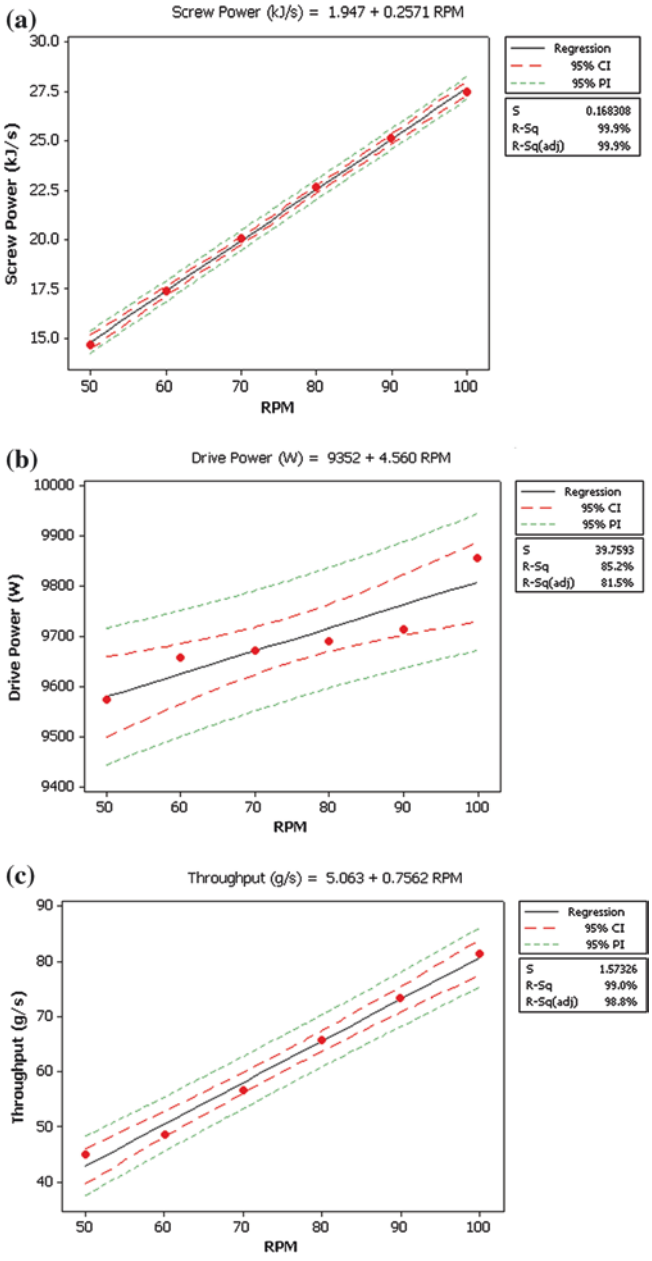

Fig. 6.10 Results of statistical analysis and model regression for the extrusion case. **a** Fitted linear model for screw power. **b** Fitted linear model for drive train power. **c** Fitted linear model for throughput rate

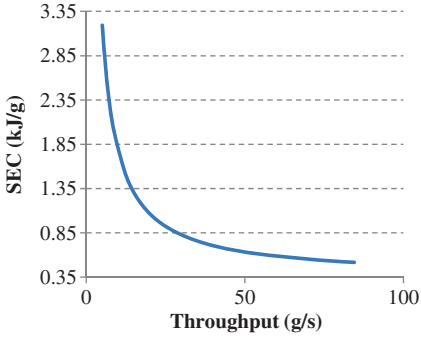

Fig. 6.11 SEC trend of the tested plastic sheet extrusion line

$$\begin{aligned} SEC &= \frac{P_{total}}{\dot{m}} = \frac{16.169 + 0.2617 \times RPM}{\dot{m}} + \varepsilon \\ &= \frac{16.169 + 0.2617 \times \frac{\dot{m} - 5.063}{0.7562}}{\dot{m}} + \varepsilon \\ &= 0.3461 + \frac{14.416}{\dot{m}} + \varepsilon \end{aligned} \tag{6.17}$$

A further validation run was conducted for 16 min at 85 screw RPM, the value of which was not used for model development. According to Eqs. 6.15 and 6.17, the predicted throughput rate was 0.069 g/s and the estimated SEC was 0.5501 kJ/g. Under this setting, the process took 962 s to product 69 kg of plastic sheet. The measured energy consumptions during this period were 23,861 kJ for the screw unit, 9334 kJ for the drive train unit and 4685 kJ for the heating unit. So the actual SEC was 0.5489. Comparing the predicted SEC with the actual value, the difference is around 2 % of the real SEC. Therefore, the derived SEC model is safe to use for estimating the energy consumption of the tested sheet extrusion line.

6.4 Improving Life Cycle Inventory (LCI) Database

The previous characterization of eco-efficiency relies on the existing LCA results of the energy and resources, such as a LCA for coolant. It is essential to improve the quality of the data source. Since the derived SEC models have achieved a great accuracy for predicting energy consumption of unit process, the life cycle inventory (LCI) database for unit process can be compared with the models.

In here, a LCI database, Ecoinvent database Version 2.2 was investigated. In the category of metal chipping unit process, the database provides LCA results

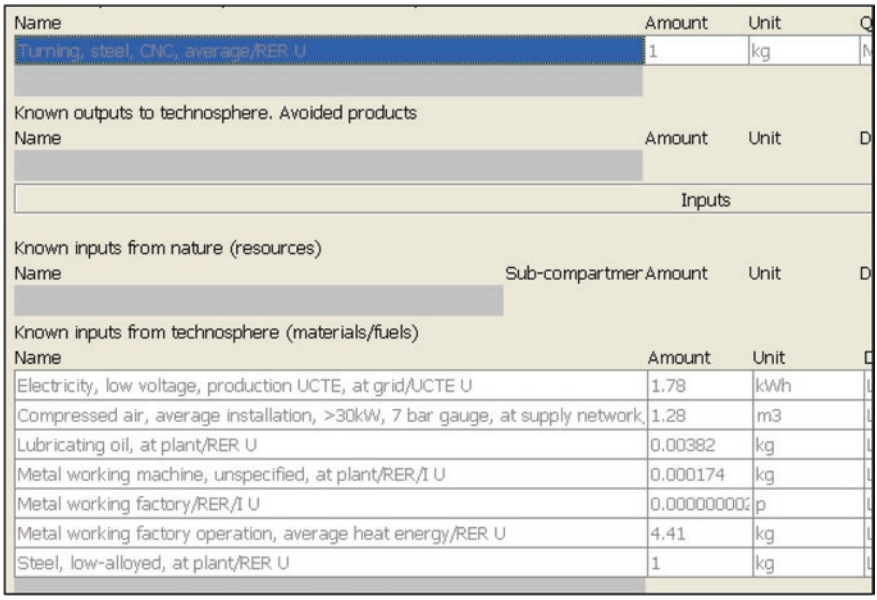

Name	Amount	Unit
Turning, steel, CNC, average/RER U	1	kg

Known outputs to technosphere. Avoided products

Name	Amount	Unit

Inputs

Known inputs from nature (resources)

Name	Sub-compartmer	Amount	Unit

Known inputs from technosphere (materials/fuels)

Name	Amount	Unit
Electricity, low voltage, production UCTE, at grid/UCTE U	1.78	kWh
Compressed air, average installation, >30kW, 7 bar gauge, at supply network,	1.28	m3
Lubricating oil, at plant/RER U	0.00382	kg
Metal working machine, unspecified, at plant/RER/I U	0.000174	kg
Metal working factory/RER/I U	0.00000000	p
Metal working factory operation, average heat energy/RER U	4.41	kg
Steel, low-alloyed, at plant/RER U	1	kg

Fig. 6.12 Screenshot of an exemplary dataset in LCI database (Ecoinvent V. 2.2)

for unit turning and milling processes, covering different workpiece materials (i.e. aluminum, cast iron, steel, etc.) and the purpose of machining (i.e. dressing, roughing, or average). The LCA results encompass the direct electricity of the process, the consumption of compressed air and lubricant oil, the removed metal, as well as the machine and factory infrastructure, an example of unit turning process is shown in Fig. 6.12.

Since the derived SEC models target only electricity consumption, the model results were compared with data in the LCI database. Table 6.3 lists the comparison for turning processes with aluminum workpiece. The MRR was assumed for each type of process, and both clustered model and a machine specific model for Colchester Tornado A50 was compared with the LCI datasets.

As the table shows, the LCI datasets overestimate the electricity consumption for turning 1 kg of material. For some cases, the real process only uses one fifth of the LCI suggested amount, which may result in a biased analysis and results. Alternatively, the SEC models can be integrated with the LCI database. Both the clustered model and machine specific models should be used, since the clustered model can be extremely useful when only limited information is available. In that way, the process parameters can be directly configured in the LCI and LCA analysis. Thus, the quality of LCI database can be definitely improved.

Table 6.3 The comparison between LCI datasets and SEC models

Process name	Turning, CNC, aluminum, average	Turning, CNC, aluminum, dressing	Turning, CNC, aluminum, roughing
Reference (kg)	1	1	1
Volume (cm^3)	352	352	352
Assumed MRR (cm^3/s)	1.0	0.25	3.0
Electricity in LCI dataset (E_I) (kWh)	1.83	3.29	0.362
Clustered model (Eq. 6.11)			
SEC (kJ/cm^3)	6.654	20.121	2.147
Electricity (E_m) (kWh)	0.65	1.97	0.21
Difference[a] (%)	64	40	42
SEC model for Colchester Tornado A50 (Eq. 4.4)			
SEC (kJ/cm^3)	3.713	10.37	2.234
Electricity (E_m) (kWh)	0.363	1.01	0.22
Difference[a] (%)	80	69	40

[a]Difference $= \frac{|E_I - E_m|}{E_I} \times 100\,\%$

6.5 Energy Efficiency Strategies for Manufacturing Processes

6.5.1 Energy Efficiency Strategies: An Operator's Perspective

From an operator point of view, a good energy efficiency measure should be easy-to-practice, no hardware investment with short pay-back period. It mainly refers to the activities relating to process and production planning and control. Based on the derived SEC models and above model analysis, energy efficiency improvements for manufacturing processes can be gained by either increasing production rate (MRR or throughput) or reducing the fixed energy consumption.

For most of the manufacturing processes, operators have a certain degree of freedom to select process parameters for producing a product. The constraints mainly refer to the surface finishing, dimensional accuracy, process type, machine tool capacity and tool life. Within the possible range, a higher material removal rate or throughput is favored according to SEC models. For the case of turning, increasing MRR can be achieved by e.g. changing cutting parameters, altering cutting tools, applying cutting fluid, etc. In addition, critical region should be avoided and prioritized for energy efficiency measures. For example, the efforts for increasing MRR in process should be encouraged as the small amount of MRR growth would result in a considerable energy reduction. However, changing

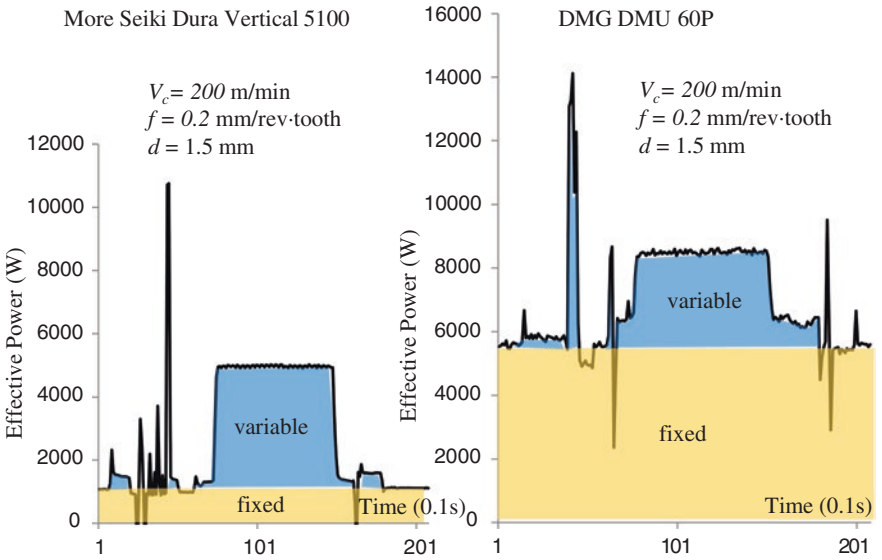

Fig. 6.13 Comparison of one milling process on different machine tools

process parameters also affects the surface finishing, dimensional accuracy, tool life, etc. Therefore, the evaluation of eco-efficiency should be used. Continuing with the case of grinding, the surface roughness, coolant consumption and the dressing processes were integrated into the evaluation, as presented in Chap. 5. The 3D figure suggests a critical region for different grinding wheels (see in Fig. 5.7). Within the critical region, the benefits from increasing material removal rate become less significant due to high requirement of surface roughness.

During the SEC decomposition, the fixed power consumption has been identified as a major contributor to coefficient c_1. Figure 6.13 compares an identical milling process performed by two different milling machine tools. It clearly shows that the difference of the total energy consumptions is mainly due to the fixed parts, where DMG DMU 60P consumes 5 times of fixed energy consumption than Mori Seiki Dura Vertical 5100 (5.45 and 1.02 kW respectively). More importantly, the fixed part not only accounts for a large proportion of the energy consumption during processing period, but also accumulates total energy consumption over other non-value adding periods. In industry, many machine tools are switched on 24/7, but only used for working in a relatively short period of time. Thus, investigation into the fixed energy consumption contains great potential for reducing energy consumption of manufacturing processes.

From an operator's point of view, the easiest approach for reducing fixed energy consumption is to switch off the machine tool when the machine is idle. However, this is not straight forward, as the fixed power ensures the machine readiness for operation and it takes time to regain the operational readiness. Therefore the question of when to switch the machine off still remains unanswered.

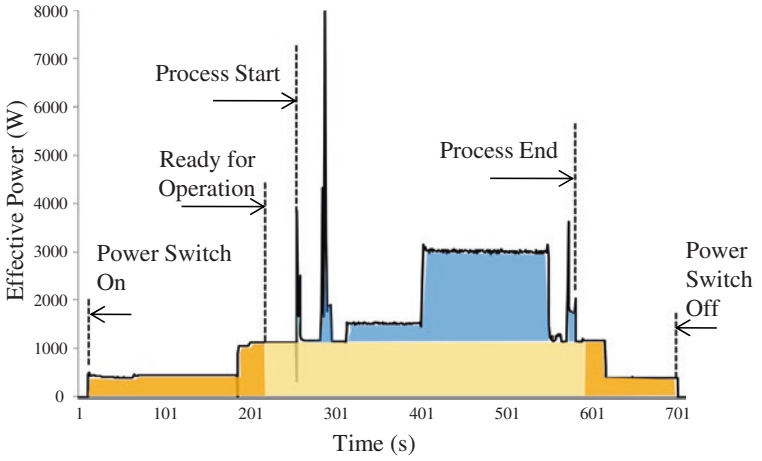

Fig. 6.14 Energy profile of the Mori Seiki NL2000MC/500

Table 6.4 List of start-up period and energy for the selected machine tools

Machine	Start-up period (s)	Start-up energy (kWh)
Colchester Tornado A50	30	0.004
Mori Seiki NL2000MC/500	150	0.038
Mori Seiki Dura Vertical 5100	110	0.021
DMG DMU 60P	100	0.096
Studer S120	110	0.036
Studer S40	250	0.256
BOY 15S (to 300 °C)	236	0.205
Battenfeld BA500CD (to 300 °C)	258	1.708

Figure 6.14 shows an entire power profile of the Mori Seiki Dura Vertical 5100 from power switch on to off.

As Fig. 6.14 suggests, the machine requires over 150 s in order to achieve operational readiness. In general, if the machine tool is scheduled to be idle for a period of time longer than start-up time, the machine needs to be switched off. Table 6.4 lists the start-up time and energy consumption for the selected machine tools. There are three machine tools requiring long period for start-up. Studer S40 needs 240 s to lubricate the driving system during machine start-up, while injection molding machines use around 4 min to reach the desired heating temperature. The high start-up energy demand for the Battenfeld BA500CD is due to the large volume of melting material, and the high rated power of heating unit (8 kW). In that case, how temperature decreases during the idle stage should be investigated as a future work in order to develop optimal switch-off strategies.

6.5.2 *Energy Efficiency Strategies: A Machine Tool Builder's Perspective*

The machine tool builders have become active to promote energy efficiency components and machine tools. The energy consumption can be reduced by retrofitting and replacing with energy efficient motors and pumps. Based on above analysis, the fixed energy consumption is of particular interest in this research. Li et al. (2011) attempted to assign the fixed power to each enabled components. But the procedure has been found problematic due to the lack of information about each component, as well as the accessibility to measure each motors. Alternatively, a component-based description of fixed power consumption was derived by using the power profile at different stage in conjunction with the wiring diagram of the machine tool, as shown in Fig. 6.15. The average fixed energy breakdown of reviewed machine tools has suggested the hydraulic system and the cooling lubrication system are the two hot-spots for energy efficiency improvements (see in Fig. 6.15d).

The new technologies such as variable speed hydraulic pumps are available in market for improving the energy efficiency of manufacturing processes. The savings are believed to be considerable, but cost efficiency and pay-back periods need to be taken into account as well.

Besides introducing new technologies, machine tool builders have a more important role for supplying energy efficiency information about their products (Zein et al. 2011). In other words, the energy consumption of the machine tools should be documented properly for the users. The proposed methodology for deriving unit process energy consumption models can be implemented at the machine tool builder's side. Therefore, a list of energy consumption indicators have been proposed to be included in the machine tool specifications (Table 6.5).

The above list can be extended to include energy consumption of each component, as well as their energy consumption trend against load and process parameters. This information is very helpful for selecting a machine tool from energy efficiency perspective, as well as configuring a process chain in an energy efficient way. For example, a shop floor has different milling and turning machine tools featuring different capacities and energy consumption behaviors. With above proposed indicators, the job can be allocated to a process which is capable but consumes least amount of energy. The interrelationship among processes can be also considered with a simulation tool (Herrmann et al. 2011). Owing to the dynamic nature of SEC models, the quality of the simulation at a process chain level or system level can be improved significantly.

Moreover, the provided information is also useful for the early stage of a product life cycle. The product designers and process planners can design the product and manufacturing processes in a way that reduces the energy consumption during the manufacturing stage.

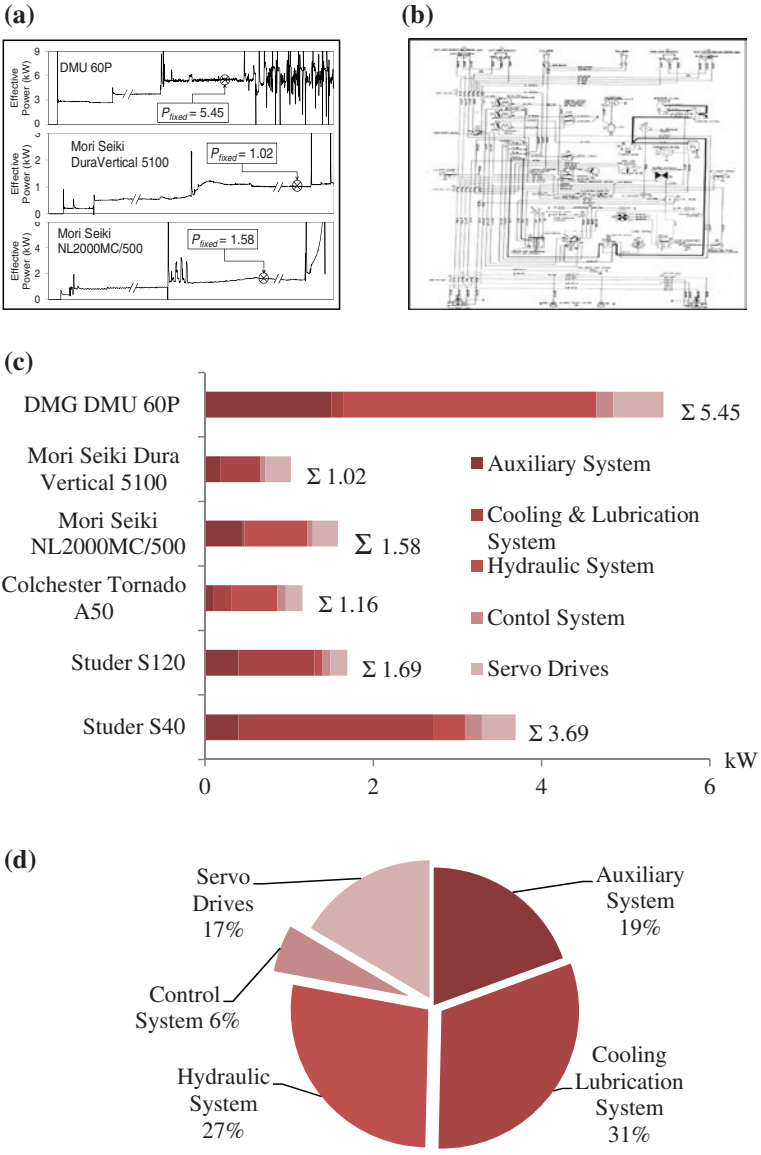

Fig. 6.15 Results of investigation into fixed energy consumption for the selected machine tools. **a** Power profile. **b** Wiring scheme. **c** Component-based description of fixed power consumption. **d** Average fixed energy breakdown of reviewed machine tools

Table 6.5 List of proposed energy consumption indicators for machine tool specifications

Proposed indicator		Unit	Example of Colchester Tornado A50
Rated power	Spindle motor	kW	5.5
	Servo motor	kW	0.5(Z axis)/0.5(X axis)/0.3(Turret)
	Hydraulic pump motor	kW	0.55
Fixed power consumption		kW	1.16
SEC model	c_0	kJ/cm^3	1.495
	c_1	kW	2.191
Start-up time		s	30
Start-up energy		kWh	0.004

6.5.3 Energy Efficiency Strategies: A Designer's Perspective

The design stage of a product life cycle is known to have a major influence on the entire product life cycle, but it is difficult to control the impacts due to the absence of physical objects (Stark 2011). Reliable models, simulations and other predicting tools can certainly ease the difficulties. Based on the derived SEC models, there are a few basic strategies for designers to reduce the energy consumption during the manufacturing stage.

- Material selection: the material properties have a direct impact on the production rate during manufacturing processes. From the SEC point of view, material with better machinability can significantly reduce the production time and energy consumption.
- Product shape: the size and geometric features of the products also affect the manufacturing processes in terms of energy consumption. The large volume of material removal are particularly inefficient from both energy and resource point of view. If a forming or casting process is in front of a material removal process, it is recommended to have formed or casted workpiece close to the end shape, resulting in a minimum volume of material removal.
- Surface finish and dimensional accuracy: the quality features of the product are essential for fulfilling product functional requirements. Without losing the surface finish or dimensional accuracy, a high MRR or throughput is preferred which can be achieved by using different cutting tools, applying higher process parameters, or efficient cutting fluid.

Although above three strategies may sound like common sense, the SEC models can quantify the changes made during design stage, and enable proactive actions to reducing the energy consumption during manufacturing stage. This can be achieved by integrating SEC models with the design software such as Computer Aided Design (CAD) software. Figure 6.16 illustrates this concept, which consists of a machine tool library, a CAD design interface, and an Energy consumption module. The machine tool library is the database for the derived SEC models for different machines and manufacturing processes. The CAD design interface

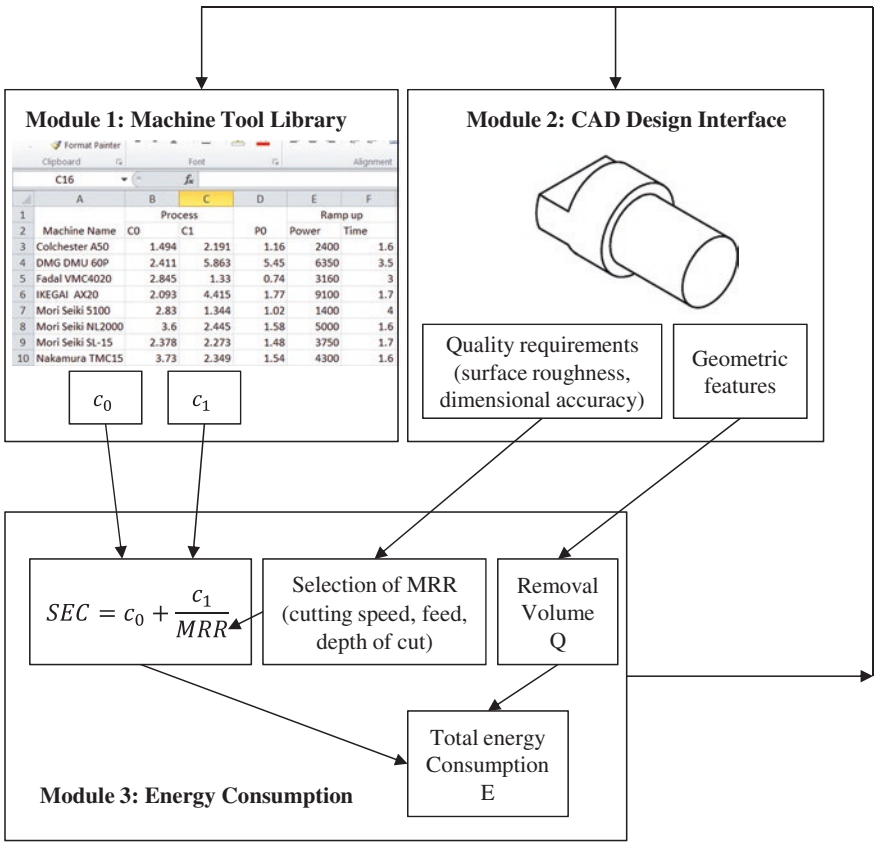

	A	B	C	D	E	F
1		Process			Ramp up	
2	Machine Name	C0	C1	P0	Power	Time
3	Colchester A50	1.494	2.191	1.16	2400	1.6
4	DMG DMU 60P	2.411	5.863	5.45	6350	3.5
5	Fadal VMC4020	2.845	1.33	0.74	3160	3
6	IKEGAI AX20	2.093	4.415	1.77	9100	1.7
7	Mori Seiki 5100	2.83	1.344	1.02	1400	4
8	Mori Seiki NL2000	3.6	2.445	1.58	5000	1.6
9	Mori Seiki SL-15	2.378	2.273	1.48	3750	1.7
10	Nakamura TMC15	3.73	2.349	1.54	4300	1.6

Fig. 6.16 Conceptual structure of integrating SEC models with CAD software

is the original environment in which the cutting volume of the workpiece can be easily calculated. The energy consumption module uses the information from the other two modules in conjunction with the selection of machine tools and process parameters, and then calculates the energy consumption for producing this part accordingly. This information can be fed back to the designers, which allows the designers to compare different options regarding the energy consumption of manufacturing processes.

This concept can be enhanced by introducing other studies such as research of surface integrity, tool wear, cost models, etc. For example, the design interface requires a certain surface roughness; the models describing the relationship process parameters and surface roughness would help the selection of process parameters and MRR. The tool wear and other cost models can be further added to provide economic information about the design. Therefore, future works are recommended to integrate unit process energy consumption models with other process studies such as surface integrity and tool wear.

It is also important to notice that reducing the environmental impacts during manufacturing stage may result in increasing impacts during other stages, e.g. usage stage. Thus, it is essential for designers to have a holistic view of the potential environmental impacts from raw material extraction to product end of life. To do so, further work is needed to improve the design tools which should offer a reliable analysis of the environmental impacts of a product throughout its entire life cycle.

6.6 Summary

This chapter has further discussed the use of unit process energy consumption models, besides the use for evaluating the energy and eco-efficiency of unit processes. The derived SEC model has been both decomposed and clustered. The SEC model decomposition has qualitatively suggested the factors related to the model coefficients. The findings have resulted in the definition of critical regions, in which unproductive energy consumption is high, and the SEC increases exponentially along decreasing MRR. The clustered model for metal machining processes has provided a useful tool for rough estimation disregarding the type of the machine tools or the processes. It also quantified the critical region for those processes, which is the MRR between 0 and 1 cm^3/s. Moreover, this chapter has modified the methodology for characterizing energy efficiency of manufacturing process in industries. The planning stage (DoE) plays a critical role for model development, where industrial requirements and practicality need to be considered with caution. An extrusion line was used to demonstrate the methodology. The resultant model shows a great ability to accurately predict energy consumption in this tested case.

The results of energy consumption models have been compared with the existing LCI database, which suggests a dynamic calculation rather than a constant value to improve the quality of the database. The energy efficiency strategies have been developed accordingly from different perspectives. The fixed energy consumption has been of particular focus, since it was believed to have great potential for reducing energy consumption during both process and non-value adding periods. Moreover, a list of energy consumption indicators has been proposed for machine tool builders. The SEC model is suggested to be included in the machine tool specifications. In addition, the energy consumption models can be integrated with design software, which provide another aspect for decision making.

References

Abele E, Altintas Y, Brecher C (2010) Machine tool spindle units. CIRP Ann Manuf Technol 59(2):781–802

Altintas Y (2000) Manufacturing automation: metal cutting mechanics, machine tool vibrations, and CNC design. Cambridge University Press, New York

Dietmair A, Verl A (2008) Energy consumption modeling and optimization for production machines. In: 2008 IEEE international conference on sustainable energy technologies, ICSET, Singapore

Gutowski T, Dahmus J, Thiriez A, Branham M, Jones A (2007) A thermodynamic characterization of manufacturing processes. In: IEEE international symposium on electronics and the environment, Orlando, FL

Herrmann C, Thiede S, Kara S (2011) Energy oriented simulation of manufacturing systems—concept and application. CIRP Ann Manuf Technol 60(1):45–48

Jedrzejewski J, Kowal Z, Kwasny W, Modrzycki W (2005) High speed precise machine tools spindle units improving. J Mater Process Technol 162–163:615–621

Kalpakjian S, Schmid SR (2005) Manufacturing engineering and technology, 5th edn. Prentice Hall, Upper Saddle River

Li W, Kara S (2011) An empirical model for predicting energy consumption of manufacturing processes: a case of turning process. In: Proceedings of the Institution of Mechanical Engineers, Part B. J Eng Manuf 225(9):1636–1646

Li W, Kara S, Kornfeld B (2013) Developing unit process models for predicting energy consumption in industry: a case of extrusion line. Re-engineering Manufacturing for Sustainability, pp 147–152

Li W, Zein A, Kara S, Herrmann C (2011) An investigation into fixed energy consumption of machine tools. In: 18th CIRP international conference on life cycle engineering, Braunschweig, Germany

SECO® Tools (2009) MN2009-turning. The machining navigator catalogue

Stark J (2011) Decision engineering: product lifecycle management: 21st century paradigm for product realisation, 2nd edn. Springer, New York

World Energy Council (2008) Energy efficiency polices around the world: review and evaluation. Online publication: http://www.worldenergy.org/publications/energy_efficiency_policies_around_the_world_review_and_evaluation/default.asp. Last visited 1 Mar 2012

Zein A, Li W, Herrmann C, Kara S (2011) Energy efficiency measures for the design and operation of machine tools: an axiomatic approach. In: 18th CIRP international conference on life cycle engineering, Braunschweig, Germany

Chapter 7
Conclusions

7.1 Concluding Remarks

As stated in the beginning of the book, the overall research objective is to develop a reliable methodology for characterizing the efficiency of manufacturing processes from both energy and ecological perspectives. The specific energy consumption, SEC, has been identified as the key indicator for the energy efficiency of unit processes. It refers to the total energy consumption of a machine tool for producing 1 unit of material. Therefore, developing SEC models for unit processes is essential for evaluating energy and eco-efficiency of manufacturing processes.

After a large number of experiments, an empirical approach for characterizing the relationship between process parameters and energy consumption has been successfully developed. This methodology has been implemented on different machine tools and manufacturing processes, including turning, milling, grinding, injection moulding processes and electrical discharge machining. For the case of material removal processes, SEC is the total energy consumption of removing 1 cm^3 material, whereas in the case of material addition process (such as injection moulding), SEC uses the weight of processed material instead of volumetric measures. Notably, the volumetric measures can be converted into the weight measures through the use of the workpiece density. Thus, this model response is generic and transferable among the tested manufacturing processes.

For each type of manufacturing process, different machine tools have been selected for model development and evaluations. Thus, the derived SEC models are machine specific. Without exception, all the derived models agree with one universal shape, where the production rate (material removal rate, through put) plays a decisive role in the model. Based on the statistical analysis, the model can exclude the sole impact of other parameters, i.e. workpiece material, tool geometry, etc. However, those factors are interrelated to the production rate. Hence, minimal input information is needed for predicting the energy consumption. More

W. Li, *Efficiency of Manufacturing Processes*, Sustainable Production,
Life Cycle Engineering and Management, DOI 10.1007/978-3-319-17365-8_7

importantly, the statistical results and additional validation runs have proved the high accuracy of the derived models. The difference between predicted and measured energy consumption remains under 10 %.

In addition to the evaluation energy efficiency, the value and the associated environmental impacts of the process have been discussed. Instead of using a market value, the value of unit process is suggested to be measured by physical characteristics, such as removal volume, processed weight, surface roughness, etc. The selection of indicators should agree with the primary objective of the unit process. A general classification has been made for the tested manufacturing processes, such as material removal process, surface finishing process, and thermoplastic processes. Grinding has been found as a special case, due to the high importance of surface integrity. Thus, the surface roughness has been added for the evaluation of eco-efficiency.

The analyses of environmental impacts of unit processes face limitations due to the absence of information regarding tools, coolant, etc. Regardless, electricity consumption is generally believed to be the main source of environmental impacts. The inverse of SEC can be directly used for evaluating the eco-efficiency for the case of turning, milling under dry machining environmental, as well as injection moulding. Since surface roughness is compulsory for grinding case, a 3D curve has been generated to describe the interrelationship among process parameters, surface roughness and CO_2 emissions.

The evaluations results have been further investigated to develop strategies for improving the energy and eco-efficiency of manufacturing processes.

The model decomposition has revealed the complexity of machine tool system, which cannot be explained by a theoretical model. It also qualitatively suggests the factors related to the derived empirical models. Although the coefficients of the models vary from machine to machine, a clustered model has been obtained for a rough estimation, and for developing energy efficiency measures. In order to implement the energy efficiency characterization in industries, a modified methodology has been developed. Due to the limited process flexibility and the costs of running experiments, a minimal number of experiments shall be planned to cover the practical range of process variances. The demonstrated case study of a sheet extrusion line has proved the reliability of the derived energy consumption models. In addition, the derived energy consumption models can certainly improve the quality of life cycle inventory (LCI) database. Both machine specific models and clustered model can be used for the future environmental analysis of a product or process.

The energy efficiency strategies have been proposed based on the derived models and the following analysis from different perspectives. Both of the model decomposition and clustering has suggested a critical region of material removal rate between 0 and 1 cm^3/s, which should be avoided if possible. The fixed power, which is the energy due to the use of auxiliary components to ensure machine readiness, has been identified as the priority for improvements. A feasible switch-off strategy and retrofitting priorities have been proposed, and the benefits can be quantified based on the derived models. The machine tool builders should also

take an important role by providing the energy consumption information of their products. In addition, the SEC models are suggested to integrate with the product design software; as a result, early actions can be taken during the early product design stage.

7.2 Research Contributions

The contributions of this research are:

- Developed a generic methodology for characterizing energy and eco-efficiency of manufacturing processes;
- Developed energy metering and monitoring strategies at unit process level;
- Derived energy consumption models for a variety of machine tools and manufacturing processes;
- Evaluated the interrelationship among process parameters, process value and environmental impacts;
- Explored the mechanism of unit process energy consumptions;
- Clustered model for all the material removal processes;
- Developed a modified methodology for characterizing energy efficiency in industries;
- Improved the data quality and accuracy for LCI database.
- Defining the critical region for selected processes;
- Developed energy efficiency strategies for unit process from different perspectives.

7.3 Recommendations for Future Works

Without a doubt, this is an on-going research topic. According to the findings from this research, there are three main areas for future efforts.

The proposed methodology for evaluating energy and eco-efficiency of manufacturing processes can be extended and implemented in other processes, such as casting process, metal forming process. The proposed methodology should be adapted and modified to suit those processes. For example, the value of a metal forming process is certainly different than the machining or injection molding. Thus, further efforts are required to evaluate the energy and eco-efficiency of other manufacturing processes.

The SEC models have their own limitations, which only capture the energy during the value adding period. The overall efficiency of a process chain or manufacturing system can be improved by integrating unit process models with system simulation tools. As a result, the unit process models deal with the dynamics of each process, while upper level simulations can manage the interrelationship among the unit processes.

The eco-efficiency provides a holistic view of unit processes. However, the value of the process and how to evaluate other processes requires further studies. In addition, the life cycle assessment of the supporting resources needs to be conducted as well, i.e. grinding wheel, different cutting fluid, etc.

In summary, this research has provided a useful foundation for the studies in the field of energy and eco-efficiency of manufacturing processes. With the joint efforts, the energy and resource efficiency will certainly be improved.

Appendix 1

Example of Experiment Schedule

Machine: Colchester Tornado A50
Workpiece Material: Aluminium alloy 2011

Standard order	Run order	Pt type	Blocks	Cutting speed V (m/min)	Feed f (mm/rev)	Depth of cut[a] d (mm)
10	1	−1	1	400	0.2	1
8	2	1	1	400	0.3	1.75
6	3	1	1	400	0.1	1.75
15	4	0	1	300	0.2	1
14	5	−1	1	300	0.2	1.75
4	6	1	1	400	0.3	0.25
3	7	1	1	200	0.3	0.25
1	8	1	1	200	0.1	0.25
12	9	−1	1	300	0.3	1
18	10	0	1	300	0.2	1
2	11	1	1	400	0.1	0.25
7	12	1	1	200	0.3	1.75
9	13	−1	1	200	0.2	1
17	14	0	1	300	0.2	1
13	15	−1	1	300	0.2	0.25
19	16	0	1	300	0.2	1
16	17	0	1	300	0.2	1
11	18	−1	1	300	0.1	1
5	19	1	1	200	0.1	0.75
20	20	0	1	300	0.2	1

[a]The levels of depth of cut were modified to a possible wide range

W. Li, *Efficiency of Manufacturing Processes*, Sustainable Production,
Life Cycle Engineering and Management, DOI 10.1007/978-3-319-17365-8

Appendix 2

Sample Data

Machine: Colchester Tornado A50
Workpiece Material: Aluminium alloy 2011

Run order	Cutting speed V (m/min)	Feed f (mm/rev)	Depth of cut d (mm)	RPM	MRR (cm^3/s)	SEC (kJ/cm^3)
1	400	0.2	1	2831	1.33	3.999
2	400	0.3	1.75	3033	3.5	1.960
3	400	0.1	1.75	3033	1.16	4.698
4	300	0.2	1	2123	1	4.978
5	300	0.2	1.75	2275	1.75	3.196
6	400	0.3	0.25	2654	0.5	9.211
7	200	0.3	0.25	1327	0.25	17.677
8	200	0.1	0.25	1327	0.083	52.275
9	300	0.3	1	2123	1.5	3.524
10	300	0.2	1	2123	1	4.928
11	400	0.1	0.25	2654	0.167	27.090
12	200	0.3	1.75	1516	1.75	3.086
13	200	0.2	1	1415	0.167	6.950
14	300	0.2	1	2123	1	4.933
15	300	0.2	0.25	1990	0.25	17.425
16	300	0.2	1	2123	1	4.861
17	300	0.2	1	2123	1	4.911
18	300	0.1	1	2123	0.5	9.131
19	200	0.1	0.75	1516	0.583	7.839
20	300	0.2	1	2123	1	4.875

W. Li, *Efficiency of Manufacturing Processes*, Sustainable Production,
Life Cycle Engineering and Management, DOI 10.1007/978-3-319-17365-8

Appendix 3

Curve-Estimation Results for Tested Machine Tools (Inverse Model)

Machine: Colchester Tornado A50

Model summary			
R	R square	Adjusted R square	Std. error of the estimate
0.997	0.993	0.993	0.596

ANOVA					
	Sum of squares	df	Mean square	F	Sig.
Regression	9432.483	1	9432.483	26,552.083	0.000
Residual	62.878	177	0.355		
Total	9495.362	178			

Coefficients					
	Unstandardized coefficients		Standardized coefficients	t	Sig.
	B	Std. error	Beta		
1/MRR (cm^3/s)	2.191	0.013	0.997	162.948	0.000
(Constant)	1.495	0.065		23.070	0.000

W. Li, *Efficiency of Manufacturing Processes*, Sustainable Production, Life Cycle Engineering and Management, DOI 10.1007/978-3-319-17365-8

Model Plots

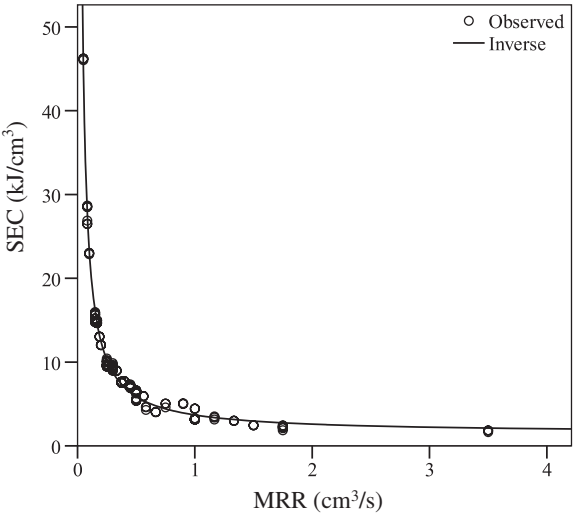

Machine: Mori Seiki NL2000MC/500

Model summary			
R	R square	Adjusted R square	Std. error of the estimate
0.963	0.927	0.926	1.541

ANOVA					
	Sum of squares	df	Mean square	F	Sig.
Regression	5327.040	1	5327.040	2244.321	0.000
Residual	422.494	178	2.374		
Total	5749.534	179			

Coefficients					
	Unstandardized coefficients		Standardized coefficients	t	Sig.
	B	Std. error	Beta		
1/MRR (cm3/s)	2.445	0.052	0.963	47.374	0.000
(Constant)	3.600	0.175		20.596	0.000

Model Plots

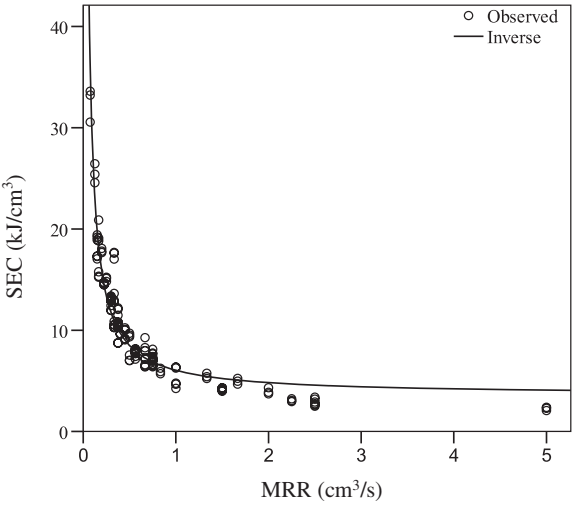

Machine: IKEGAI AX20

Model summary			
R	R square	Adjusted R square	Std. error of the estimate
0.991	0.981	0.981	1.512

ANOVA					
	Sum of squares	df	Mean square	F	Sig.
Regression	15,646.335	1	15,646.335	6840.151	0.000
Residual	299.653	131	2.287		
Total	15,945.988	132			

Coefficients					
	Unstandardized coefficients		Standardized coefficients	t	Sig.
	B	Std. error	Beta		
1/MRR (cm3/s)	4.415	0.053	0.991	82.705	0.000
(Constant)	2.093	0.193		10.832	0.000

Model Plots

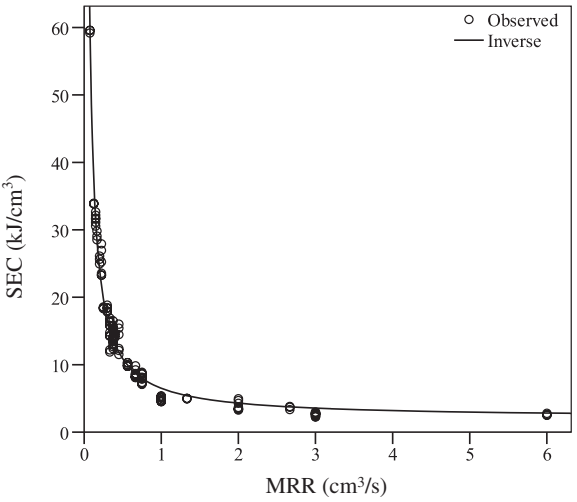

Machine: Mori Seiki SL-15

Model summary			
R	R square	Adjusted R square	Std. error of the estimate
0.970	0.940	0.940	1.393

ANOVA					
	Sum of squares	df	Mean square	F	Sig.
Regression	4324.108	1	4324.108	2227.515	0.000
Residual	275.654	142	1.941		
Total	4599.762	143			

Coefficients					
	Unstandardized coefficients		Standardized coefficients	t	Sig.
	B	Std. error	Beta		
1/MRR(cm^3/s)	2.273	0.048	0.970	47.197	0.000
(Constant)	2.378	0.168		14.130	0.000

Model Plots

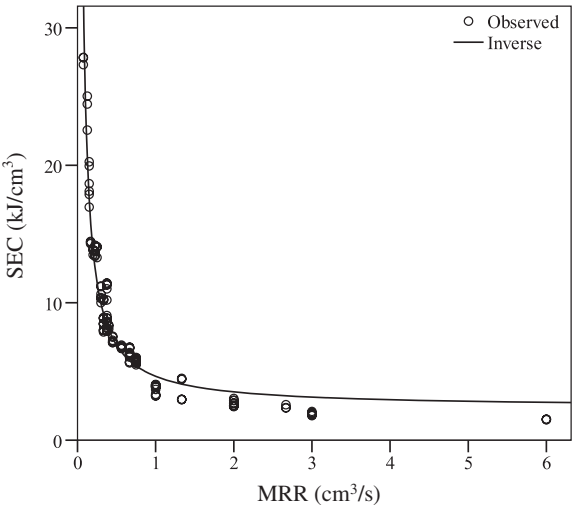

Machine: Nakamura TMC-15

Model summary			
R	R square	Adjusted R square	Std. error of the estimate
0.964	0.929	0.929	1.567

ANOVA					
	Sum of squares	df	Mean square	F	Sig.
Regression	4433.744	1	4433.744	1806.164	0.000
Residual	336.305	137	2.455		
Total	4770.049	138			

Coefficients					
	Unstandardized coefficients		Standardized coefficients	t	Sig.
	B	Std. error	Beta		
1/MRR (cm3/s)	2.349	0.055	0.964	42.499	0.000
(Constant)	3.730	0.197		18.975	0.000

Model Plots

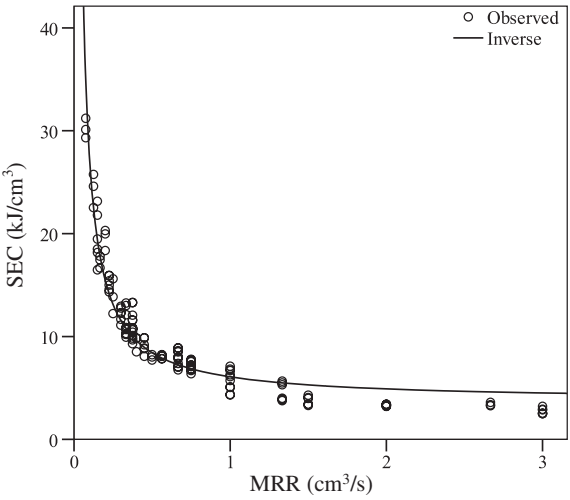

Machine: Mori Seiki Dura Vertical 5100 (Dry Machining)

Model summary			
R	R square	Adjusted R square	Std. error of the estimate
0.973	0.947	0.947	1.867

ANOVA					
	Sum of squares	df	Mean square	F	Sig.
Regression	34,318.546	1	34,318.546	9844.944	0.000
Residual	1934.678	555	3.486		
Total	36,253.223	555			

Coefficients					
	Unstandardized coefficients		Standardized coefficients	t	Sig.
	B	Std. error	Beta		
1/MRR (cm3/s)	1.344	0.014	0.973	99.222	0.000
(Constant)	2.830	0.106		26.816	0.000

Model Plots

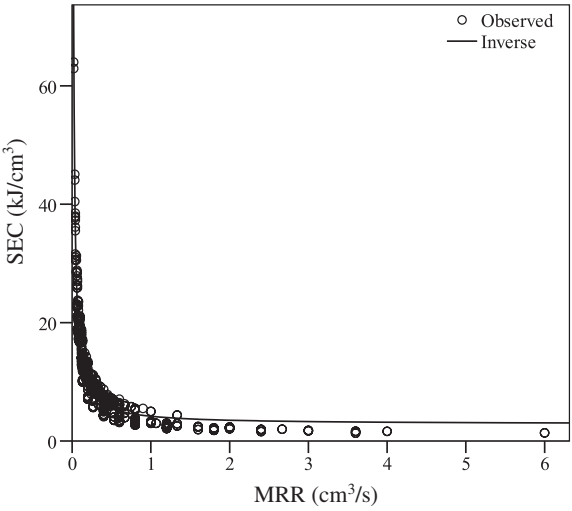

Machine: Fadal VMC 4020 (Dry Machining)

Model summary			
R	R square	Adjusted R square	Std. error of the estimate
0.986	0.971	0.971	1.463

ANOVA					
	Sum of squares	df	Mean square	F	Sig.
Regression	42,668.595	1	42,668.595	19,921.793	0.000
Residual	1261.523	589	2.142		
Total	43,930.118	590			

Coefficients					
	Unstandardized coefficients		Standardized coefficients	t	Sig.
	B	Std. error	Beta		
1/MRR (cm^3/s)	1.330	0.009	0.986	141.145	0.000
(Constant)	2.845	0.079		36.130	0.000

Model Plots

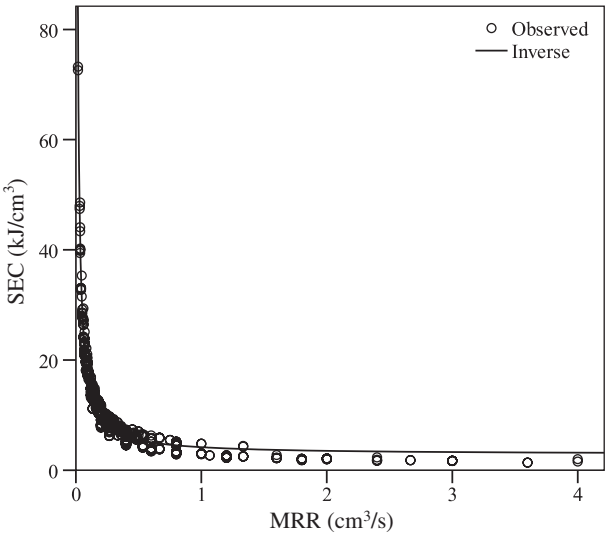

Machine: DMG DMU 60P (Dry Machining)

Model summary			
R	R square	Adjusted R square	Std. error of the estimate
0.998	0.997	0.997	1.893

ANOVA					
	Sum of squares	df	Mean square	F	Sig.
Regression	659,710.361	1	659,710.361	184,086.087	0.000
Residual	2035.545	568	3.584		
Total	661,745.905	569			

Coefficients					
	Unstandardized coefficients		Standardized coefficients	t	Sig.
	B	Std. Error	Beta		
1/MRR (cm3/s)	5.863	0.014	0.998	429.053	0.000
(Constant)	2.411	0.106		22.789	0.000

Model Plots

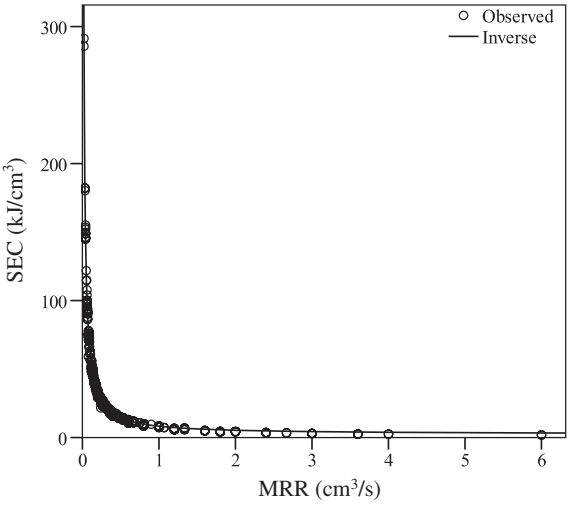

Machine: Mori Seiki Dura Vertical 5100 (Wet Machining)

Model summary			
R	R square	Adjusted R square	Std. error of the estimate
0.991	0.982	0.982	1.823

ANOVA					
	Sum of squares	df	Mean square	F	Sig.
Regression	60,196.323	1	60,196.323	18,116.539	0.000
Residual	1103.146	332	3.323		
Total	61,299.469	333			

Coefficients					
	Unstandardized coefficients		Standardized coefficients	t	Sig.
	B	Std. error	Beta		
1/MRR (cm3/s)	2.018	0.015	0.991	134.598	0.000
(Constant)	2.955	0.134		22.122	0.000

Model Plots

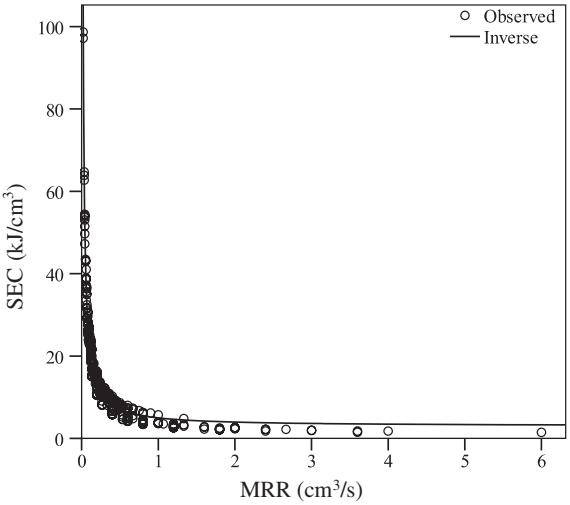

Machine: Fadal VMC 4020 (Wet Machining)

Model summary			
R	R square	Adjusted R square	Std. error of the estimate
0.988	0.976	0.976	1.628

ANOVA					
	Sum of squares	df	Mean square	F	Sig.
Regression	38,153.415	1	38,153.415	14,386.779	0.000
Residual	933.496	352	2.652		
Total	39,086.911	353			

Coefficients					
	Unstandardized coefficients		Standardized coefficients	t	Sig.
	B	Std. error	Beta		
1/MRR (cm^3/s)	1.397	0.012	0.988	119.945	0.000
(Constant)	3.078	0.114		27.086	0.000

Model Plots

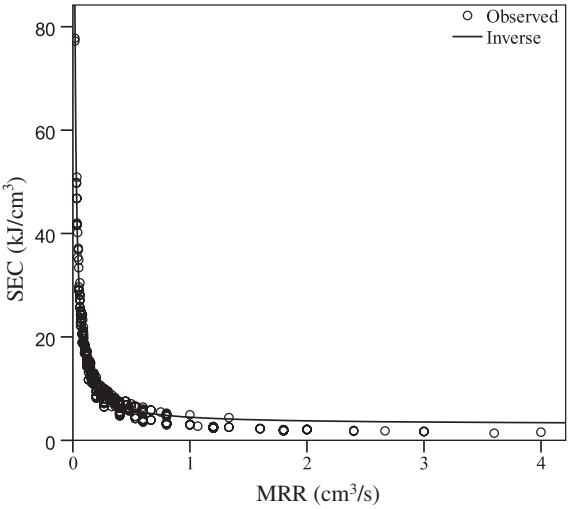

Machine: DMG DMU 60P (Wet Machining)

Model summary			
R	R square	Adjusted R square	Std. error of the estimate
0.994	0.987	0.987	4.865

ANOVA					
	Sum of squares	df	Mean square	F	Sig.
Regression	613,966.400	1	613,966.400	25,937.998	0.000
Residual	8000.642	338	21.671		
Total	621,967.043	339			

Coefficients					
	Unstandardized coefficients		Standardized coefficients	t	Sig.
	B	Std. error	Beta		
1/MRR (cm3/s)	6.422	0.040	0.994	161.053	0.000
(Constant)	2.425	0.356		6.820	0.000

Model Plots

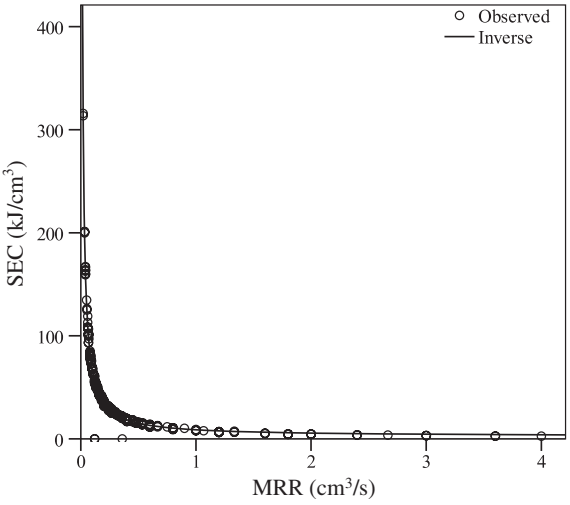

Machine: Reinecker ISA 110

Model summary			
R	R square	Adjusted R square	Std. error of the estimate
0.991	0.983	0.982	45.479

ANOVA					
	Sum of squares	df	Mean square	F	Sig.
Regression	6,739,931.668	1	6,739,931.668	3258.593	0.000
Residual	119,964.657	58	2068.356		
Total	6,859,896.325	59			

Coefficients					
	Unstandardized coefficients		Standardized coefficients	t	Sig.
	B	Std. error	Beta		
1/MRR (cm3/s)	3.399	0.060	0.991	57.084	0.000
(Constant)	47.269	12.060		3.920	0.000

Model Plots

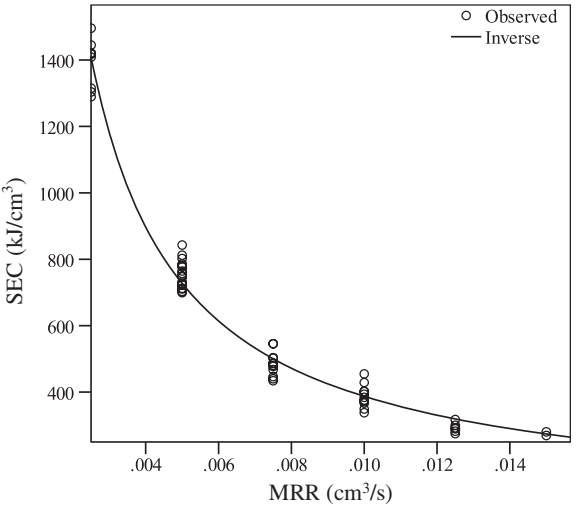

Machine: Studer S120

Model summary			
R	R square	Adjusted R square	Std. error of the estimate
0.998	0.996	0.996	29.928

ANOVA					
	Sum of squares	df	Mean square	F	Sig.
Regression	15,526,649.95	1	15,526,649.95	17,335.020	0.000
Residual	58,219.272	65	895.681		
Total	15,584,869.22	65			

Coefficients					
	Unstandardized coefficients		Standardized coefficients	t	Sig.
	B	Std. error	Beta		
1/MRR (cm3/s)	4.781	0.036	0.998	131.663	0.000
(Constant)	70.240	6.846		10.260	0.000

Model Plots

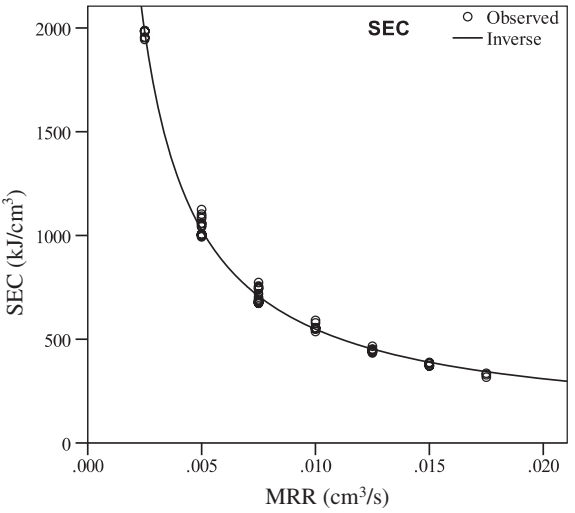

Machine: Studer S40

Model summary			
R	R square	Adjusted R square	Std. error of the estimate
0.994	0.988	0.988	70.334

ANOVA					
	Sum of squares	df	Mean square	F	Sig.
Regression	24,619,331.12	1	24,619,331.12	4976.690	0.000
Residual	286,921.844	58	4946.928		
Total	24,906,252.96	58			

Coefficients					
	Unstandardized coefficients		Standardized coefficients	t	Sig.
	B	Std. error	Beta		
1/MRR (cm3/s)	6.510	0.092	0.994	70.546	0.000
(Constant)	135.103	17.325		7.798	0.000

Model Plots

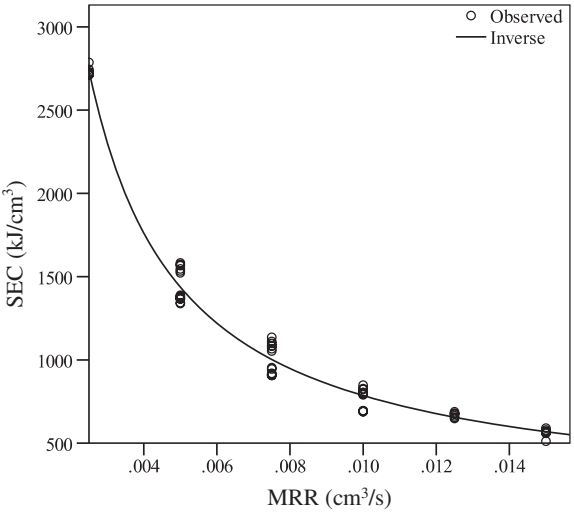

Machine: BOY 15S

Model summary			
R	R square	Adjusted R square	Std. error of the estimate
0.991	0.982	0.982	0.779

ANOVA					
	Sum of squares	df	Mean square	F	Sig.
Regression	32,782.975	1	32,782.975	54,054.513	0.000
Residual	605.267	998	0.606		
Total	33,388.242	998			

Coefficients					
	Unstandardized coefficients		Standardized coefficients	t	Sig.
	B	Std. error	Beta		
1/MRR (cm3/s)	1.933	0.008	0.991	232.496	0.000
(Constant)	3.552	0.049		72.268	0.000

Model Plots

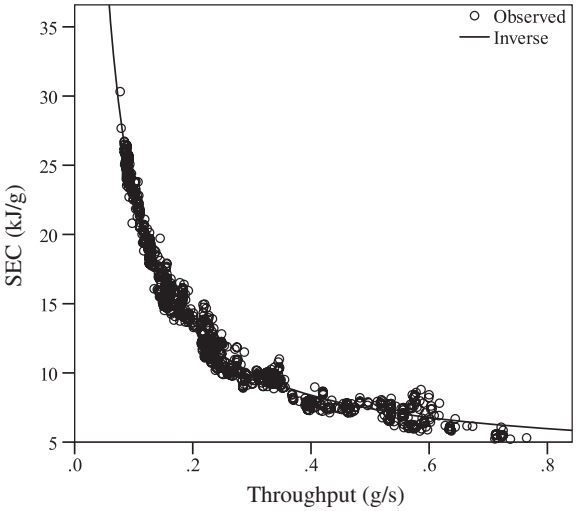

Machine: Bettenfeld BA500CD

Model summary			
R	R square	Adjusted R square	Std. error of the estimate
0.983	0.966	0.965	0.110

ANOVA					
	Sum of squares	df	Mean square	F	Sig.
Regression	9.947	1	9.947	816.269	0.000
Residual	0.353	29	0.012		
Total	10.301	30			

Coefficients					
	Unstandardized coefficients		Standardized coefficients	t	Sig.
	B	Std. error	Beta		
1/MRR (cm^3/s)	3.816	0.134	0.983	28.570	0.000
(Constant)	1.582	0.103		15.434	0.000

Model Plots

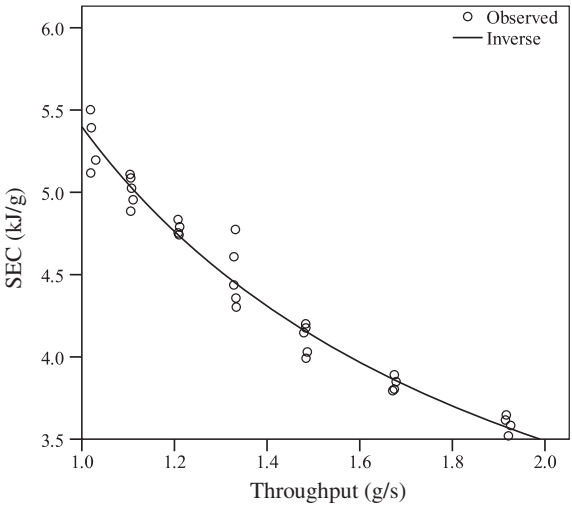

Machine: BOY 15

Model summary			
R	R square	Adjusted R square	Std. error of the estimate
0.980	0.961	0.960	0.903

ANOVA					
	Sum of squares	df	Mean square	F	Sig.
Regression	923.508	1	923.508	1133.699	0.000
Residual	37.471	46	0.815		
Total	960.979	47			

Coefficients					
	Unstandardized coefficients		Standardized coefficients	t	Sig.
	B	Std. error	Beta		
1/MRR (cm^3/s)	2.239	0.066	0.980	33.670	0.000
(Constant)	2.201	0.446		4.937	0.000

Model Plots

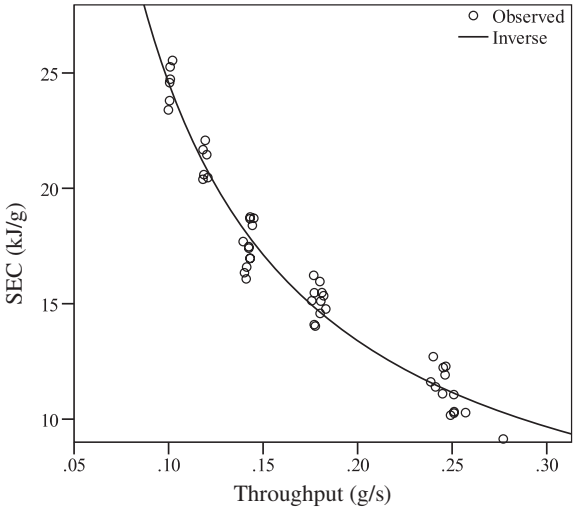
Observed
Inverse
SEC (kJ/g)
25
20
15
10
.05
.10
.15
.20
.25
.30
Throughput (g/s)

Appendix 4

Results of Model Validation

Turning Machine Tools

Machine: Colchester Tornado A50

	Brass		Bright mild steel 1045	
	Test 1	Test 2	Test 3	Test 4
V (m/min)	350	350	160	160
f (mm/rev)	0.2	0.1	0.2	0.1
d (mm)	2	0.5	1.25	0.8
MRR (cm^3/s)	2.333	0.292	0.667	0.213
Q (mm^3)	8792	2041	7497	4391
Predicted SEC (kJ/ cm^3)	2.433	9.006	4.781	11.764
Predicted E (J)	21,390.9	18,381.2	35,838.2	51,656.8
Measured E_i (J)	23,491.4	19,990.5	39,385.4	54,052.8
Difference (%) (Eq. 3.10)	8.94	8.05	9.01	4.44

Machine: Mori Seiki NL2000MC/500

	Brass		Bright mild steel 1045	
	Test 1	Test 2	Test 3	Test 4
V (m/min)	350	350	160	160
f (mm/rev)	0.2	0.1	0.2	0.1
d (mm)	2	0.5	1.25	0.8
MRR (cm^3/s)	2.333	0.292	0.667	0.213
Q (mm^3)	8792	2041	7497	4391
Predicted SEC (kJ/ cm^3)	4.648	11.983	7.268	15.061
Predicted E (J)	40,864.0	24,457.0	54,482.6	66,132.2
Measured E_i (J)	41,099.6	25,610.3	53,222.6	65,971.0
Difference (%) (Eq. 3.10)	0.57	4.50	2.37	0.24

W. Li, *Efficiency of Manufacturing Processes*, Sustainable Production,
Life Cycle Engineering and Management, DOI 10.1007/978-3-319-17365-8

Machine: IKEGAI AX20

	Bright mild steel 1045	
	Test 1	Test 2
V (m/min)	160	160
f (mm/rev)	0.2	0.1
d (mm)	1.25	0.8
MRR (cm^3/s)	0.667	0.213
Q (mm^3)	7497	4391
Predicted SEC (kJ/ cm^3)	8.716	22.788
Predicted E (J)	65,337.9	100,062.9
Measured E_i (J)	68,443.7	109,988.3
Difference (%) (Eq. 3.10)	4.54	9.02

Machine: Mori Seiki SL-15

	Bright mild steel 1045	
	Test 1	Test 2
V (m/min)	160	160
f (mm/rev)	0.2	0.1
d (mm)	1.25	0.8
MRR (cm^3/s)	0.667	0.213
Q (mm^3)	7497	4391
Predicted SEC (kJ/ cm^3)	5.788	13.033
Predicted E (J)	43,387.4	57,226.2
Measured E_i (J)	42,113.6	53,908.3
Difference (%) (Eq. 3.10)	3.02	6.15

Machine: Nakamura TMC-15

	Bright mild steel 1045	
	Test 1	Test 2
V (m/min)	160	160
f (mm/rev)	0.2	0.1
d (mm)	1.25	0.8
MRR (cm^3/s)	0.667	0.213
Q (mm^3)	7497	4391
Predicted SEC (kJ/ cm^3)	7.254	14.741
Predicted E (J)	54,377.7	64,727.1
Measured E_i (J)	57,761.5	70,302.9
Difference (%) (Eq. 3.10)	5.86	7.93

Milling Machine Tools

Machine: Mori Seiki Dura Vertical 5100

Workpiece	High tensile steel 4140			Bright mild steel (1045)		
Cutter	32 mm; 3-tooth			63 mm; 4-tooth		
Cutting parameters	$V = 160$ m/min; N = 1600 rpm; $d = 1.8$ mm			$V = 160$ m/min; N = 900 rpm; $d = 1.8$ mm		
Tool path number	1	2	3	1	2	3
w (mm)	5	25	20	15	10	25
f (mm/rev·tooth)	0.2	0.18	0.14	0.18	0.2	0.16
MRR (cm^3/s)	0.144	0.648	0.403	0.292	0.216	0.432
Q (cm^3)	1.8	9.0	7.2	5.4	3.6	9.0
Predicted SEC (kJ/cm^3)	12.16	4.90	6.16	7.44	9.05	5.94
Predicted E (kJ)	21.89	44.14	44.38	40.17	32.59	53.47
Measured E_i (kJ)	24.05	47.40	48.01	41.78	33.71	55.95
Difference (%)	8.97	6.88	7.57	3.85	3.32	4.43

Machine: Fadal VMC 4020

Workpiece	High tensile steel 4140			Bright mild steel (1045)		
Cutter	32 mm; 3-tooth			63 mm; 4-tooth		
Cutting Parameters	$V = 160$ m/min; N = 1600 rpm; $d = 1.8$ mm			$V = 160$ m/min; N = 900 rpm; $d = 1.8$ mm		
Tool path number	1	2	3	1	2	3
w (mm)	5	25	20	15	10	25
f (mm/rev·tooth)	0.2	0.18	0.14	0.18	0.2	0.16
MRR (cm^3/s)	0.144	0.648	0.403	0.292	0.216	0.432
Q (cm^3)	1.8	9.0	7.2	5.4	3.6	9.0
Predicted SEC (kJ/cm^3)	12.08	4.90	6.14	7.41	9.00	5.92
Predicted E (kJ)	21.75	44.08	44.23	39.99	32.41	53.31
Measured E_i (kJ)	22.34	45.20	45.99	41.32	34.01	54.21
Difference (%)	2.65	2.48	3.82	3.21	4.70	1.65

Machine: DMG DMU 60P

Workpiece	High tensile steel 4140			Bright mild steel (1045)		
Cutter	32 mm; 3-tooth			63 mm; 4-tooth		
Cutting parameters	$V = 160$ m/min; N = 1600 rpm; $d = 1.8$ mm			$V = 160$ m/min; N = 900 rpm; $d = 1.8$ mm		
Tool path number	1	2	3	1	2	3
w (mm)	5	25	20	15	10	25
f (mm/rev·tooth)	0.2	0.18	0.14	0.18	0.2	0.16
MRR (cm^3/s)	0.144	0.648	0.403	0.292	0.216	0.432
Q (cm^3)	1.8	9.0	7.2	5.4	3.6	9.0
Predicted SEC (kJ/cm^3)	43.13	11.46	16.95	22.51	29.55	15.98

Workpiece	High tensile steel 4140			Bright mild steel (1045)		
Cutter	32 mm; 3-tooth			63 mm; 4-tooth		
Cutting parameters	$V = 160$ m/min; N = 1600 rpm; $d = 1.8$ mm			$V = 160$ m/min; N = 900 rpm; $d = 1.8$ mm		
Tool path number	1	2	3	1	2	3
Predicted E (kJ)	77.63	103.13	122.06	121.59	106.40	143.84
Measured E_i (kJ)	79.91	105.85	126.05	123.67	109.29	151.13
Difference (%)	2.85	2.57	3.17	1.68	2.65	4.82

Grinding Machine Tools

Machine	Reinecker ISA 110	Studer S120	Studer S40
Grinding wheel	CBN	Al_2O_3	CBN
Workpiece	100Cr6	100Cr6	16MnCr5
w (mm)	10	10	10
Q'_w (mm^3/mm·s)	0.8	0.4	1.2
V'_w (mm^3/mm)	250	120	250
MRR (cm^3/s)	0.008	0.004	0.012
Q (cm^3)	2.5	1.2	2.5
Predicted SEC (kJ/cm^3)	472.14	1265.49	677.60
Predicted E (kJ)	1180.36	1518.59	1694.01
Measured E_i (kJ)	1132.67	1498.04	2510.11
Difference (%)	4.21	1.37	3.52

Injection Machine Tools

Machine: BOY 15S

Material	HDPE	LDPE	PS
Density (g/cm^3)	0.941	0.920	1.05
Injection Volume, Q (cm^3)	12.42	12.42	12.42
Cycle time (s)	80	70	25
Mass, m (g)	11.69	11.43	13.04
Throughput rate, $\dot{m}$ (g/s)	0.146	0.163	0.522
Predicted SEC (kJ/g)	16.8	15.4	7.3
Predicted E (kJ)	196.15	175.90	94.65
Measured E_i (kJ)	209.251	184.15	98.25
Difference (%)	6.26	4.48	3.67

Machine: Battenfeld BA500CD

Material	HDPE	LDPE	PS
Density (g/cm^3)	0.941	0.920	1.05
Injection volume, Q (cm^3)	58.29	58.29	58.29
Cycle time (s)	60	50	40

Material	HDPE	LDPE	PS
Mass, m (g)	54.85	53.63	61.20
Throughput rate, $\dot{m}$ (g/s)	0.914	1.073	1.53
Predicted SEC (kJ/g)	5.8	5.1	4.1
Predicted E (kJ)	315.73	25.64	249.47
Measured E_i (kJ)	301.59	272.64	274.548
Difference (%)	4.69	1.1	9.14

Machine: BOY 15

Material	HDPE	LDPE
Density (g/cm^3)	0.941	0.920
Injection Volume, Q (cm^3)	3.51	3.51
Cycle time (s)	30	25
Mass, m (g)	3.30	3.23
Throughput rate, $\dot{m}$ (g/s)	0.11	0.129
Predicted SEC (kJ/g)	22.5	19.5
Predicted E (kJ)	74.44	63.08
Measured E_i (kJ)	78.729	68.169
Difference (%)	5.45	7.46

Index

W. Li, *Efficiency of Manufacturing Processes*, Sustainable Production, Life Cycle Engineering and Management, DOI 10.1007/978-3-319-17365-8